

博士論文

論文題目

**Analyses of movement patterns and individual  
interactions in the animal behavior**

(動物行動における動きのパターンと相互作用の解析)

氏名 阿部 真人

# Table of contents

Chapter 1. General introduction .....	2
Chapter 2. Lévy walk search strategy under predation risks .....	7
Chapter 3. Theoretical analysis and experiment of random avoidance behavior .....	31
Chapter 4. Detecting information transfer in ant society.....	46
Chapter 5. Network structure of dominance hierarchy of ant workers .....	76
Chapter 6. General discussion .....	114
Acknowledgement.....	119
References .....	120

# Chapter 1

## General introduction

### Introduction

Movements, defined as changes in the spatial locations of individuals, are fundamental characteristics of animals, and therefore, can define animals. In the 4<sup>th</sup> century B.C., Aristotle said in *De Motu Animalium* (*On the Movement of Animals*) that we must consider the common reason for the movements of animals (Nussbaum, 1978). Even in modern behavioral science, the question remains unchanged: How and why do animals move? In order to examine this, studies in the animal behavior research field of behavioral ecology have been conducted to analyze animal behaviors in terms of adaptive optimization through natural selection (Wilson, 1975; Krebs and Davies, 1978). Although a number of theoretical and empirical studies have successfully revealed optimal foraging strategies and social structure, most analyses have been limited to shorter temporal and smaller spatial scales due to the difficulties in collecting data. Actually, by moving in the environment throughout their lifetime, animals have the ability to search for desirable things (e.g., food, prey, and mates) and avoid harmful things (e.g., predator and disease) (Nathan et al., 2008). Moreover, animals in groups can collectively move through direct interactions with other individuals in the group, which leads to collective decision-making or efficient information transfer (Camazine et al., 2003, Sumpter, 2010, Vicsek and Zafeiris, 2012). Therefore, we need to quantitatively investigate movements on a larger scale. Recently, techniques that can be used to collect movement data, such as GPS or image analysis, have been developed, and they allow researchers to obtain long-term and high-resolution quantitative movement data (Dell et al., 2014). Thus, movement ecology is a proposed research field that focuses on quantifying and analyzing movements (Nathan et al., 2008).

Another important characteristic of animals is interactions with other individuals, including prey-predator interactions, interspecific or intraspecific competition, and

cooperation (Solé and Bascompte, 2006; Nowak, 2006). These interactions are considered one of the factors that drive the evolution of animal behavior through natural selection because the consequences of interactions critically determine fitness. Furthermore, individual interactions can directly influence ecological phenomena, such as population dynamics and the spread of invaders and pathogens, and determine structures, such as the food web structure and the spatial structure (Solé and Bascompte, 2006; Kondoh, 2003; Ishii and Shimada, 2012). These remain a primary concern in ecology. Clearly, interactions are critically associated with the movements of animals as movement patterns can influence interactions and vice versa.

A number of studies of individual movement (i.e., not grouped) showed that movements often fit into a special class of random walks called Lévy walks (Bartumeus et al., 2003; Reynolds and Frye, 2007; Sims et al., 2008; Humphries et al., 2010; Viswanathan et al., 2011). However, these studies have only examined interactions with targets, and, thus, the effects of other interactions are less understood. In studies of collective behavior, fascinating results have clarified the relationship between the interaction rule and movements in schools of fish or flocks of birds with high polarization. However, groups that are composed of diverse individuals and that exhibit complex dynamics (e.g., social insects) have not been analyzed. Thus, the current understanding of the relationship between interactions and movements is not sufficient.

## **Thesis outline and chapter abstracts**

### **Outline**

In this thesis, I consider both movements and interactions and investigate the relationship between them. First, I concentrate on prey-predator interactions at the individual level in terms of searching strategies (Chapter 2) and avoidance strategies (Chapter 3) and theoretically investigate efficient movement patterns. Second, I examine the group level and investigate conspecific interactions in social insects based on movement data (Chapter 4) and dominance behavior (Chapter 5). Finally, I discuss the movements and interactions of animals (Chapter 6).



## **Chapter 2: Lévy walk search strategy under predation risks**

All animals search for desirable things, such as food, prey, and mates. Previous studies on search behavior have predicted that animals perform a special class of random walk, called a Lévy walk, to obtain more targets (Viswanathan et al., 1999; Viswanathan et al., 2011). However, the findings of some empirical studies have not supported this prediction (Edwards et al., 2007), and the relationship between search strategies and ecological factors is still unclear. I concentrated on ecological factors, such as the predation risk, and analyzed whether Lévy walks are preferred, even with the influence of ecological factors. I found that ecological factors often altered an optimal search strategy from a Lévy walk to a Brownian walk, depending on the speed of the predator's movement, the density of the predators, and the lifecycle of the searcher. I will discuss the relationship between random search strategies and ecological factors.

## **Chapter 3: Theoretical analysis and experiment on random avoidance behavior**

Animals often exhibit random spontaneous decision-making patterns in movements (i.e., step length or stop/go timing), such as Lévy walks (Viswanathan et al., 2011; Proekt et al., 2012; Wearmouth et al., 2014). An adaptive aspect of such randomness is the unpredictability of an individual's movements so that it cannot be readily anticipated by other individuals (Domenici et al., 2008; Brembs, 2011). To elucidate the adaptive unpredictability of random movements, I focused on avoidance behavior for a predator because most animals are usually exposed to predation risks in nature. In this chapter, I theoretically analyzed the optimal avoidance strategy and conducted an experiment on subjects (human beings) that seek and catch an individual evading on a computer screen. I showed that Lévy walk movement patterns were superior to Brownian movements for avoiding predators. I discuss the relationship between randomness and the adaptive predator-avoidance strategy.

## **Chapter 4: Detecting information transfer in ant society**

Collective behaviors in animals' groups, such as fish schools, bird flocks, and colonies of social insects, include rapid and accurate decision-making in uncertain environments or efficient division of labor (Camazine et al., 2003; Sumpter, 2010, Vicsek and Zafeiris, 2012). Although determining how such collective behaviors emerge from local interactions is important, little is known about the groups that are composed of diverse individuals and that exhibit complex dynamics (e.g., social insects). In this chapter, I applied a novel time-series analysis, Convergent Cross Mapping (Sugihara et al., 2012), to quantify and analyze the local interactions in the movement data of ants of *Diacamma* sp. The method showed causality in multivariate time series. Therefore, the interactions between ant individuals were obtained from the time series. I provided a framework to analyze collective behavior. I discuss the interaction pattern and information transfer.

## **Chapter 5: Network structure of the dominance hierarchy of ant workers**

Dominance hierarchy in groups of animals has been a central topic in behavioral ecology for decades (Wilson, 1975; Shizuka and McDonald, 2012). A prevalent theoretical and statistical method to analyze such data, the tournament, is powerful in analyses of small and dense groups of animals. However, the detection and quantification of dominance hierarchy in large groups are difficult mainly due to sparse interactions in the group. In this chapter, I analyze the aggressive dominance hierarchy that was formed by worker ants in large directed networks. Although very recent studies have asked similar questions by using a local analysis method (triad census), analyses of the global network structures of directed dominance networks have been surprisingly absent in ecology and sociobiology. I illustrated the observed networks with (approximate) directed acyclic graphs and conducted further network analysis. I discuss the evolutionary implications of the discovered properties of dominance networks.

## **Chapter 6: General discussion**

Finally, I summarize the conclusions of the thesis, discuss the movements and interactions in animals, and describe future studies.

# Chapter 2

## Lévy walk search strategy under predation risks

### Introduction

How should we move to search for targets when we have no information about their location? This is called the random search problem, which has attracted the attention of researchers in various fields (Viswanathan et al., 2011). The problem can be applied to various phenomena, including molecular-level movements within an organism, cell movements, movements of an individual animal, and the movement of robots (van Dartel et al., 2004; van den Broek et al., 2008; Harris et al., 2012). For example, animals search their environment for food, prey, mates, and nesting locations, and DNA-binding proteins search for a specific DNA sequence to initiate gene expression. The search strategy has evolved to be more efficient through the process of natural selection because successful searches increase fitness, especially at the individual level in animals.

The Lévy walk search (or foraging) hypothesis was proposed to solve the random search problem (Viswanathan et al., 1999). A Lévy walk is a special class of random walk models in which the probability function of step length  $l$  has a power-law tail:  $P(l) \sim l^{-\mu} (1 < \mu \leq 3)$ , where  $\mu$  is a power-law exponent, such that rare ballistic movements occur among a number of relatively short steps. Comparisons of the efficiency of random searches showed that a Lévy walk with  $\mu \approx 2$  was a highly efficient search strategy in environments where patchy prey were sparsely distributed (Viswanathan et al., 1999; Bartumeus et al., 2002; Bartumeus et al., 2005; Viswanathan et al., 2011). On the other hand, Lévy walks had almost the same efficiency as Brownian walks when the targets were abundant (Bartumeus et al., 2002). Therefore, the Lévy walk foraging hypothesis predicts that most animals should perform Lévy walks while searching unless there are abundant targets.

Although many empirical studies have reported that diverse organismal components and taxa (e.g., T cells, insects, and human beings) perform Lévy walks (Bartumeus et al., 2003; Reynolds and Frye, 2007; Reynolds et al., 2007; Sims et al., 2008; Reynolds and Rhodes, 2009; Humphries et al., 2010; Viswanathan et al., 2011; Harris et al., 2012; Humphries et al., 2012; Raichlen et al., 2014), several recent analyses demonstrated that some animals had various Lévy exponents  $\mu$ , or they exhibited Brownian walks (Edwards et al., 2007; Benhamou, 2007; Humphries et al., 2010; Petrovskii et al., 2011; Horibe, 2011; Humphries et al., 2012). For example, rigorous statistical analyses of deer and bumblebees failed to provide strong evidence for Lévy walks (Edwards et al., 2007). Thus, the question changed from whether animals have Lévy walk movement patterns to when or why animals perform Lévy walks. In general, the diversity of organisms is the result of varying ecological and environmental factors as well as complex biotic interactions with conspecific and heterospecific individuals (Wearmouth et al., 2014). Theoretical reports of random searches have generally focused only on search efficiency to evaluate the fitness of the searcher (Viswanathan et al., 1999; Bartumeus et al., 2002; Raposo et al., 2003; Santos et al., 2004; Bartumeus et al., 2005; Bartumeus and Levin, 2008; Reynolds, 2008; Viswanathan et al., 2011). Moreover, most of these studies paid little attention to other relevant ecological factors such as death rate with predation risk, interactions with other individuals, and the metabolic costs of foraging. Although a few theoretical studies have considered such factors (Zollner and Lima, 1999; Faustino et al., 2007; Reynolds and Bartumeus, 2009; de Jager et al., 2011; de Jager et al., 2014), including predation risk (Visser, 2007; Reynolds, 2010; Reynolds 2013), the relationships between these factors are still poorly understood.

Here, I focus on the fact that search efficiency represents the probability of an encounter with anything existing in the environment. Highly efficient search strategies may correspond to more frequent encounters with predators, and thus higher death rates. Therefore, search efficiency, as defined in previous studies, may not reflect the actual fitness, because fitness is not only determined by the efficiency of searching for targets (i.e., benefits), but also by the death rate caused by predation (i.e., cost) (Lima et al., 1985).

Reynolds (2010, 2013) reported that predation risk altered the optimal strategy, but did not consider predators (Reynolds, 2010) or the fitness of the searcher (Reynolds, 2010). In this chapter, I explicitly introduce predation risk and life-cycle types to the previous simulations, and extend the random search scenario to correctly estimate the fitness of a searcher to determine an animal's optimal search strategy.

## Methods

### Basic assumption

First, I considered a searcher performing either the Lévy walk (hereafter, LW) or the Brownian walk (hereafter, BW) at movement velocity  $v_s (= 1)$  in an environment in which patchy targets were sparsely distributed. Then,  $N_p$  predators were randomly placed in the environment. To explore the effect of the predators' movements, I considered four cases with respect to the predators' movement velocity  $v_p$ :  $v_p = 0$  (sit-and-wait);  $v_p / v_s = 0.2$  (slow);  $v_p / v_s = 1$  (middle); and  $v_p / v_s = 5$  (fast). If  $v_p > 0$ , I assumed that a predator performed LW with  $\mu = 2$  (or BW in Text S1). For simplicity, I assumed that if the searcher encountered a predator, the searcher died from predation.

Second, if the death effect arising from encounters with predators was considered, search time became an important factor because the length of rest during searches was associated with fitness. Thus, each searcher had a maximum searching time,  $T_{\max}$ , that could be cut off by an encounter with a predator.

Finally, when calculating fitness (i.e., lifetime reproductive success), I incorporated the life-cycle type of the searcher. In the simplest case, finding a target directly led to increased fitness in a linear fashion (life-cycle type I). For example, when a female parasitoid wasp finds and attacks a host, and then searches for another target, I presume that its fitness increases linearly. Furthermore, when a male finds a female and mates, its fitness as a searcher also increases linearly. In contrast, animals characterized by life-cycle type II would need to survive until their reproductive stage to obtain higher fitness. In life-cycle

type II, individuals that die from predation prior to maturity have no offspring and have a fitness of zero.

## General relationship between fitness and the rate of encounter with targets and predators

Here, I show the general relationship between fitness and the rate of encounter with targets and predators as well as the robustness of  $T_{\max}$  to my results. I denote the encounter rate with a predator per unit time  $\Delta T$  as  $\gamma$ . The probability of an encounter with the predator at the  $m$ -th time unit is expressed as

$$(1-\gamma)^{m-1}\gamma. \quad (2.1)$$

Therefore, when  $T_{\max}$  is divided into  $n$  (i.e.,  $T_{\max} = \Delta T n$ ), the mean search time  $\bar{T}$  is

$$\bar{T} = \sum_{m=1}^n \{m(1-\gamma)^{m-1}\gamma\} + n(1-\gamma)^n = \frac{1-(1-\gamma)^n}{\gamma}, \quad (2.2)$$

where  $n(1-\gamma)^n$  indicates the case in which the searcher never encounters predators. When the mean number of encounters with predators for  $n$  is  $k$ ,  $n\gamma = k$  and  $(1-\gamma)^n \approx e^{-k}$  for  $\gamma \ll 1$  and a large  $n$ , thus

$$\bar{T} \approx \frac{n(1-e^{-k})}{k}. \quad (2.3)$$

### Life-cycle type I

Here, I assume that an encounter with a target increases the fitness of the searcher by  $\alpha$ . I denote the probability of the searcher encountering the target per unit time by  $\eta$ . The mean fitness of the searcher is

$$\phi = \alpha\eta\bar{T} \approx \frac{\alpha\eta n(1-e^{-k})}{k} \quad (2.4)$$

Hence, the relative fitness ratio of the Lévy walk to the Brownian walk is

$$\frac{\phi_{\text{LW}}}{\phi_{\text{BW}}} \approx \frac{\eta_{\text{LW}}k_{\text{BW}}(1-e^{-k_{\text{LW}}})}{\eta_{\text{BW}}k_{\text{LW}}(1-e^{-k_{\text{BW}}})}. \quad (2.5)$$

Thus, this value is independent of the maximum search time  $T_{\max}$ , and is determined by the balance between the mean number of encounters with predators at  $T_{\max}$  and the search efficiency for targets per unit time.

### Life-cycle type II

Next, I consider the case in which finding a target leads to a non-linear increase in fitness and stock targets until the reproductive stage (here  $T_{\max}$ ). Therefore, the expected fitness is  $n\alpha\eta(1-\gamma)^n \approx n\alpha\eta e^{-k}$  for a large  $n$ . The relative fitness ratio of the Lévy walk to the Brownian walk is

$$\frac{\phi_{\text{LW}}}{\phi_{\text{BW}}} \approx \frac{\eta_{\text{LW}} e^{-k_{\text{LW}}}}{\eta_{\text{BW}} e^{-k_{\text{BW}}}}. \quad (2.6)$$

Thus, this value is also independent of the maximum search time  $T_{\max}$ . Unlike type I, in life-cycle type II, an encounter with targets does not directly impact fitness.

### Simulation

I calculated the fitness of LW and BW strategies in the ecological context using computer simulations because the encounter rate cannot be derived analytically. Using the methods described previously (Viswanathan et al., 1999; Bartumeus et al., 2005; Benhamou, 2007), I simulated one searcher roaming in a 2-D environment in which some targets (e.g., food, hosts, mates) and predators were distributed. Although the species at higher trophic levels are lower in number in real ecosystems, I introduced only one searcher. This is because I focused on the fitness of a single searcher, and my main results must be robust if I introduce a number of searchers. The searcher had no prior information about the locations of both targets and predators, and wandered at a constant velocity  $v_s = 1$  (per unit time) in a 2-D continuous field with length  $L^2 = 500 \times 500$  in which the boundary condition is periodic (Bartumeus et al., 2005).

The LW was characterized by a distribution function  $P(l) \sim l^{-\mu}$  ( $1 < \mu \leq 3$ ). In my simulations, I derived step lengths from the following equation to obtain LW, generating a



uniform random number  $u$  ( $0 < u \leq 1$ ):

$$l = l_0 u^{(1-\mu)^{-1}}, \quad (2.7)$$

where the minimum step length  $l_0$  is 1 (Bartumeus et al., 2005). For the BW simulation, to obtain an exponentially decaying distribution of the move length, each successive step length was drawn from a Gaussian distribution, where the mean was the minimum step length  $l_0 = 1$  and the variance was equal to 1 (Bartumeus et al., 2005). In LW or BW, after walking in a straight-line motion until reaching a step length  $l$ , the searcher turns in the angle drawn from a uniform distribution  $[-\pi, \pi]$ .

I assumed that the dynamics of targets were destructive and that the distribution of targets was patchy. Non-destructive targets were not used because they were considered to be unrealistic (Benhamou, 2007; Reynolds, 2010). Alternatively, I used destructive patchy targets, and set the mean number as 20 since non-destructive targets corresponded to the limit of patchy destructive targets (Viswanathan et al., 1999). The center of each patch was random, and the radius of each patch was equal to 10. In my simulation, the centers of 50 patches were spotted randomly, and thus the total number of targets was 1000.  $R_t$  and  $R_s$  represented the radius of the targets and searcher, respectively, and  $R'_s$  and  $R'_p$  represented the radius of perception of the searcher and predators. If the distance between the searcher and a target was less than  $R_t + R'_s = 1$ , the searcher obtained the target, and the target disappeared. Then the step length of the searcher is truncated and recalculated, and the direction is drawn from a uniform distribution. After the searcher migrated a 500 path length, the depleted target regenerated to maintain the specified target density (Benhamou, 2007). Similarly, the searcher died if the distance between the searcher and a predator was less than  $R_s + R'_p = 1$ . The mean free path  $\lambda$ , which represents the mean distance or travel time between patches or targets, was expressed as  $L^2/2RN$  for the 2-D environment (Bartumeus et al., 2005). Hence, in my simulation,  $\lambda_{\text{patch}} = 2500$  and  $\lambda_{\text{target}} = 125$  for detection distance  $R=1$ . This is equivalent to the low-resource scenario of previous studies (e.g., Bartumeus and Levin, 2008). The maximum search time  $T_{\text{max}}$  was  $10^4$ . To

converge the results, the total time for a single parameter set (i.e., searcher's movement pattern and density of predators) was  $10^7$  for sit-and-wait, slow, or middle predator conditions, and  $5 \times 10^7$  for fast conditions. Then,  $k, \eta, \gamma$  were calculated, and the relative fitness was obtained using equations (2.5) and (2.6).

## Results

The results of the relative fitness ( $\phi_{LW} / \phi_{BW}$ ) calculation for life-cycle type I are presented in Figure 2-1. When predators were absent ( $N_p = 0$ ), the relative fitness  $\phi_{LW} / \phi_{BW}$  was  $>2$ . Thus, LW with intermediate-level  $\mu$  had the highest fitness, which was consistent with the findings of previous studies (Viswanathan et al., 1999; Bartumeus et al., 2005). However, as the number of predators increased, the  $\phi_{LW} / \phi_{BW}$  ratio gradually declined to  $\sim 1$  or slightly less than 1 when the predator strategy was sit-and-wait or slow LW (Figure 2-1A, B). When the predator strategy was middle or fast LW,  $\phi_{LW} / \phi_{BW}$  was maintained at a high value, and LW could be an efficient strategy (Figure 2-1C, D).

Likewise, in the case of a searcher with life-cycle type II, the relative fitness  $\phi_{LW} / \phi_{BW}$  decreased substantially as the number of predators increased when the predator strategy was sit-and-wait or slow LW (Figure 2-2A, B). Even when the strategy of predators was middle LW,  $\phi_{LW} / \phi_{BW}$  decreased as the number of predators increased. These results were robust to other search strategies (i.e., correlated random walk or composite Brownian walk) (Figures 2-S1–S4) and to Brownian walk predators (Figure 2-S5). The relative fitness decreased because the searcher was likely to encounter a predator. The search time was shortened by death in a manner dependent on the search efficiency, and the relative mean searching time  $\bar{T}_{LW} / \bar{T}_{BW}$  depended on the search strategy (Figure 2-3). These results indicated that the LW strategy could lead to a high predator-encounter rate; therefore, BW could potentially be a risk-averting strategy.

To investigate these results, the relationship between the relative fitness and the encounter rate with targets and predators was examined (Figure 2-4). This result is not limited to my simulation results or to the relative fitness of LW or BW, but it describes a general trend. The relative encounter rates with targets and predators and the expected encounter number of BW for my simulation are presented in Figure 2-5. When the encounter rate with predators was low (i.e., low  $k_{BW}$ ), the fitness of random search strategies clearly depended on the encounter rate with targets (Figure 2-4A, D). Hence, LW had higher fitness in my simulation (Figure 2-5A). On the other hand, for intermediate or high  $k_{BW}$ , fitness also changed depending on the encounter rate with predators (Figure 2-4B, C, E, F). Furthermore, fast predators displayed the same high predator encounter rates of high  $k_{BW}$  and  $\gamma_{LW}/\gamma_{BW} \approx 1$  (Figure 2-5B, C). Thus, LW had higher fitness under the fast-predator conditions for life-cycle type I and almost equal fitness for life-cycle type II. Similarly, the fitness of other random search strategies was determined by the encounter rate with targets and predators. The degree of encounter rate improvement not only depends on the search strategy, but also on the distribution or density of the targets (Viswanathan et al., 1999; Bartumeus et al., 2005), suggesting that the conditions for the optimal search strategy are complex.

I assumed that the death rate caused by predators was equal to 1. Unlike searches for food or prey, animals do not search for other predators in a given location after an encounter with a predator, but instead depart from sit-and-wait predators or hide from moving predators. Therefore, even if the death rate was  $<1$ , the lower density of predators at death rate =1 could correspond to the same situation. In addition, although I did not consider the distribution of predators, my results did not qualitatively change depending on the distribution at a death rate =1. These findings arose from the asymmetrical property of the encounter rate with benefit and cost factors.

## Discussion

### **Predators alter optimal searching strategy**

My results revealed that the random search strategy affected the death rate arising from predation, and that trade-offs could occur between foraging efficiency and predation risk. In nature, animal species have different ecological traits or interactions associated with their foraging behavior (MacArthur and Pianka, 1966; Charnov, 1976; Lima et al., 1985). Considering such ecological factors, optimal foraging theory, as it currently exists, successfully predicts various types of animal behaviors from the viewpoint of maximizing fitness through natural selection (MacArthur and Pianka, 1966; Charnov, 1976). However previous studies of random search movements have only focused on foraging (i.e., search efficiency for targets), which may be unrealistic when considering the diversity of ecological characteristics and biotic interactions in nature. Lima et al. (1985) reported that animals performed more efficient strategies in response to ecological factors, including risks, with such trade-offs. My simulations predicted that where predators were abundant, a searcher performing a LW might have lower fitness depending on its ecological characteristics and those of the predators. This suggests that the optimal search strategy may change. Therefore, the parameter range in which the LW is advantageous may be narrower than previously estimated (Figure 2-4). The mechanism explaining these dynamics was that LWs not only increased the encounter rate of targets, but also of predators, which shortened the lifespan in exchange for the capture of more targets. The rare ballistic movements of LWs led to the high encounter rate with predators (Figure 2-5C), and this effect has been reported as a high encounter rate of randomly distributed destructive targets (Bartumeus et al., 2005). In the presence of predators, a searcher was confronted with conditions similar to the destructive search problem, because encounters with predators resulted in the death of the searcher. Although I suppose the ecological context in this chapter, such searching-avoiding trade-offs in the random search problem that I revealed here may occur in other contexts such as protein-DNA interactions (van den Broek et al., 2008; Bénichou et al., 2011).

## **Relation to empirical studies**

Many empirical studies have reported that the movement patterns of animals, from insects to human beings, are expressed as LWs with  $\mu \approx 2$  (Viswanathan et al., 2011). However, the power-law exponents fitted to movement patterns sometimes ranged from 2 to 3 (Viswanathan et al., 2011), suggesting that movement patterns may be diverse. Additionally, the data best fitted to the exponential decay distribution (i.e., BWs) has also been reported (Edwards et al., 2007; Humphries et al., 2010; Petrovskii et al., 2011; Humphries et al., 2012; Hays et al., 2012; de Jager et al., 2014). In theoretical studies, the first attempt reported that LWs with  $\mu \approx 2$  were optimal for targets that can be revisited (i.e., non-destructive) or those that are extremely patchy (Viswanathan et al., 1999). Moreover, LWs with  $\mu \rightarrow 1$  (i.e., straight movement) were the optimum for randomly distributed destructive targets. After the study, the results of several versions of simulations suggested that LWs with  $1 < \mu \leq 2$  are more efficient depending on the prey distribution and other factors (Raposo et al., 2003; Santos et al., 2004; Reynolds and Bartumeus, 2009). For the power-law exponent  $\mu > 3$  (i.e., BW), it has been theoretically reported that the foraging efficiency is similar to LW under high-resource conditions (Bartumeus et al., 2002). My results suggests that under high predation risk, animals with power-law exponents close to three have higher fitness than  $\mu \approx 2$  or  $\mu < 2$  (Figures 2-1, 2), and those under intermediate predation risk, LW with  $2 < \mu < 3$  also benefit. Therefore, it can be an alternative explanation for the diversity of power-law exponents.

## **Mechanisms for Brownian movement**

There is a question of whether Brownian movements in animals are spontaneous patterns for adaptation or a reflection of interactions with targets or complex environments (de Jager et al., 2014). de Jager et al. experimentally explained Brownian movement patterns of mussels by truncations resulted from encounters with conspecific individuals, which is the original mechanism of Einstein's collision-induced BWs (Einstein, 1905; de Jager et al.,

2014). In contrast, my findings suggested that spontaneous BWs were beneficial, and this conclusion is supported by the fact that the pattern can spontaneously change depending on internal physiological states (Martin et al., 2001; Sorribes et al., 2011). Of course, my hypothesis does not contradict the claim of de Jager et al., because the spontaneous LW pattern has higher efficiency in the absence of risk.

### **Changing search strategy**

Furthermore, my results suggest that animals can change their search strategy according to their developmental stage or in response to predator cues. For example, a juvenile individual under high predation pressure might adopt the BW strategy to avoid predator encounters, but an adult might adopt the LW strategy to obtain more targets in the absence of predators or under low predation pressure. In smaller scale responses, when an individual receives a chemical cue (kairomone) that indicates the presence of a predator, switching the internal pattern from LW to BW may represent an adaptive searching strategy, because the stochastic or random pattern can arise from internal processes (Cole, 1995; Maye et al., 2007; Sorribes et al., 2011; Proekt et al., 2012). Although such switching strategies depending on the target distribution have been investigated (Bartumeus et al., 2003; Humphries et al., 2010; Humphries et al., 2012; Hays et al., 2012; Sims et al., 2012), the response to predators is less understood (Lenz et al., 2012) and may be a topic for further study.

### **Estimation of animal movements**

Tracking animal movements over a prolonged period of time (biologging) is a method developed within the last decade that can lead to the understanding of dynamic phenomena ranging from the individual level to population and community levels (Rutz and Hays, 2009; Dell et al., 2014). Because the differences in searching strategies influence diffusiveness and movement patterns of animals, it is crucial to identify the search strategy that animals adopt in a natural environment. The tracking of animal movements within the framework of movement ecology requires information on biotic interactions and

interactions between individual animals (Nathan et al., 2008; Getz and Salts, 2008; Wittemyer et al., 2008); therefore, the context in my model should be common to various animal species in nature, because most animals are exposed to predation pressures or to the risk of death during searching. Likewise, predators may be exposed to the risks of higher-order predators. For further investigation, it will be interesting to explore the complex dynamics via the interactions between movement and population dynamics. Thus, considering that ecological factors can lead to an understanding of the dynamics at various scales.

## Supporting Information

### Analysis of other search strategies under predation risk

I analyzed the fitness of a searcher performing the alternative search strategy correlated random walk (CRW) and composite Brownian walk (CBW) proposed by previous studies (Bartumeus et al., 2005; Benhamou, 2007). CRW is positively correlated with previous direction when the direction changes, and I selected the directional change from a wrapped Cauchy distribution with shape parameter  $\rho$  (Haefner and Crist, 1994; Zollner and Lima, 1999; Bartumeus et al., 2005). For  $\rho = 0$ , CRW corresponds to BW, and CRW becomes a straight-line movement as  $\rho$  approaches 1. The directional change  $\Delta\theta$  is drawn from the following equation

$$\Delta\theta = 2 \arctan \left[ \left( \frac{1-\rho}{1+\rho} \right) \tan \left[ \pi \left( u - \frac{1}{2} \right) \right] \right] \quad (2.S1)$$

where  $u$  is a uniform random variable from 0 to 1. Each step length between two successive directional changes is drawn from a normal distribution where the mean value is the minimum step length 1 and the variance is 1.

The CBW is composed of BW and straight motion. CBW performs a straight motion until it encounters a target, at which point it changes to BW. Then, CBW returns to straight motion after moving a certain distance (i.e., giving-up length). Therefore, CBW exploits targets within a patch and then explores a new patch. Benhamou (2007) reported that the step length distribution of CBW was similar to that of LW as a result of interaction with the environment (i.e., targets) and that CBW had high search efficiency.

The other parameters and assumptions for calculating relative fitness of CRW and CBW, namely  $\phi_{\text{CRW}}/\phi_{\text{BW}}$  and  $\phi_{\text{CBW}}/\phi_{\text{BW}}$ , are the same as those of the LW simulation in the Main Text. The results are presented in Figures 2-S1–S4. As was the case for LW, BW outperformed the CRW and CBW when predators were abundant.

### LW searcher vs. BW predators



If BW has higher fitness than LW under predation risk, a predator for a searcher should also perform the BW. Here, I analyzed the fitness of LW and BW under BW predators (Figure 2-S5). The simulation method is the same as that under LW predators. A LW searcher has lower fitness under some BW predators because fast or middle BW with lower dispersal ability plays a role similar to that of a slow LW predator. This indicates that if the numbers of a top predator in a food web increase, the presence of that top predator may affect the strategy of animals in the second and third levels from the top by a cascade effect.

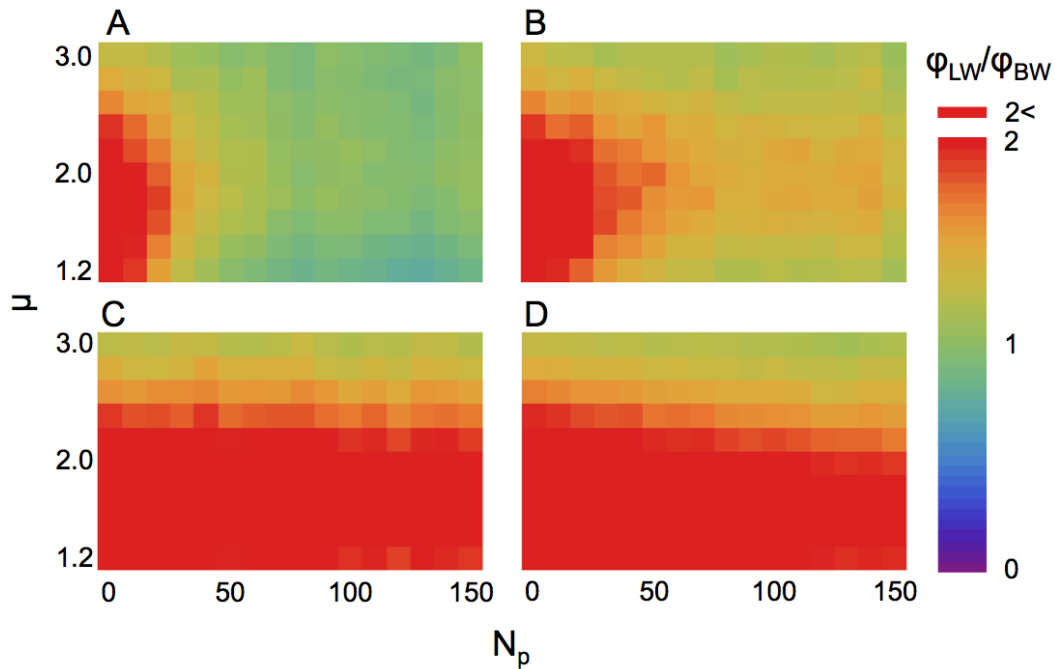


**Figure 2-1. The relative fitness of a Lévy searcher with life-cycle type I changes depending on the density and velocity of predators.**

The strategy of predators is (A) sit-and-wait ( $v_p = 0$ ); (B) slow Lévy walker ( $v_p / v_s = 0.2$ ); (C) middle Lévy walker ( $v_p / v_s = 1$ ); and (D) fast Lévy walker ( $v_p / v_s = 5$ ). The horizontal axis represents the number of predators introduced, and the vertical axis represents the Lévy index  $\mu$  of the searcher. The total search time is  $10^7$  for sit-and-wait, slow, and middle predator conditions and  $5 \times 10^7$  for fast predator conditions.

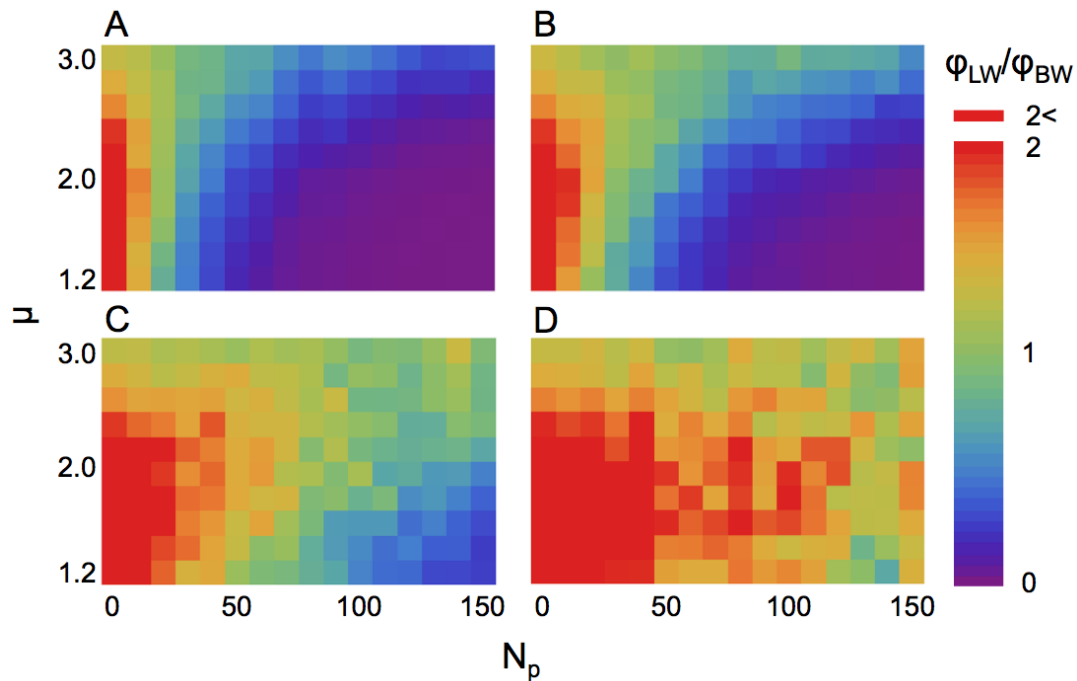


**Figure 2-2. The relative fitness of a Lévy searcher with life-cycle type II changes depending on the density and velocity of predators.**

The strategy of predators is (A) sit-and-wait ( $v_p = 0$ ); (B) slow Lévy walker ( $v_p / v_s = 0.2$ ); (C) middle Lévy walker ( $v_p / v_s = 1$ ); and (D) fast Lévy walker ( $v_p / v_s = 5$ ). The horizontal axis represents the number of predators introduced, and the vertical axis represents the Lévy index  $\mu$  of the searcher. The total search time is  $10^7$  for sit-and-wait, slow, and middle predator conditions and  $5 \times 10^7$  for fast predator conditions.

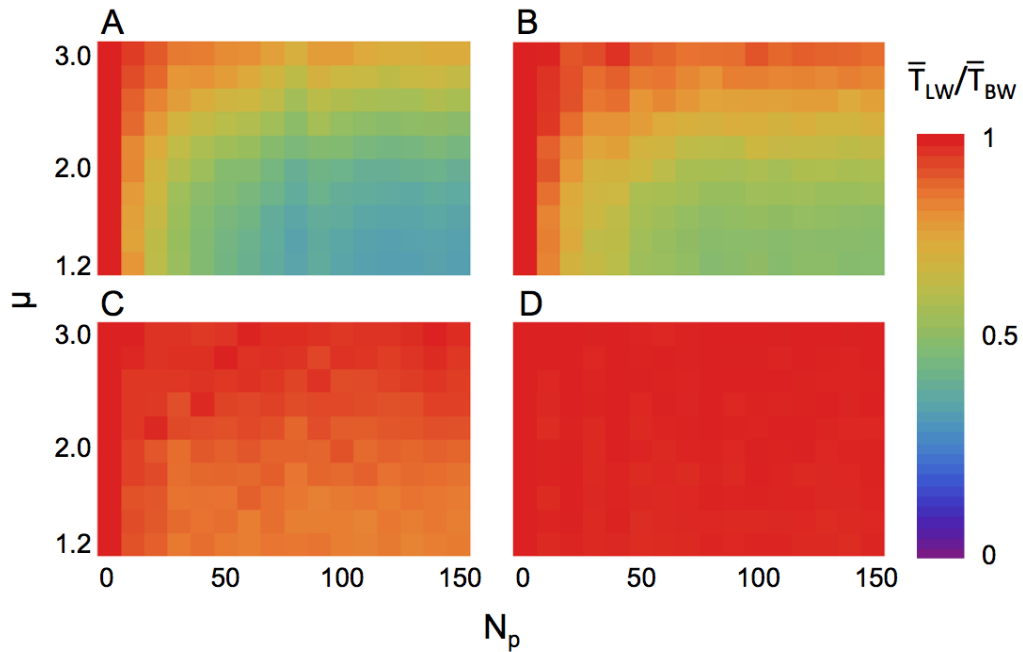


**Figure 2-3. The relative mean search time changes depending on the density and velocity of predators.**

The strategy of predators is (A) sit-and-wait; ( $v_p = 0$ ); (B) slow Lévy walker ( $v_p / v_s = 0.2$ ); (C) middle Lévy walker ( $v_p / v_s = 1$ ); and (D) fast Lévy walker ( $v_p / v_s = 5$ ). The horizontal axis represents the number of predators introduced, and the vertical axis represents the Lévy index  $\mu$  of the searcher. The total search time is  $10^7$  for sit-and-wait, slow, and middle predator conditions and  $5 \times 10^7$  for fast predator conditions.

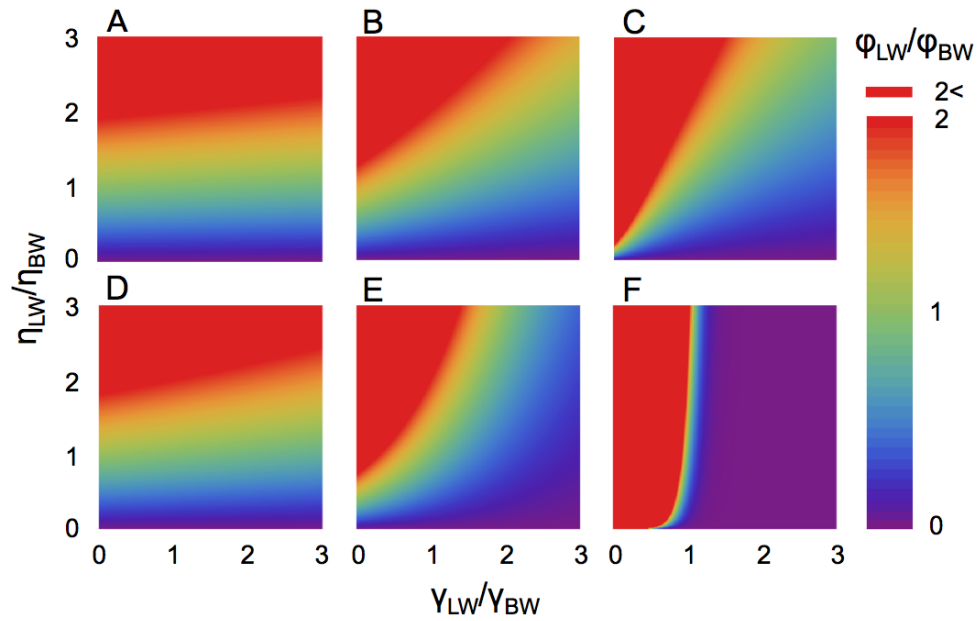


**Figure 2-4. The relationship between relative encounter rates of targets and predators.** Data in (A–C) and (D–F) correspond to life-cycle types I and II, respectively. (A and D) The lower encounter rate condition,  $k_{BW} = 0.1$  (e.g., lower predator density or slower predators). (B and E) The middle encounter rate condition,  $k_{BW} = 1$ . (C and F) The higher encounter rate condition,  $k_{BW} = 10$  (e.g., higher predator density or faster predators).

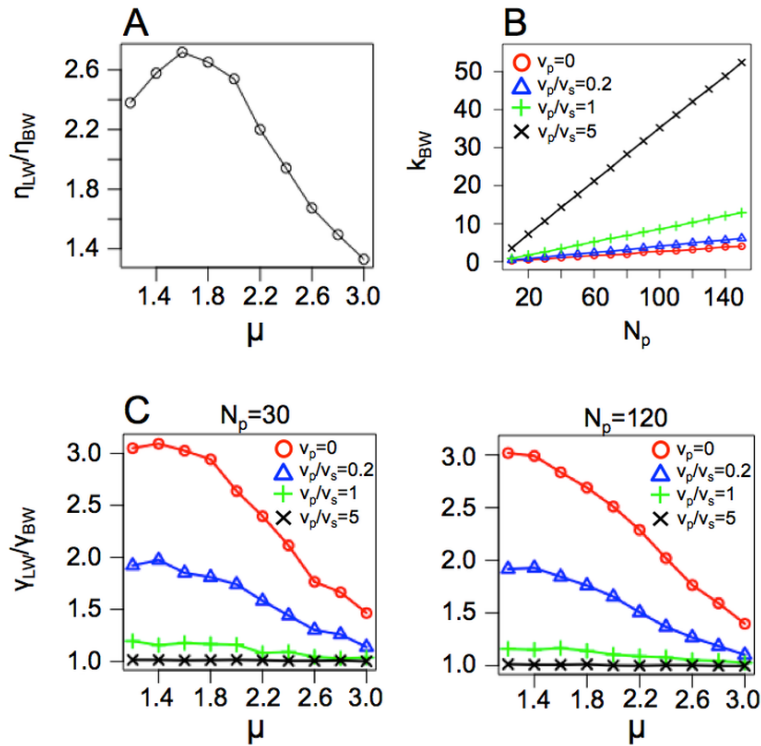


**Figure 2-5. Encounter rates with targets and predators in my simulation setting.**

(A) The relative encounter rate to targets increases at an intermediate  $\mu$ . (B) The mean encounter number of a BW searcher ( $k_{BW}$ ) for  $T_{max}$ . As the number or velocity of predators increases, the encounter number increases. (C) The relative encounter rate with predators increases when the movement of a searcher approaches a straight line (i.e., smaller  $\mu$ ). However, the faster the movement of predators, the lower the rate of increase. Similar results for  $N_p = 30$  (left) and  $N_p = 120$  (right) indicate that the relative encounter rate does not change at low predator densities (e.g.,  $N_p \approx 10^2$ ) in my simulation.

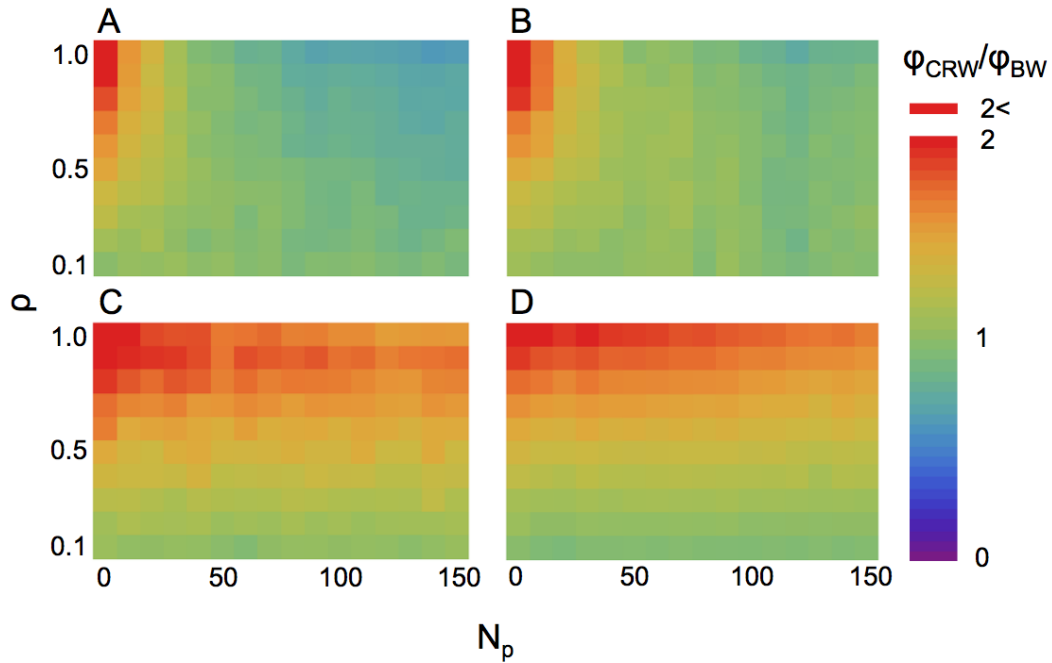


**Figure 2-S1. The relative fitness of a CRW searcher with life-cycle type I changes depending on the density and velocity of predators.**

The strategy of predators is (A) sit-and-wait ( $v_p = 0$ ); (B) slow Lévy walker ( $v_p / v_s = 0.2$ ); (C) middle Lévy walker ( $v_p / v_s = 1$ ); and (D) fast Lévy walker ( $v_p / v_s = 5$ ). The horizontal axis represents the number of predators introduced, and the vertical axis represents the shape parameter  $\rho$  of the searcher. The total search time is  $10^7$  for sit-and-wait, slow, and middle predator conditions and  $5 \times 10^7$  for fast predator conditions.

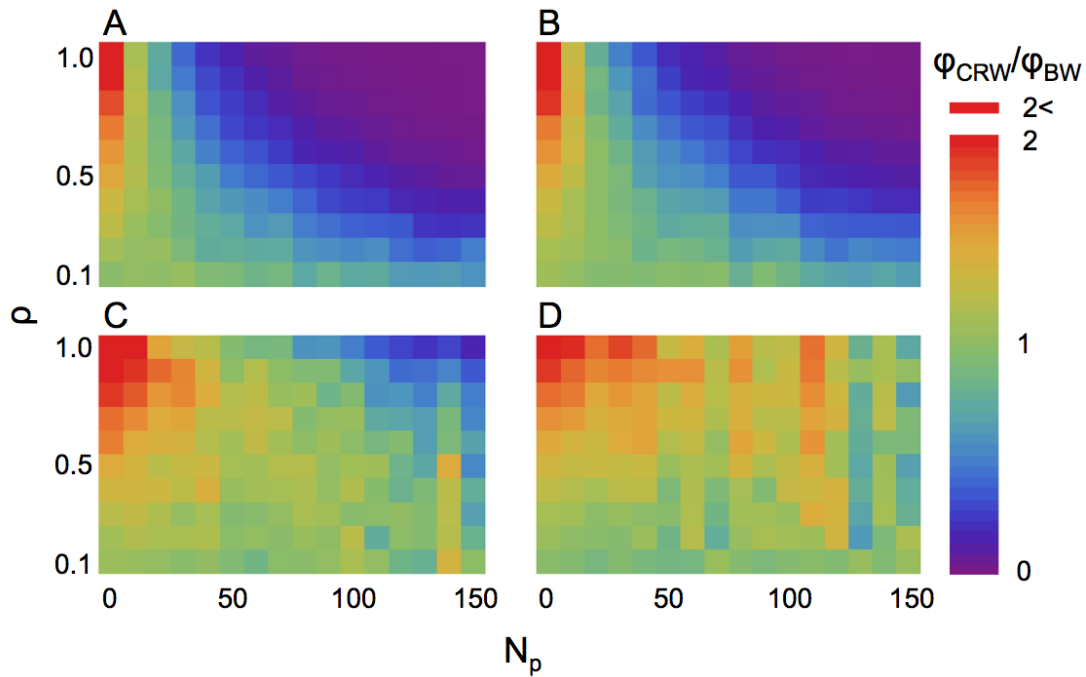


**Figure 2-S2. The relative fitness of a CRW searcher with life-cycle type II changes depending on the density and velocity of predators.**

The strategy of predators is (A) sit-and-wait ( $v_p = 0$ ); (B) slow Lévy walker ( $v_p / v_s = 0.2$ ); (C) middle Lévy walker ( $v_p / v_s = 1$ ); and (D) fast Lévy walker ( $v_p / v_s = 5$ ). The horizontal axis represents the number of predators introduced, and the vertical axis represents the shape parameter  $\rho$  of the searcher. The total search time is  $10^7$  for sit-and-wait, slow, and middle predator conditions and  $5 \times 10^7$  for fast predator conditions.



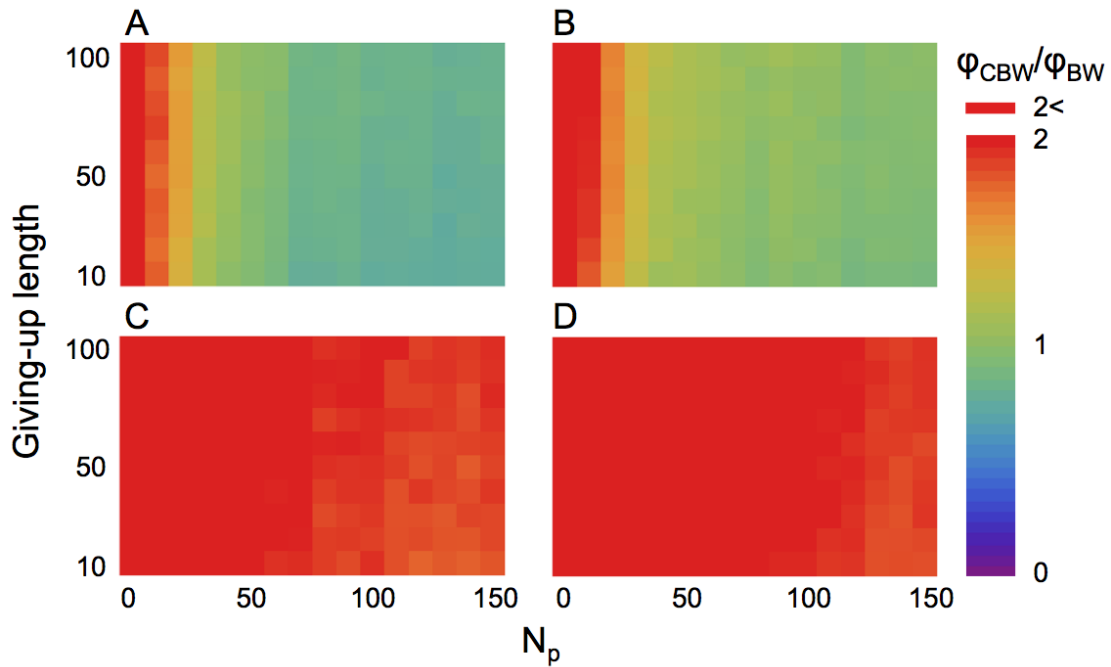


**Figure 2-S3. The relative fitness of a CBW searcher with life-cycle type I changes depending on the density and velocity of predators.**

The strategy of predators is (A) sit-and-wait ( $v_p = 0$ ); (B) slow Lévy walker ( $v_p / v_s = 0.2$ ); (C) middle Lévy walker ( $v_p / v_s = 1$ ); and (D) fast Lévy walker ( $v_p / v_s = 5$ ). The horizontal axis represents the number of predators introduced, and the vertical axis represents the giving-up length of the searcher. The total search time is  $10^7$  for sit-and-wait, slow, and middle predator conditions and  $5 \times 10^7$  for fast predator conditions.

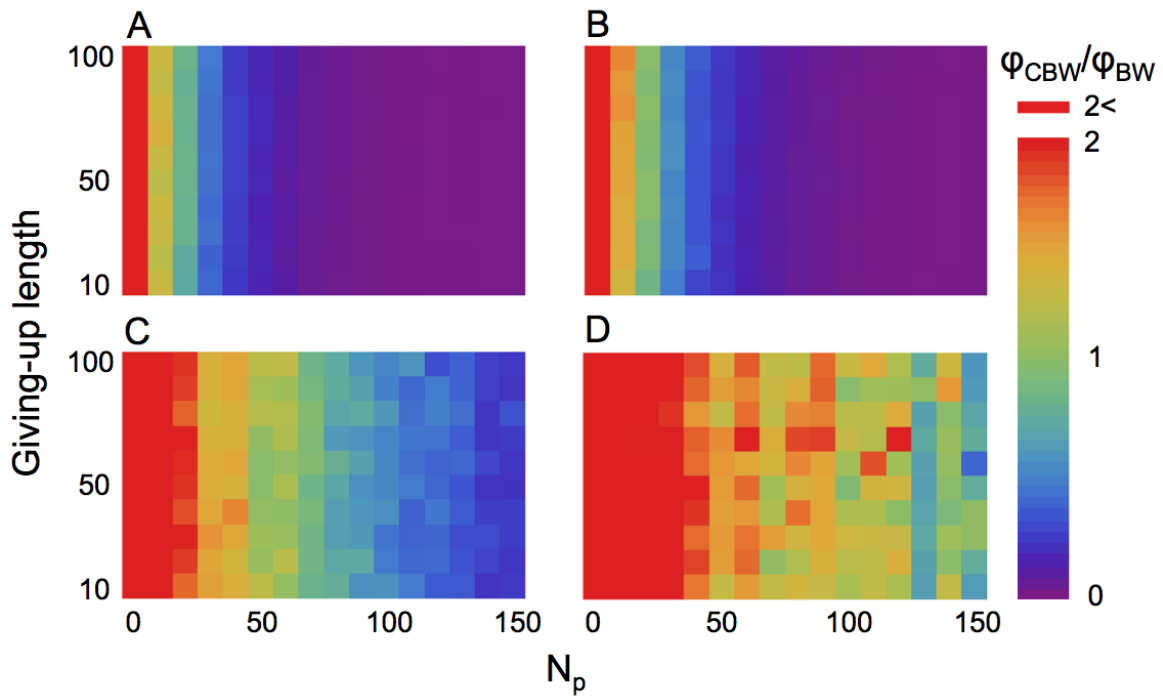


**Figure 2-S4. The relative fitness of a CBW searcher with life-cycle type II changes depending on the density and velocity of predators.**

The strategy of predators is (A) sit-and-wait ( $v_p = 0$ ); (B) slow Lévy walker ( $v_p / v_s = 0.2$ ); (C) middle Lévy walker ( $v_p / v_s = 1$ ); and (D) fast Lévy walker ( $v_p / v_s = 5$ ). The horizontal axis represents the number of predators introduced, and the vertical axis represents the giving-up length of the searcher. The total search time is  $10^7$  for sit-and-wait, slow, and middle predator conditions and  $5 \times 10^7$  for fast predator conditions.

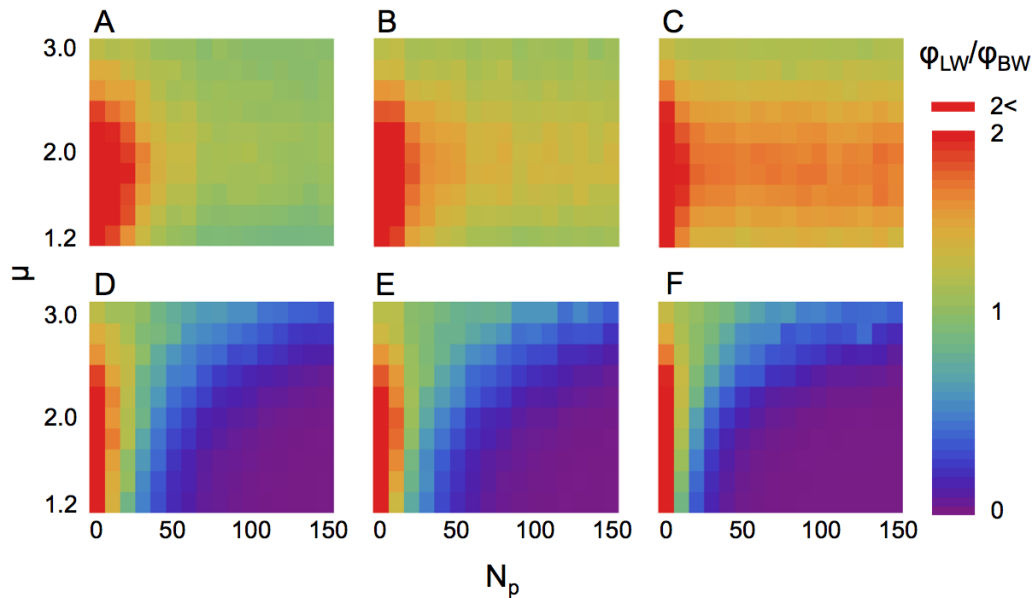


**Figure 2-S5. The relative fitness of a LW searcher with life-cycle type I (A–C) and life-cycle type II (D–F) in the presence of BW predators changes depending on the density of predators.**

The strategy of predators is (A, D) slow Brownian walker ( $v_p / v_s = 0.2$ ); (B, E) middle Brownian walker ( $v_p / v_s = 1$ ); and (C, F) fast Brownian walker ( $v_p / v_s = 5$ ). The horizontal axis represents the number of predators introduced, and the vertical axis represents the giving-up length of the searcher. The total searching time is  $10^7$  for sit-and-wait, slow, and middle predator conditions and  $5 \times 10^7$  for fast predator conditions.

# Chapter 3

## Theoretical analysis and experiment of random avoidance behavior

### Introduction

Animal behavior often appears to be random and unpredictable to an observer or experimenter. Even if experimental apparatuses for studying animal behavior or external stimulus are identical, variability or randomness in behavior can be often observed (Maye et al., 2007; Domenici et al., 2008; Proekt, 2011). The mechanistic explanation for variability is that the brain is an input/output system which is capable of initiating spontaneous actions (Maye et al., 2007; Brembs, 2011; Proekt et al., 2011; Sorribes et al., 2011; Wearmouth et al., 2014). Hence, it is important to understand the evolutionary significance of the variation in animal behavior. Some hypotheses have proposed that such variability is an adaptive trait (Maye et al., 2007; Brembs, 2011). One of the most important hypotheses states that variability may improve the efficiency of the prey-predator interactions (Humphries, 1970; Brembs, 2011). If the prey moves in the same manner each time, the predator can easily predict the movement of the prey. Most organisms are exposed to predation risk, and they need to exhibit a movement that predator cannot predict easily. Therefore, the optimal avoidance strategy, which is familiar in behavioral ecology, should be explained based on its costs and benefits (Krebs and Davies, 1978). The highly variable behavior of a prey that prevents a predator from predicting its position includes random movements. A previous study claims that randomness is important when the prey pauses and then runs away from the predator (Domenici et al., 2008).

Various types of avoiding behaviors from predators have been reported (known as “Protean behavior”) (Driver and Humphries, 1970). Recent study indicated that the variability in the direction of movement may be adaptive trait, a response to the predator that approaches the prey (Domenici et al., 2008). Animal escapology, focusing on how

animals escape from a threatening stimulus on a short time scale, has been proposed (reviewed in Domenici et al., 2011a, b). Another important situation in an ecosystem is the predator's attack on the moving prey; for example, a bird's attack on an insect moving on the ground.

As mentioned in Chapter 2, since the late 1990s, the trajectory of animal movement has been modeled as a special class of random walk called Lévy walk (LW), which has been studied as a search behavior in the field of behavioral ecology (Viswanathan et al., 1999, 2011; Bartumeus et al., 2005; Sims et al., 2008; Humphries et al., 2010). The power-law distribution, which explains the step length of LW, has been shown to be relevant in several other situations, such as in the bursty dynamics of human decision-making (Barabasi, 2005) and in spontaneous activity (Maye et al., 2007; Proekt et al., 2012; Wearmouth et al., 2014). Therefore, the power law is universal in behaviors, including movements. However, the adaptive aspects of the power-law behavior characteristics are less understood, except in the adaptive search behavior.

Clearly, a prey's movement is crucial in prey-predator interactions because the prey that keeps pausing at a position becomes an easy target for the predator. It is considered that there are two cases of prey-predator interactions in which prey moves. The first case includes a situation in which the predator pursues the prey after the prey-predator encounter and catches it (Nahin, 2007). In this case, both the predator's and prey's movements are important for successful capture of the prey. The second situation is simpler, in which the predator predicts the future position of the moving prey and tries to catch it. To model the second situation, I considered an individual that avoids a predator that can observe an open arena (Figure 3-1A) and investigate what class of random walk is efficient. The predator predicts the trajectory of the prey to attack it. In the movements, the most unpredictable strategy may be Brownian walk (BW) due to frequent changes in direction, whereas straight walk (SW) is the most easy to predict. However, the straight-like movements have high diffusivity, which leads to short-time exposure to predation. LW is an intermediate strategy between BW and SW. I focus on the trade-off between the unpredictability and the time of exposure to predation risk to analyze the adaptive

avoidance behavior.

Although unpredictability of the movement in the prey-predator interaction is crucial, little is known about the optimal strategy used in this interaction. Here, I address the following questions: (1) What strategy is efficient in avoidance? (2) Why is that particular strategy efficient? To answer these questions, I constructed a framework of predator avoidance behavior based on the random-walk paradigm and analyzed the theoretical model to describe the efficiency of avoidance. To examine the adaptive avoidance behavior, I conducted an experiment in which a human subject attacks the virtual prey on a computer screen.

## Methods

### Models

I considered one prey individual, set at the center of the 2-D circular field with radius  $R$ , and one predator that can observe the entire field. Then, the prey starts to move and performs one type of random walk (LW or BW) at a constant velocity. I assumed that the predator perceives the present and past positions of the prey and has to predict the future position (after time step  $\tau$ ) to attack the prey, while the prey cannot obtain any information about the predator. Once the prey reaches the safety area, the individual is regarded as having survived (i.e., the absorbing boundary condition).

I denoted the actual position of the prey at time  $t$  as  $P_t(x_t, y_t)$  and the predicted position by the predator as  $\hat{P}_{t+\tau}(\hat{x}_{t+\tau}, \hat{y}_{t+\tau})$ . Because I considered a class of random walk that does not change the probability distribution of step length and direction depending on position, I simplified the prediction rule and used the following equation, which represents the prediction by a straight line:

$$\begin{pmatrix} \hat{x}_{t+\tau} \\ \hat{y}_{t+\tau} \end{pmatrix} = \frac{\tau}{\sqrt{(x_t - x_{t-1})^2 + (y_t - y_{t-1})^2}} \begin{pmatrix} x_t - x_{t-1} \\ y_t - y_{t-1} \end{pmatrix} + \begin{pmatrix} x_t \\ y_t \end{pmatrix} \quad (3.1)$$

where  $(x_{t-1}, y_{t-1})$  is the past position of the prey that defines the direction of the movement

(Figure 3-1B). When the distance between the predicted position  $\hat{P}_{t+\tau}(\hat{x}_{t+\tau}, \hat{y}_{t+\tau})$  and the actual position  $P_{t+\tau}(x_{t+\tau}, y_{t+\tau})$  is less than the attacking radius  $r$ , the predator can capture the prey.

If the movement of the prey is close to SW the amount of time for reaching the safety area decreases, but the predator can easily predict the prey's future position. Conversely, if the prey often reorients, the amount of time for reaching the safety area increases, but the predator often fails to predict the prey's position. Thus, there is a trade-off in the framework. The survival rate  $\phi$  of a prey is denoted by

$$\phi = (1 - Q)^{T/s} \quad (3.2)$$

Where  $Q$  is the predictability of movements of the prey by the predators,  $T$  is the average time to reach the safety area, and  $s$  is the mean attack waiting time of the predator.  $s$  represents the time from the previous attack to the next attack and reflects the characteristic of the predator, but it does not change the shape of the function  $\phi$  qualitatively. Thus, the parameters  $Q$  and  $T$  depend only on the strategy of the prey. To simplify the random avoidance behavior, I assume that reorientation angle is derived from uniform distribution ( $-\pi \leq \theta \leq \pi$ ) and adopted truncated LW, because by changing one parameter  $\mu$  the random behavior varies from Brownian-like motion ( $\mu = 3$ ) to straight-like motion ( $\mu \rightarrow 1$ ) (Viswanathan et al., 1999) and BW with scaling parameter  $\lambda$ . The step length of BW follows the distribution  $P(l) \sim \lambda \exp(-\lambda l)$ . When  $\lambda$  is small, the movement is close to a straight motion while keeping the characteristic of BW. The difference between these two models is whether the distribution of each step length between reorientation is scale-free or not. Furthermore, I set  $l_{\min}$  and  $l_{\max}$  as the lower and upper cutoff values of the step length derived from the distribution in order to make step lengths realistic. These cutoff values were used when fitting the probability distribution by applying rigorous statistical methods (Humphries et al., 2012; Wearmouth et al., 2014). Thus,  $Q$  and  $T$  is the function of  $\mu$  or  $\lambda$ , but the explicit expression is limited ( $Q$  for  $r \rightarrow 1$ , see Supporting information). The prediction by a predator is defined to be forecasting the position of the prey  $\tau$  seconds after observing the position (Figure 3-1B). For example, when the prey

performs a perfect straight motion, then the prediction probability  $Q$  is 1 for any  $\tau$ . In contrast, for the movement with randomness, the prediction probability  $Q$  depends on  $\tau$  and attacking radius  $r$ . Under these assumptions, I explored the strategy to maximize the survival rate using simulations.

## Experiments

To elucidate the success rate of the random avoidance behavior for the actual predator, I generated one virtual prey that performed random walk on a computer screen and could be attacked using a mouse click by a human subject (student). The subject can perceive the virtual prey, observe the circular field, and attack (i.e., click) wherever he or she wants in the field. Initially, the virtual prey stands in the center of the circular field. Then, the prey performs random walk and is exposed to attacks by the subject. If the distance between the click position and prey's position is within the attacking radius  $r$ , the attack is regarded as success. Otherwise, the attack is treated as a failure. The subject could not attack the prey 0.5 s from the start and after a failed click. This rule prevents the subject from instantly clicking. When the virtual prey reached the circumference of the field, the prey was considered to have survived (i.e., reached the safety area). One trial ends with either successful attack by the subject or successful survival of the prey. The velocity  $v$  of the prey roughly corresponds to  $\tau$  in the theoretical model because there is a time difference between the moment the subject decides to attack and the moment it actually attacks (clicks). When the prey moves very slowly, the time between making the decision and clicking is short (i.e., small  $\tau$ ) and vice versa. I set LW ( $\mu = 1.4$ ) and BW ( $\lambda = 0.05$ ) as prey's avoiding strategy because theoretical analysis showed that these parameters increased the efficiency of each strategy. Ten people (students) over the age of 18 participated as subjects. Each subject conducted 20 trials  $\times$  three strategies (i.e., LW, BW, and SW). SW has a random initial direction at the starting point. I defined the survival rate of the prey's strategy as the success (i.e., survival) frequency of 20 trials. The experiments were performed using a computer (iMac, 27-inch, 2560  $\times$  1440, Apple Inc., Cupertino, CA, USA) using a library, OpenGL 2.0 (Khronos Group, Beaverton, OR, USA). To set the same



conditions as in the theoretical model, the radius of the field where the prey wanders and the attacking radius were 115 mm and 3.45 mm, respectively, and their ratio was  $r/R = 0.03$ . The velocity of the prey was set at 74 mm/s.

## Results

First, I calculated the prediction rate of the predator and the time to reach the safety area using computer simulations. Figure 3-2A and 3-2B show the relationships between the prediction rate and the avoiding strategy (i.e., exponent  $\mu$  or  $\lambda$ ) and the time to reach the safety area and the avoiding strategy, respectively. Each value is an average of 10,000 trials. As the exponent  $\mu$  or  $\lambda$  increases, the prediction rate decreases, indicating that the movement strategy with large  $\mu$  or  $\lambda$  is difficult to predict. This is because LW or BW with large  $\mu$  or  $\lambda$  has frequent reorientations. However, the time to reach the safety area increases with increasing the exponents, suggesting that there is a trade-off between the unpredictability and the time of exposure to predation risk.

Next, I observed the survival rate for each strategy using simulations, and the results of the survival rate for  $r/R = 0.03$  are shown in Figure 3-3 (results for  $r \rightarrow 0$  are presented in Figure 3-S1). For a small prediction time  $\tau$ , LW strategy has higher survival rate at intermediate  $\mu$ , whereas BW strategy has a lower survival rate than LW. These results suggest that LW can be an efficient avoiding strategy in the prey-predator interaction. For a large  $\tau$ , LW with  $\mu = 3$  (i.e., BW-like strategy) has a higher survival rate than LW with  $\mu < 3$ , and BW is more efficient than LW ( $\mu = 3$ ), suggesting that for a large  $\tau$  the strategy with lower prediction rate is more efficient. These trends were observed for  $r \rightarrow 0$ , hence, they may be considered general trends.

Finally, I observed the survival rate of the virtual prey generated on the computer screen. The survival rate of the three distinct avoiding strategies (LW with  $\mu = 1.4$ , BW with  $\lambda = 0.05$ , and SW) was calculated from the average of 10 subjects and the results are shown in Figure 3-4. The survival rate of LW was significantly higher than that of BW and

SW, and the survival rate of SW was significantly higher than that of BW (ANOVA,  $df = 2$ ,  $F = 11.081$ ,  $p < 0.001$ , and paired Bonferroni's multiple comparison test, LW-SW:  $p < 0.001$ , LW-BW:  $p < 0.001$ , SW-BW:  $p < 0.05$ ). These results suggest that the LW strategy has the highest survival rate among the three strategies.

## Discussion

In this chapter, I investigated the random avoidance behavior both theoretically and experimentally in terms of prey-predator interactions. Simulations show that LW could outcompete BW in survival rate. The experiment using a virtual moving individual on a computer screen being hunted by a human subject suggests that the LW strategy has a higher survival rate. The reason for such higher survival rate of LW is that the intermediate movements between BW and SW can resolve the trade-off between the prediction rate and the time of exposure to the predator. Although I used humans as predators in the experiment, prediction of the movement in this experiment may not be specific to humans. Mammals, birds, and even insects can predict the future state from the present and past states (Mischiati et al., 2015). Therefore, the framework used here can be applied to various prey-predator interactions.

Recent long-term observations of animal movements have revealed that the trajectory often follows a LW pattern (Sims et al., 2008; Humphries et al., 2010; Viswanathan et al., 2011). From the evolutionary perspective, LW pattern has been considered to have a higher rate of target encounter (i.e., food, prey, mates) (Viswanathan et al., 1999, 2011; Humphries et al., 2010), and therefore the LW foraging hypothesis has been proposed (Viswanathan et al., 1999). However, foraging efficiency is not the only benefit of LW (de Jager et al., 2011). The variability or randomness and the characteristics of the spontaneous scale-free movement may not be essential for the foraging behavior because the combination of exploration of a patch by straight movement and exploitation of targets within the patch are also efficient (Benhamou, 2007). Therefore, understanding LW from the evolutionary perspective except search behavior is crucial. Based on the results of the present study, I propose the LW avoidance hypothesis.

The relationship between movement patterns of preys such as and decision making of the predator remains less understood. For predators, in most situations, the hunting strategy is not just a reflective response to their prey's movements. The predators, including vertebrates and invertebrates, can predict the future position of a prey by using internal models (Mischiati et al., 2015). The evolution of a neural circuit associated with such a prediction capability may be driven by the randomness of preys.

In my framework, the condition of the environment was limited (i.e., circle). Although the natural conditions are far more complex, a trade-off between the prediction rate and the time of exposure to the predation risk must exist. Further studies are needed to address how the heterogeneity of environment (Getz and Saltz, 2008; Raposo et al., 2011; Lenz et al., 2012) and the dependency of strategy on the environment affect the evolutionary consequence of movement patterns. Furthermore, understanding the situation that predator predicts the prey's movement and prey predicts the predator's movement is challenging. In this way, my results raise open question: how other factors can alter the optimal avoidance strategy.

## Supporting Information

### Generating Lévy walk and Brownian walk

LW is characterized by a distribution function  $P(l) \sim l^{-\mu}$  ( $1 < \mu \leq 3$ ). In my simulations, the step lengths were derived from the following equation to obtain LW, generating a uniform random number  $u$  from  $0 < u \leq 1$ :

$$l = l_{\min} u^{(1-\mu)^{-1}} \quad (3.S1)$$

where  $l_{\min}$  is the minimum step length (Bartumeus et al., 2005). Furthermore, to exclude the values that were more than  $l_{\max}$ , instead of using the value that was more than  $l_{\max}$ , I generated a new one.

The step length of BW follows the equation  $P(l) \sim \lambda \exp(-\lambda l)$ . Each step length was obtained from:

$$l = -\frac{1}{\lambda} \log(1-u) + l_{\min} \quad (3.S2)$$

where,  $u$  is a uniform random number from  $0 \leq u < 1$ .

### Analysis of the prediction rate for $r \rightarrow 0$

I show the case in which the attacking radius  $r$  is close to 0. The length of a straight line of LW,  $l$ , follows the equation:

$$P(l) \sim l^{-\mu} \quad (3.S3)$$

where,  $\mu$  ( $1 < \mu \leq 3$ ) is the scaling exponent. I denoted the minimum and maximum step lengths as  $l_{\min}$  and  $l_{\max}$  that serve as the lower and upper cutoff value of distribution, respectively. The probability density function  $l$  ( $l_{\min} \leq l \leq l_{\max}$ ) is

$$P_1(l) = \frac{P(l)}{\int_{l_{\min}}^{l_{\max}} P(x) dx}. \quad (3.S4)$$

When an animal performing LW is observed, the probability that the animal has selected  $l$  is

$$P_2(l) = \frac{lP_1(l)}{\int_{l_{\min}}^{l_{\max}} xP_1(x) dx}. \quad (3.S5)$$

Moreover, the probability that the rest length is longer than  $m$  is

$$\frac{l-m}{l}. \quad (3.S6)$$

Therefore, the probability that the predator can forecast the prey's position  $\tau$  seconds after observing the prey is

$$\begin{aligned} \int_{\tau}^{l_{\max}} \frac{l-\tau}{l} P_2(l) dl &= \int_{\tau}^{l_{\max}} \frac{(l-\tau)P_1(l)}{\int_{l_{\min}}^{l_{\max}} xP_1(x) dx} dl \\ &= \int_{\tau}^{l_{\max}} \frac{(l-\tau)l^{-\mu}}{\int_{l_{\min}}^{l_{\max}} x^{(-\mu+1)} dx} dl. \end{aligned} \quad (3.S7)$$

Finally, the explicit expression of prediction rate is

$$Q(\tau, \mu, l_{\min}, l_{\max}) = \frac{l_{\max}^{2-\mu} - \tau^{2-\mu}}{l_{\max}^{2-\mu} - l_{\min}^{2-\mu}} + \frac{\tau(2-\mu)(\tau^{1-\mu} - l_{\max}^{1-\mu})}{(1-\mu)(l_{\max}^{2-\mu} - l_{\min}^{2-\mu})} \quad (3.S8)$$

when  $\mu \neq 2$ .

For  $\mu = 2$ , I set  $h = 2 - \mu$ , then

$$\begin{aligned} \lim_{h \rightarrow 0} Q &= \lim_{h \rightarrow 0} \left( \frac{l_{\max}^h - \tau^h}{l_{\max}^h - l_{\min}^h} + \frac{\tau h (\tau^{h-1} - l_{\max}^{h-1})}{(h-1)(l_{\max}^h - l_{\min}^h)} \right) \\ &= \lim_{h \rightarrow 0} \frac{l_{\max}^h - \tau^h}{h} \frac{h}{l_{\max}^h - l_{\min}^h} + \lim_{h \rightarrow 0} \frac{\tau (\tau^{h-1} - l_{\max}^{h-1})}{(h-1)} \frac{h}{(l_{\max}^h - l_{\min}^h)} \\ &= \frac{\log l_{\max} - \log \tau}{\log l_{\max} - \log l_{\min}} + \frac{\tau - l_{\max}}{l_{\max}} \frac{1}{\log l_{\max} - \log l_{\min}} \end{aligned} \quad (3.S9)$$

is obtained.

Likewise, the prediction rate for BW, the step length of which follows  $P(l) = \lambda e^{-\lambda l}$  ( $\lambda > 0$ ), is

$$Q(\tau, \lambda, l_{\min}, l_{\max}) = \frac{(\lambda \tau - \lambda l_{\max} - 1)e^{-\lambda l_{\max}} + e^{-\lambda \tau}}{(\lambda l_{\min} + 1)e^{-\lambda l_{\min}} - (\lambda l_{\max} + 1)e^{-\lambda l_{\max}}}. \quad (3.S10)$$

The time to reach the safety area is calculated by using simulations. The survival probability is derived from the prediction rate and time. The results are shown in Figure 3-S1.

Figure 1

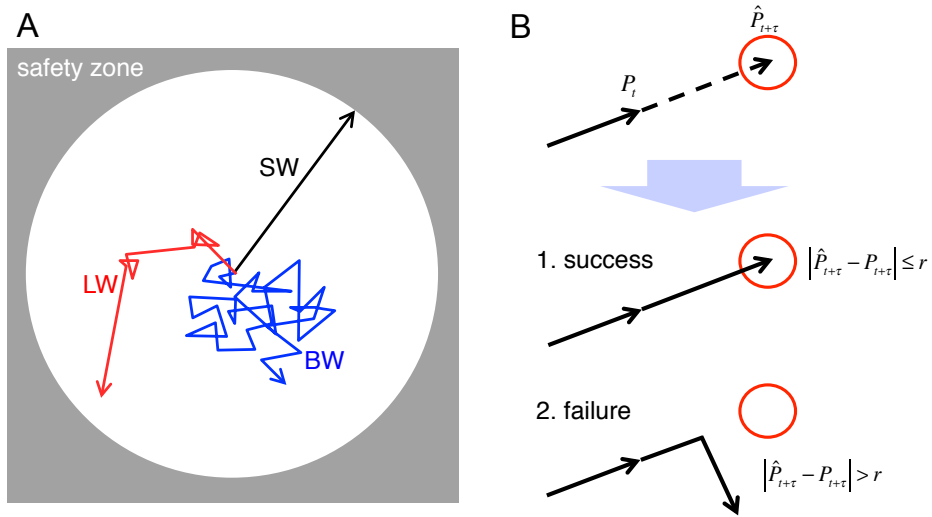


**Figure 3-1. Avoidance-capture framework.**

(A) A predator's view. One prey wanders in the white area. The gray area is a safety zone. The lines represent the example of movement path of prey's strategy (LW: Lévy walk, BW: Brownian walk, SW: straight walk). (B) The prediction by predator. At time  $t$  the predator predicts the future (time step  $\tau$  after) position of the prey. A red circle is a prediction circle (attacking) with radius  $r$  and the center is  $\hat{P}_{t+\tau}$ . If the prey moves within the circle after time step  $\tau$ , it is regarded that the predator succeeds in capturing the prey (success case). When the prey is outside the circle after time step  $\tau$ , the predator's attack is regarded as a failure (failure case).

Figure 2

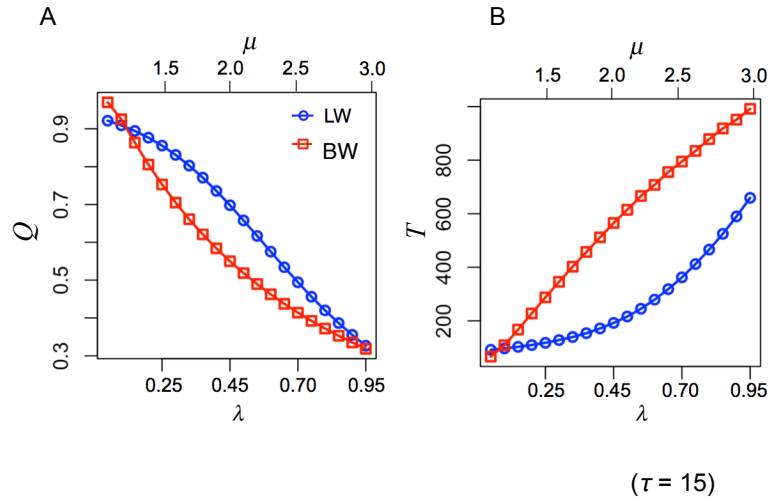


**Figure 3-2. The relation between predictability and time of exposure to predation risk.**

The horizontal axis is a prey's strategy parameter of LW ( $1 < \mu \leq 3$ ) or BW ( $\lambda > 0$ ). (A) The vertical axis is the predictability and (B) time of exposure to predation risk. The blue circle and red square represents LW and BW, respectively. The ratio  $r/R = 0.03$ . The cutoffs of step length  $l_{\min} = 1$  and  $l_{\max} = 100$ . The prediction time  $\tau = 15$ . The number of samples is 100,000.

Figure 3

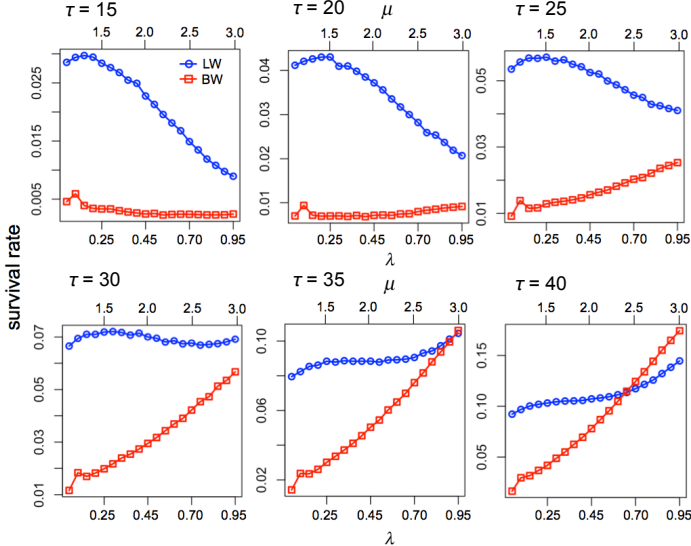


**Figure 3-3. The survival rate in simulation.**

The horizontal axis is a prey’s strategy parameter of LW ( $1 < \mu \leq 3$ ) or BW ( $\lambda > 0$ ) and the vertical axis is a survival rate of the prey. For the legends, see Fig. 3-2.



Figure 4

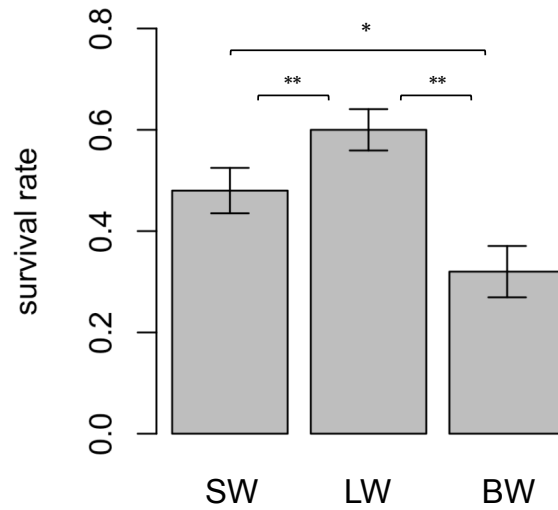


**Figure 3-4. The survival rate in human experiment.**

The vertical axis is the survival rate of the virtual prey on computer screen. The ratio  $r/R = 0.03$ . The cutoffs of step length  $l_{\min} = 1.15\text{mm}$  and  $l_{\max} = 115\text{mm}$ . The number of subjects is 10. \*  $p < 0.05$ . \*\* $p < 0.001$  (ANOVA, paired Bonferroni's multiple comparison test). The error bars represent SEM (n=10).

Figure S1

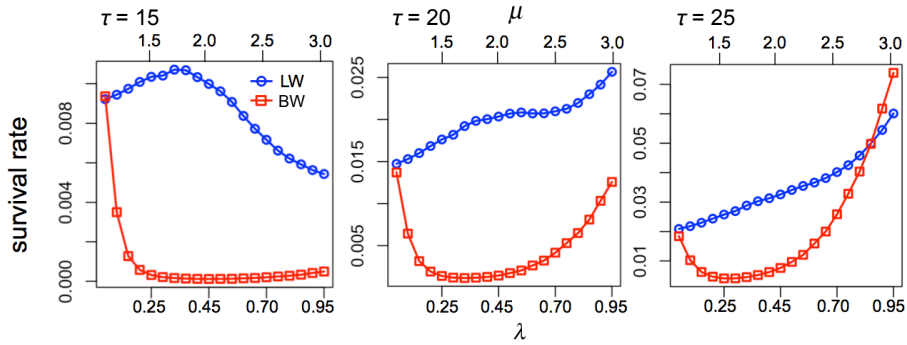


**Figure 3-S1. The survival rate in simulation  $r \rightarrow 0$ .**

The horizontal axis is a prey's strategy parameter of LW ( $1 < \mu \leq 3$ ) or BW ( $\lambda > 0$ ) and the vertical axis is a survival rate of the prey. The blue circle and red square represents LW and BW, respectively. The cutoffs of step length  $l_{\min} = 1$  and  $l_{\max} = 100$ . The number of samples is 100,000.

# Chapter 4

## Detecting information transfer in ant society

### Introduction

The collective behavior of animal groups, such as flocks of birds, schools of fish, or colonies of social insects, has been a focus of attention in various fields, including behavioral ecology, physics, and social science (Camazine et al., 2003; Couzin and Kraus, 2003; Castellano et al., 2009; Sumpter, 2010; Vicsek and Zafeiris, 2012). The sophisticated regulatory systems observed in these animal groups—information transfer, collective decision-making, and division of labor—can arise from local interactions whose rules have evolved through natural selection (Camazine et al., 2003; Couzin and Kraus, 2003; Sumpter, 2010). Therefore, the two central questions are how the individuals interact locally with other individuals, and how this order emerges at the collective level. Previous studies conducted on birds and fish have revealed how to transfer information, in addition to properties of collective behavior such as scale-free correlations (Cavagna et al., 2010; Ward et al., 2011; Katz et al., 2011; Chen et al., 2012; Tunsrøm et al., 2013). Clearly, in most situations, the individuals in such groups show strong synchronization, allowing group members to collectively establish a high degree of order or polarization. On the other hand, in most situations, the individuals in groups of social insects and mammals are considered to be a weakly coupled system in terms of dynamics. Here, “weakly coupled” means that each individual can exhibit spontaneous activities (e.g., solitary foraging patterns, inactivity patterns) (Viswanathan et al., 2011; Proekt et al., 2012) that are independent of interactions with other individuals, as well as interact with other individuals. Information transfer in systems consisting of individuals that undertake both spontaneous and interactive activities are poorly understood because of the difficulty of detecting individual interactions within complex group dynamics.

Network analysis is a useful tool for understanding relationships among interacting elements. Recently, many different networks have been analyzed, from gene

regulatory networks to the food webs (Milo et al., 2002; May, 2006). The method of network analysis applied to animal groups is based on the observation of behavior, or the distance between the positions of a pair of individuals (Flack et al., 2006; Wey et al., 2006). Recently, these analyses of animal group behavior have revealed the relationship between spatial patterns and individual interactions (Pinter-Wollman et al., 2011; Mersch et al., 2013). However, animals often interact through a variety of means, including touch, sound, visual cues, and chemical cues. When one considers that each individual influences the others through several simultaneous kinds of interactions, it becomes clear that distinguishing between these types of interactions is a difficult task. Moreover, interactions involving visual or chemical cues are difficult to detect by observation alone. When one considers dynamics of individuals, the most significant question is not what types of interactions are involved, but in what way the individual interactions influence group behavior (e.g., activity) and aid in the transfer of information. Furthermore, although the constant probability can be assumed as a degree of the effect in the case of a contact network (e.g., transmission of pathogen through interactions), the effect of interactions may be non-linearly dependent on the state of the individual (e.g., activity). Thus, it is crucial to understand whether the individuals in a group influence other individuals in dynamics. A time-series must not only include internal dynamics, but also the influence by other individuals. Therefore, a multivariate time-series is suitable for analyzing the truly meaningful interactions.

I will analyze the dynamics of activity, and quantify the influence of individual interactions using time-series data. The conventional method of detecting relationships using multivariate time-series is the Granger causality test (Granger, 1969). However, this can only detect causality in linear systems, or in strongly coupled stochastic nonlinear systems (Granger, 1969). Furthermore, this method detects “Granger causality” rather than true causality, as the test is based on the accurate estimation of future values. As a result, spurious correlations can be detected (Granger, 1969). In this chapter, I use a novel method, convergent cross mapping (CCM), as proposed by Sugihara et al. (2012), to analyze multivariate time-series. The method is based on the concept of a deterministic dynamical

system and detects true causality between deterministic multivariate time-series. Using this method, we can determine who interacts with whom.

For studies of systems in which the individuals are weakly coupled, it is most appropriate to analyze social insects such as ants and bees. This is because, in most situations, the behavior of each individual is not completely synchronized with its neighbors. In addition, sophisticated collective behavior emerges because in these systems, cooperation arises from a high degree of relatedness, which is not the case with most social mammals (Wilson, 1975; Goss et al., 1989; Bonabeau et al., 2000; Couzin and Franks, 2003). Finally, both the experiment and its associated observations are easy to conduct using insects (Dell et al., 2014).

It has been reported that an individual ant exhibits chaotic dynamics, whereas collective ant activity displays short-term periodicity (Cole, 1991a, b; Boi et al., 1999). Moreover, phase transition and chaotic dynamics have been reported to occur at the collective level under external forces (i.e., temperature) (Beekman et al., 2001; Nicolis et al., 2013). However, only theoretical studies have addressed the question of how these dynamics arise from local interactions between individuals and the associated mechanisms of information transfer (Miramontes et al., 1993; Boi et al., 1999; Delgado and Sole, 2000; Nicolis et al., 2013).

In this chapter, I observe the movements of individual ants placed in a featureless environment. This was carried out using a tracking technique. Then, I detect the interactions between individuals using time-series data analyzed via CCM. Thus, I will provide a framework for the analysis of the collective behavior of weakly coupled animal groups.

## **Materials and Methods**

### **Social insects and experimental setups**

I used an ant species *Diacamma* sp. as a social insect. The colonies were collected from Okinawa, Japan and had been kept in the laboratory for several months before the experiments. The cultures of ant colonies were under the constant condition of 25°C and

16L: 8D photoperiod. All ant individuals were colored by different colors to exactly discriminate each individual when the ant movements were tracked. The five ant individuals (in detail in the next paragraph) randomly chosen from a colony were introduced into 90mm×90mm featureless arena with no environmental changes. There was an only tube for supplying water to prevent ants from being thirsty at the center of the arena. The fluorine compound powder (Fluon, Asahi Glass, Japan) that prevents the ants from climbing was applied to the wall of the arena. There was no cover on the arena for clear recordings of the ant movements. The light was turned on during the experiments to exactly track the individuals, and the temperature was kept at 25°C. The six groups as replicates are derived from different six colonies. I recorded the movies from above (24 hours, 1fps, 800 × 600 pixels) using a web camera (C920, Logicoool, Japan), and automatically tracked the 2-D positions of each individual using a computer (Mac mini core i7, Apple Inc.) and a homemade code based on a computer vision library, Open CV. The start time of recordings was within 6 p.m. ±1hour. Thus, I obtained the movement data consisting of totally 2.6 million time steps. The example of trajectories is shown in Figure 4-1A.

In social insects, the division of labor can often be accomplished (Wilson, 1995; Camazine et al., 2003). To elucidate the influence of the caste such as a queen and worker, in the three groups (A, B, C) of six groups the all five ants were workers, and in the second three groups (D, E, F) the five ants include a queen and the four workers. The worker number in this chapter represents the order of eclosion.

## **Convergent Cross Mapping**

The CCM can detect the causality between multivariate time-series (Sugihara et al., 2012). Consider two time-series  $X=\{X(1), X(2), \dots, X(T)\}$ ,  $Y=\{Y(1), Y(2), \dots, Y(T)\}$ . The behavior of a variable  $X$  in a dynamical system includes the information about that of other variables  $Y$  if the causality from  $Y$  to  $X$  exists. Therefore, plotting the vectors embedded from one time-series we can reconstruct the attractor with the same characteristics of original one (Takens' embedding theorem; Takens, 1981). In the first step, we make two attractors  $M_X$  and  $M_Y$  from  $X$  and  $Y$ , respectively. Consider making  $M_X$  from  $X$ . Set an embedding

dimension  $E$  and time-delay  $\tau$  and then make a vector

$$x(t) = (X(t), X(t - \tau), X(t - 2\tau), \dots, X(t - (E - 1)\tau)). \quad (4.1)$$

This represents a point in  $E$  dimensional space and the set of vectors is the reconstructed attractor  $M_X$ . The distance between the two points means the similarity of time evolution  $(E - 1)\tau$ . In my analysis, I used  $E=3$  and  $\tau = 1$ .

In CCM,  $Y$  is estimated from  $M_X$  and  $X$  is estimated from  $M_Y$ . The evaluation of the estimate accuracy provides us the inference of causalities. When one estimates  $y_t$  from  $M_X$ , search the  $E+1$  most neighbors of  $x(t)$ . These are denoted by  $x(t_1), x(t_2), \dots, x(t_{E+1})$  in ascending order of the distance between  $x(t)$  and  $x(t_i)$ . Then  $y_t$  is estimated by using  $y(t_1), y(t_2), \dots, y(t_{E+1})$  in  $M_Y$  corresponding to  $x(t_1), x(t_2), \dots, x(t_{E+1})$ . The estimated value  $\hat{y}(t)$  is calculated as

$$\hat{y}(t) = \sum_{i=1}^{E+1} w_{t,i} y(t_i) \quad (4.2)$$

where  $w_{t,i}$  is a weight determined by

$$w_{t,i} = \frac{u_{t,i}}{\sum_{j=1}^{E+1} u_{t,j}}. \quad (4.3)$$

Note that  $u_{t,i} = \exp\{-d[x(t), x(t_i)] / d[x(t), x(t_1)]\}$  and  $d[x(a), x(b)]$  is the Euclidean distance between two vectors.

The  $\hat{y}(t)$  for all time is calculated and the first element  $\hat{Y}(t)$  is the estimated value of  $Y(t)$ . Then the correlation coefficient  $\rho$  between actual  $Y(t)$  and estimated  $\hat{Y}(t)$  is calculated and used for the estimate accuracy of mapping.

To distinguish the causal relationship and spurious correlation, observe the dependencies of the estimate accuracy on the number of vectors  $L$  used for reconstruction of the attractor. When the causality exists, the  $\rho$  increases as the  $L$  increasing (convergence). On the other hand, in the case of the spurious correlation, the  $\rho$  remains positive but does not change as the  $L$  increasing (Sugihara et al., 2012).

## Statistical tests for CCM

When one investigates the causality between two time-series, the statistical test is important because even if no causality exists, the results of CCM  $\rho$  are likely to have the variation due to sampling errors, so that one may conclude that the causality exists. Therefore, I made 100 surrogate time-series  $x^s(t)$  under a null hypothesis “no causality” and compared them with observed original data  $x(t)$ . In Sugihara et al. (2012), the method preserving power spectrum (e.g. Fourier Transform, iterative Amplitude Adjusted Fourier Transform) was used for a surrogate method (Sugihara et al., 2012). However, this method is not adequate because the surrogate data from this method has no characteristics of nonlinear systems. Here I adopted the twin surrogate method proposed by Thiel et al. (2006), which preserving the nonlinearity but having different initial states, so that I can obtain two time-series with no causality. The algorithm is following. Step 1) I made the vectors  $x(i)$  by embedding an original time-series and calculated recurrence matrix

$$R_{i,j} = \Theta(\delta - \|x(i) - x(j)\|) \quad (4.4)$$

for  $i, j = 1, \dots, N$  where  $\Theta(\cdot)$  is a heviside function,  $\|\cdot\|$  represents a maximum norm, and  $\delta$  is a threshold. This recurrence matrix has information about original nonlinear dynamics (Thiel et al., 2004). Step 2) The pair of  $x(i)$  and  $x(j)$  holding  $R_{i,k} = R_{j,k}$  for  $k = 1, \dots, N$  is called a twin. I found twins for all pairs. Step 3) Select randomly  $x(i)$  from original embedded time-series and set  $x^s(1) = x(i)$ . Step 4) Consider  $x^s(j) = x(m)$ . If  $x(m)$  has no twins then set  $x^s(j+1) = x(m+1)$ . If  $x(m)$  has a twin  $x(n)$  then set  $x^s(j+1) = x(m+1)$  or  $x^s(j+1) = x(n+1)$  with equal probability. When the number of twins are equal to or more than 2, similarly set  $x^s(j+1)$  from the candidates with equal probability.

Iteratively doing step 4 produces the surrogate time-series with the same length as the original data. It is said that the threshold  $\delta$  ranged from 0.05 to 0.2 is almost robust to the result (Thiel et al., 2006). Therefore, I used  $\delta = 0.125$ .



The sample result is shown in Figure 4-S1. It is consisted of the correlation coefficient for observed data (solid line), the mean correlation coefficient for surrogate data (dashed line) and 95% confidence interval (shade). If the observed line increases as  $L$  and exceeds the shade, the causality statistically significantly exists (Figure 4-S1A). Figure 4-S1B represents the result of a pair of time-series with the spurious correlation.

Two graphs are drawn for one paired time-series. If the both graphs suggest the existence of causality, the causality is bidirectional. If the one graph suggests the existence of causality, the causality is unidirectional.

## Results

I constructed the activity time-series from a position  $(X(t), Y(t))$  of each individual. The activity is defined as

$$a(t) = \sqrt{(X(t) - X(t-1))^2 + (Y(t) - Y(t-1))^2} . \quad (4.5)$$

Then I used the time-series collected every minute. The time-series for six groups are shown in Fig. 4-2 and Fig. 4-S2. Clearly, the dynamics of activities highly fluctuated and therefore the causality cannot be detected from an apparent observation of time-series. For the analysis, each time-series was divided into 6 parts in every 240 min (i.e., 1-240, 241-480, 481-720, 721-960, 961-1200, 1201-1440 min), because the rule of information transfer (i.e., the interaction strength) may change over time.

First, I calculated the auto correlation and cross correlation (Fig. 4-S3-S7). The auto correlation is defined as the correlation coefficient between a time-series and the lagged one, and thus gives us the characteristic of periodicity in a single time-series. The cross correlation provides us the correlation between paired time-series, namely degree of synchronization between two individuals. Fig. 4-S3-S7 suggests that the activity of most ants and pairs does not exhibit periodicity and synchronization. However, in some cases, for example, A 961-1200, the five ants exhibited the relatively strong periodicity of period about 18 min, which was consistent with short term cycle reported in previous studies (Cole, 1991a; Boi et al., 1999). Then, the relatively high cross correlations were also observed.

The result of CCM for the 1-240 section in the group A is shown in Fig. 4-2A. In my experiments, I drew the  ${}_5P_2=20$  graphs for the five ant individuals. In the 20 panels, the result of one directional causality in a pair of individuals is presented from rows to columns. For example, the panel placed in the first row and fifth column represents the influence from worker 1 to worker 5. Fig. 4-2A indicates the presence of causalities from worker 2 to worker 3, from worker 3 to worker 4, from worker 4 to worker 2 and from worker 5 to worker 1 in spite of low auto correlations and cross correlations.

One causation network can be derived from the results of CCM, shown in Fig. 4-2B. When the both two conditions are hold: (1) the correlation coefficient of the observed data at maximum library length is higher than 95% confidence interval, (2) the correlation coefficient at the maximum library length is 0.05 higher than that at the minimum library length (i.e., condition for convergence), I concluded the presence of causality and drew the arrow between two individuals whose direction represents the direction of causality. Then, I observed the time evolution of causation networks by analyzing 6 parts of time-series (Fig. 4-3). This indicates that causation networks can drastically change in course of time. The results for the other groups are shown in Fig. 4-S3-S7. Totally, 69% pairs have no interactions, 24% pairs have unidirectional causality and 7% pairs have bidirectional causality. Although the time-series was divided into 6 parts in every 240 min, the results for 12 parts in every 120 min showed the similar trends (data not shown).

I investigated whether the interactions was associated with the degree of movement activity or not. It is possible that an individual with high activity is likely to influence other individuals. The relation between in- or out-degree of causality networks for all groups and the mean activity is shown in Fig. 4-4A, B. In-degree and out-degree represents the number of individuals influencing a focal individual and that of individuals a focal individual influences, respectively. The Pearson's correlation coefficient between in- or out-degree and the mean activity is -0.076 and -0.033, respectively. This result suggests that the interactions were not correlated with the degree of activity (in-degree:  $p=0.312$ , out-degree:  $p=0.663$ ). Then, in order to investigate the effect of spatial factors of individuals, I examined the relation between the presence of causality and the mean

distance between the pair. The mean distance is thought to roughly correspond to the number of touches. The Fig. 4-4C shows the mean distances of the pairs with no causality, unidirectional causality or bidirectional causality. The results of statistical test suggested that the mean distances were not significantly different among three causal relationships (i.e., no causality, unidirectional causality and bidirectional causality) (ANOVA,  $F=2.2$ ,  $p=0.14$ ), but the difference between no-bidirectional or unidirectional-bidirectional was marginal (Tukey multiple comparison, no-bidirectional:  $p=0.072$ , unidirectional-bidirectional:  $p=0.08$ ), suggesting that the mean distance of the pair with bidirectional causality might be shorter than that of the pair with no causality or unidirectional causality.

Fig. 4-5 shows the effect of the queen on the mean activity and the mean number of in- and out-degree of each individual. The mean activity of queen individuals was significantly higher than that of workers in groups without queen (group A-C) (ANOVA;  $F=4.22$ ,  $p=0.03$ , and Tukey multiple comparison for queen-worker (A-C);  $p=0.02$ ). Likewise, I compared the in- and out-degree of the individuals in the network. Fig. 4-5B indicates that the number of in-degree was significantly different among workers in A-C, workers in D-F and queen (Kruskal-Wallis test;  $p=0.04$ ). The result of multiple comparisons suggests no significant differences, but the difference of workers in A-C and D-F was marginal (Scheffes' multiple comparison;  $p=0.07$ ). In Fig. 4-5C the out-degree of worker in A-C was significantly different from that of queen (Kruskal-Wallis test;  $p<0.01$  and Scheffes' multiple comparison;  $p=0.02$ ).

## Discussions

In this chapter, I observed the activity of each ant individual in a group using a tracking technic and detected the causality (i.e., information transfer) in a weakly coupled system from the time-series by a novel time-series analysis, CCM which is based on the dynamical system and provides us the causality between paired individuals. The observed activities include the complex dynamics (Fig. 4-1 and Fig. 4-S2) in spite of no environmental changes, and most of that have low degree of periodicity and synchronization (Fig.

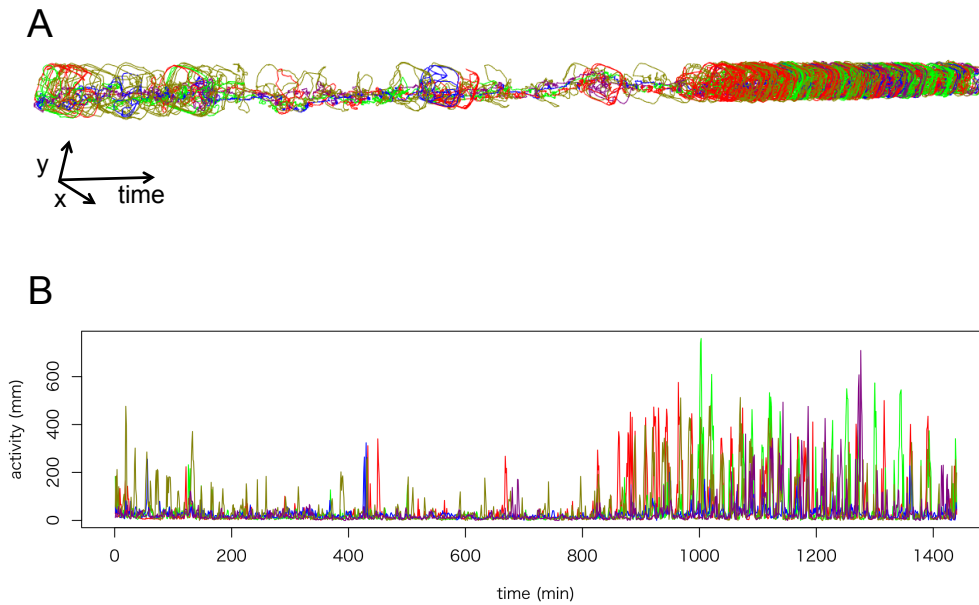
4-S3-S7). However, the result of CCM suggests that the causality in some pairs exist (Fig. 4-2, Fig. 4-3 and Fig. 4-S8-12). This is consistent with the fact that the ant individual exhibits chaotic dynamics and the ant colony is a non-linear system consisted of the coupled elements with chaotic dynamics (Cole, 1991). Thus, we can detect the true consequence of interactions from the multivariate time-series.

The directed networks representing causality can be drawn from the result of CCM. The network structures indicate who influenced whom. The observed networks have some bidirectional interactions and cycles (Fig. 4-3, 4-S8-S12). Therefore, they did not have hierarchy structures observed in my previous study of dominance networks in *Diacamma* sp. (Shimoji et al., 2014). The direction of information transfer observed in the present chapter would not be associated with the rank of individuals. Although the leadership in a group has been observed in several taxa (e.g., birds and mammals) and often plays an important role in collective decision-making (Couzin et al., 2006; Nagy et al., 2010), there was not the obvious leader in my ant groups. Even queen individuals can influence workers and vice versa. However, the queen could suppress the interaction (Fig. 4-5). Moreover, the result of each part of time-series suggests that the interaction strengths and the density of networks were not fixed but changed over time (Fig. 4-3 and Fig. 4-S8-S12). My experimental conditions included no stimuli and environmental changes, and thus the change in interaction strength is considered to be spontaneous. The number of interactions (i.e., in- or out-degree) was independent of its activity (Fig. 4-4A, B). This does not support a hypothesis that individuals with high activity are likely to affect other individuals. Furthermore, the interaction strength was independent on the distance between ant individuals (Fig. 4-4C). This result may reflect the interactions based on chemical or visual stimuli, and thus this relationship among individuals cannot be detected from the observation of touch interactions or the distance of individuals that were used for definition of interactions in the previous studies (Blonder and Dornhaus, 2011; Pinter-Wollman et al., 2011; Water and Fewell, 2012; Mersch et al., 2013).

In the present study, I observed the ants' activity without environmental changes and tasks, namely default states. The future topics include revealing the effect of the

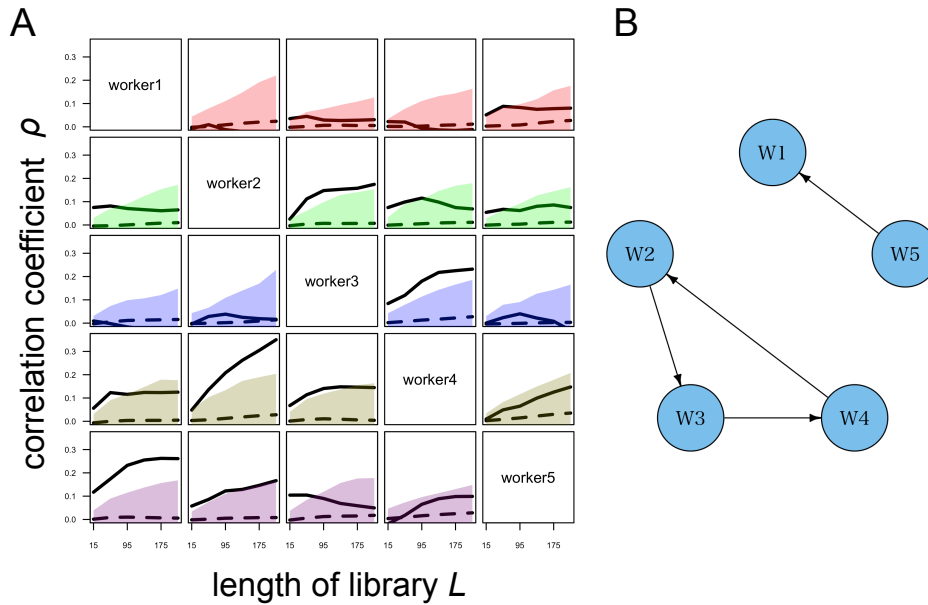
stimulus and environmental changes on the information transfer and investigating how the network structures and fluctuating activity in the default state can lead to adaptive biological systems (Hidalgo et al., 2014). The weakly coupled system is likely to exhibit chaotic dynamics unlike strongly coupled system. It is worth noting that some theoretical studies reveal such systems can exhibit intriguing phenomena like clustering of synchronization, itinerancy of quasi-attractors and tuning to external force (Kaneko, 1990; Nicolis et al., 2013).

I propose the framework to analyze the collective behavior in weakly coupling animal groups. This method can also be applied for other dynamics in animal collective behavior such as luminescent in firefly and vocalization in mammals (Strogatz and Stewart, 1993; Takahashi et al., 2013). As for movements, most animals have spontaneous activity whose timing is often considered to follow a distribution with power-law tail (Proekt et al., 2012; Viswanathan et al., 2011; Maye et al., 2007). Spontaneous activity can influence interaction pattern and vice versa. Therefore, when one understand the collective behavior, it would be crucial to consider both such spontaneous activity in each individual and interactions with other individuals.



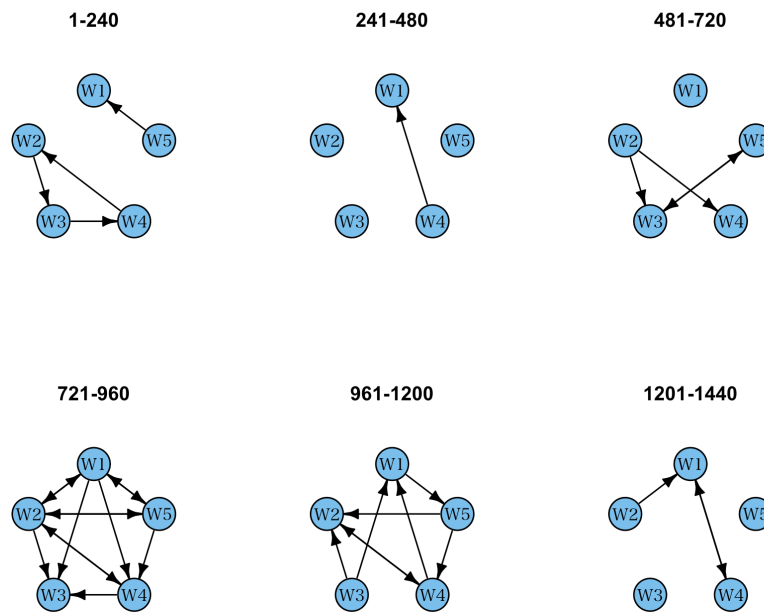
**Figure 4-1. Examples of the trajectory of ant movements and time-series of activity.**

(A) The five lines are the trajectories of five ant individuals obtained by tracking the movements. Each color of lines corresponds to each individual. The horizontal axis and the other two axes represent time and spatial positions, respectively. (B) The horizontal and vertical axes are time (min) and activity (mm) per a minute, respectively. Each color corresponds to each individual and is identical with one used in movement trajectories. The other five time-series for B-F are shown in Fig. 4-S2.



**Figure 4-2. Examples of a result of CCM and a causality network.**

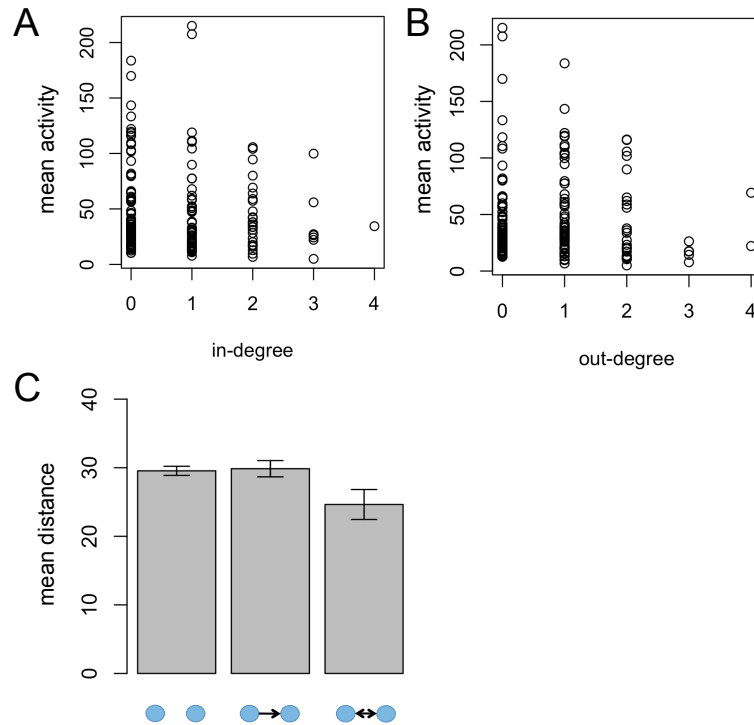
(A) The result of CCM for five ant workers (group A, 1-240 min) (The details of graphs are written in the text and the example of interpretation for the graph is shown in Fig. 4-S1). This indicates the existence of causality from worker 2 to worker 3, from worker 3 to worker 4, from worker 4 to worker 2 and from worker 5 to worker 1. (B) The causality network obtained from the result of CCM. A node and edge with a direction represent an individual and causality between nodes, respectively. The characters in a node mean the name of an ant individual. For instance, W1 means worker 1.



**Figure 4-3. The time evolution of causality network.**

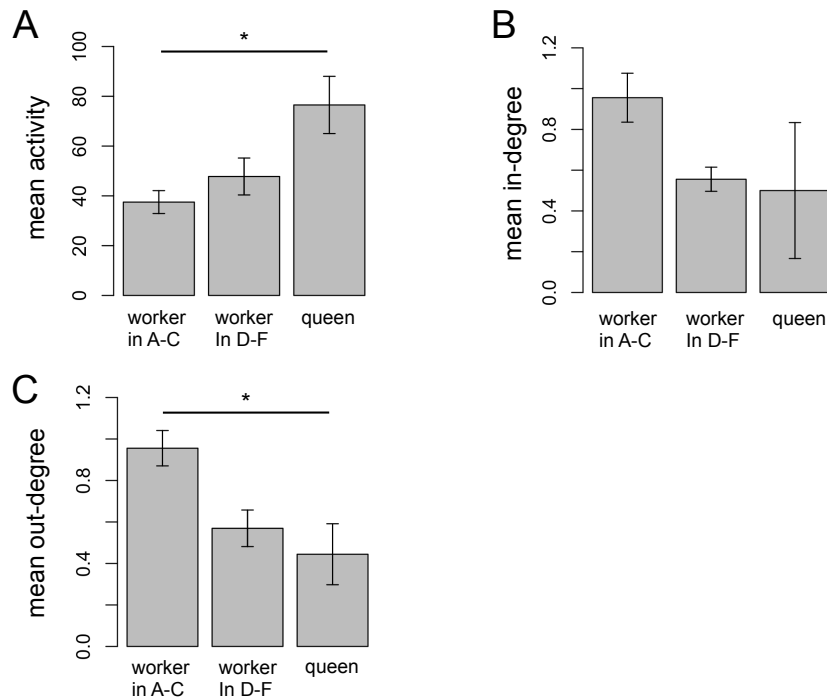
The six causality networks of five workers (group A). The number over each network indicates the time used for CCM.





**Figure 4-4. The effects of activity and distance on causality.**

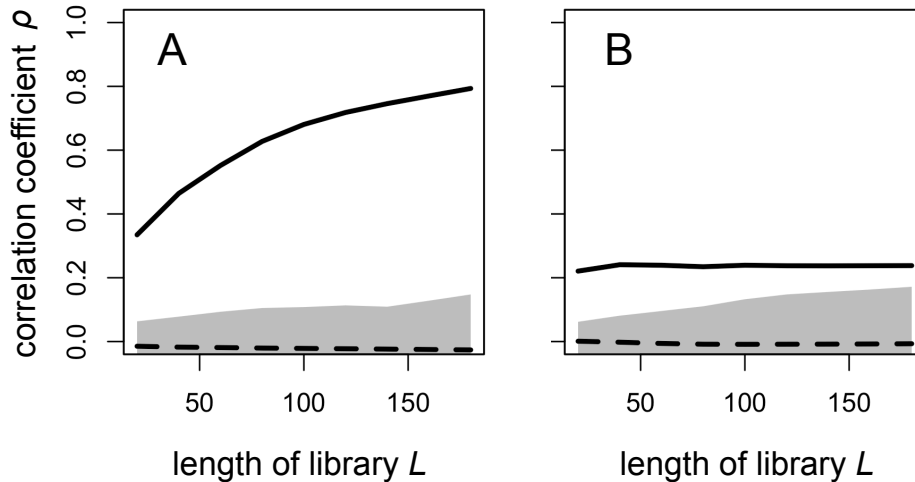
(A, B) The relation between in- or out-degree and mean activity. The mean activity was not different depending on in-degree or out-degree (correlation coefficient=-0.076 and -0.033,  $p=0.31$  and  $0.66$ , respectively). (C) The relation between causality and distance between a pair of ant individuals. The nodes and edges under bar graphs illustrate no causality, unidirectional causality and bidirectional causality. The statistical test suggested that the mean distances were not significantly different among the kinds of causality (ANOVA,  $F=2.2$ ,  $p=0.14$ ). Multiple comparisons also provided no significance, but the mean distance of the pair with bidirectional causality might be shorter than that of the pair with no causality or unidirectional causality (Tukey multiple comparison, bidirection-no:  $p=0.072$ , bidirection-unidirection:  $p=0.08$ ). Error bars are standard errors.



**Figure 4-5. The effect of the presence of queen on activity and degree of interaction.**

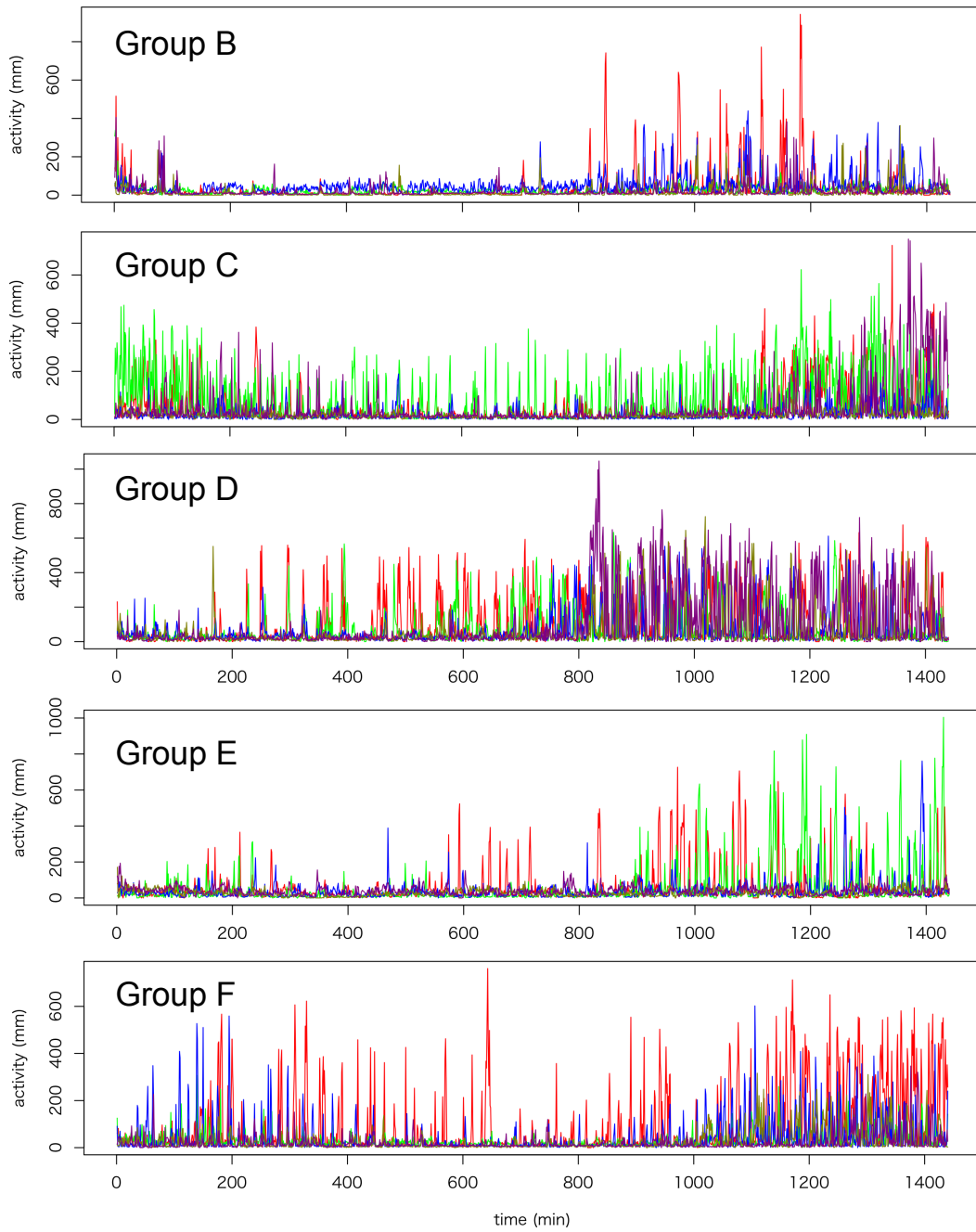
The workers in group A-C had no chance of interaction with queen (n=15). The workers in group D-F were under the presence of queen (n=12). The replication number of queen is three. The asterisk represents  $p < 0.05$ . Error bars are standard error. (A) Mean activity of worker in A-C, worker in D-F and queen. The mean activity of worker in A-C and queen was significantly different (Tukey multiple comparison). (B, C) Mean in- and out-degree of worker in A-C, worker in D-F and queen. The mean out-degree of worker in A-C and queen was significantly different (Scheffes' multiple comparison).

## Supporting information



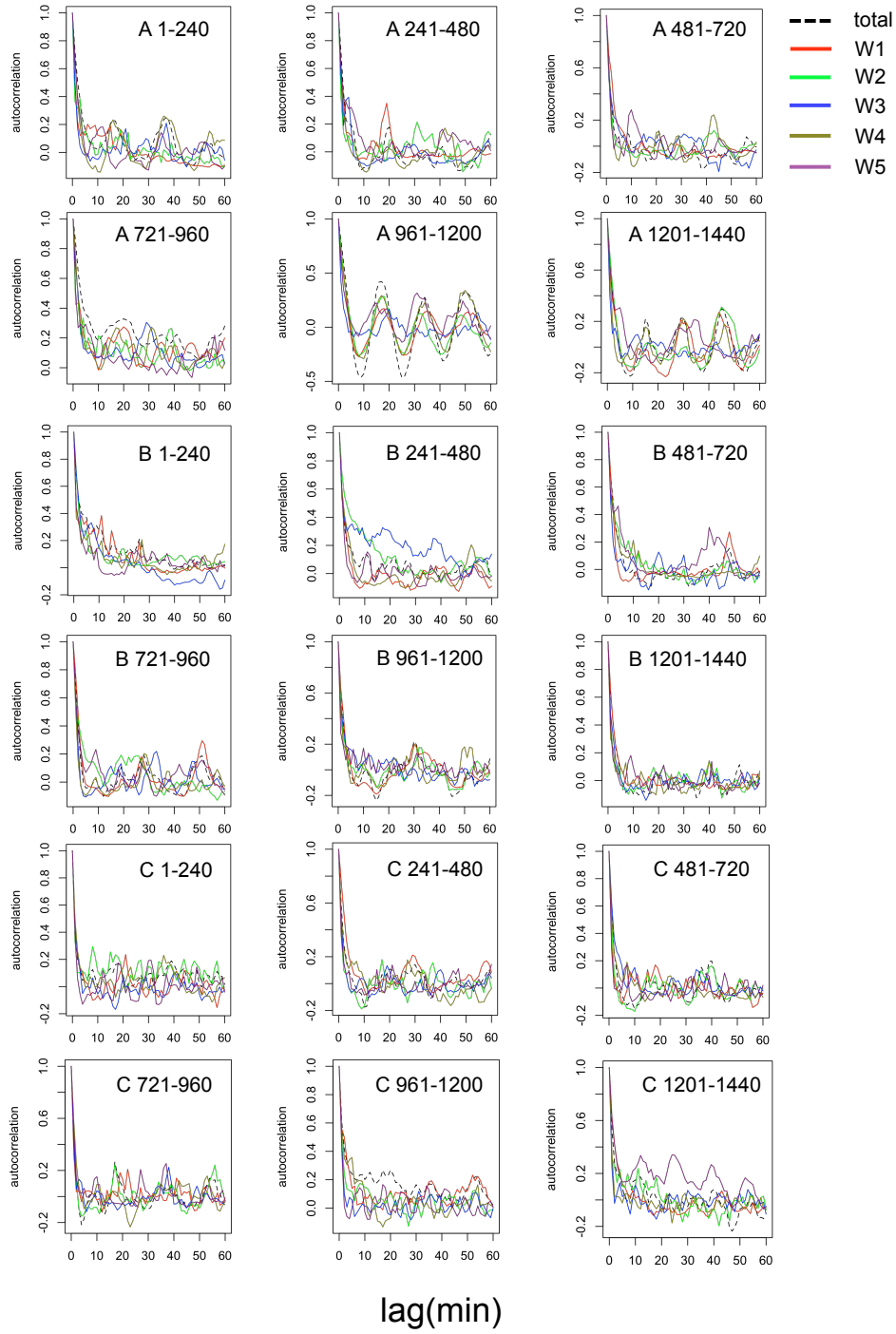
**Figure 4-S1. The example of results of CCM**

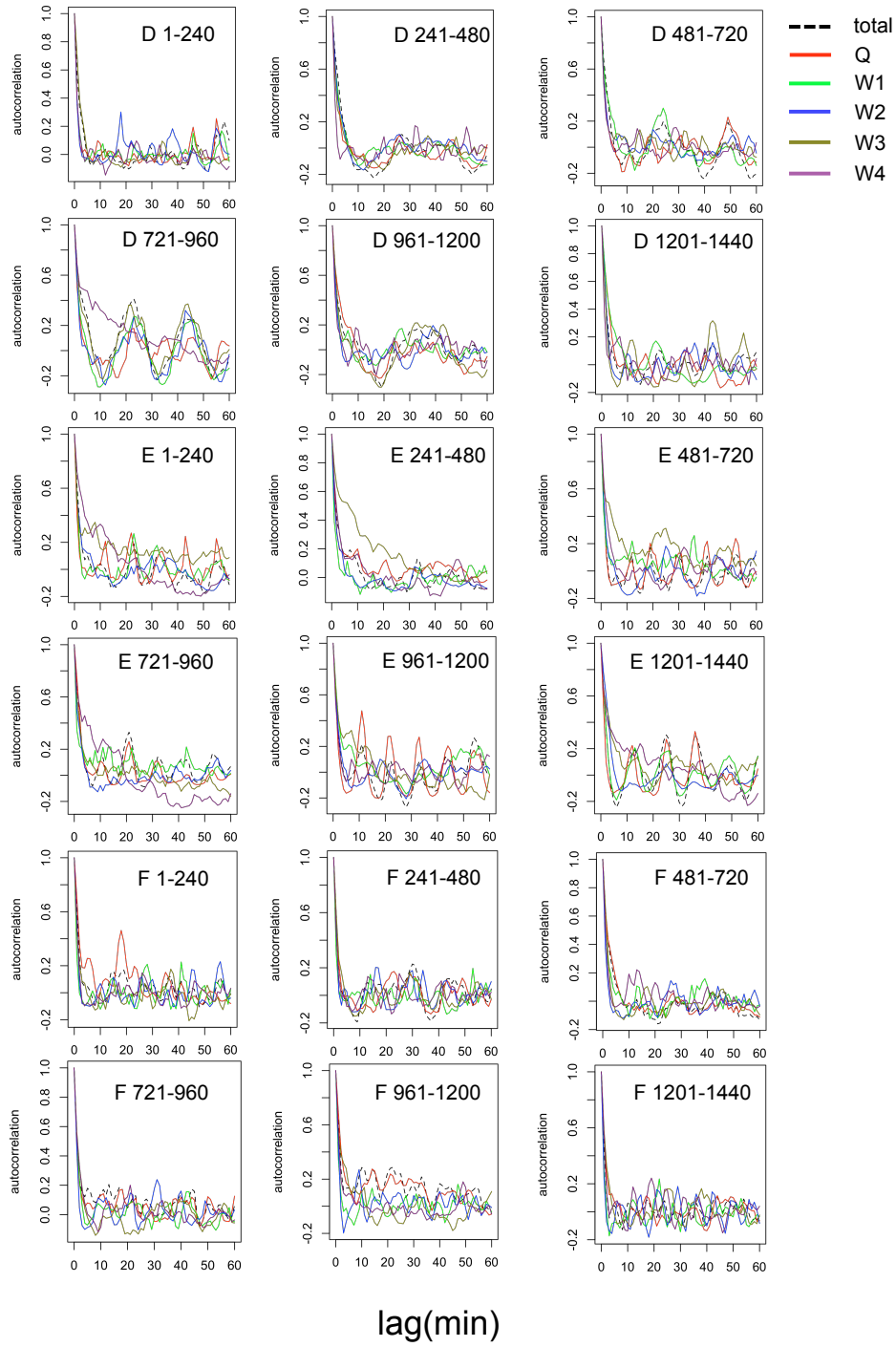
The horizontal axis is the length of library  $L$  used for reconstruction of attractor. The vertical axis is the correlation coefficient between predicted and actual value that is assumed as the cause. The solid line is the result of observed value and the dashed line is the mean value of results for 100 surrogate data. The shade represents the one-tailed 95% confidence interval. (A) This is the case of existence of causality, so that the correlation coefficient increases as  $L$  increasing and the observed value goes beyond the shade. (B) The case of spurious correlation. The positive correlation coefficient remains constant.



**Figure 4-S2. The time-series of ant's activity for each group.**

The time-series of activities of groups B-F are shown. Each color corresponds to each ant individual. In groups D-F, the activity of queen is represented as a red line. The activity of group A is shown in Fig. 4-1A.

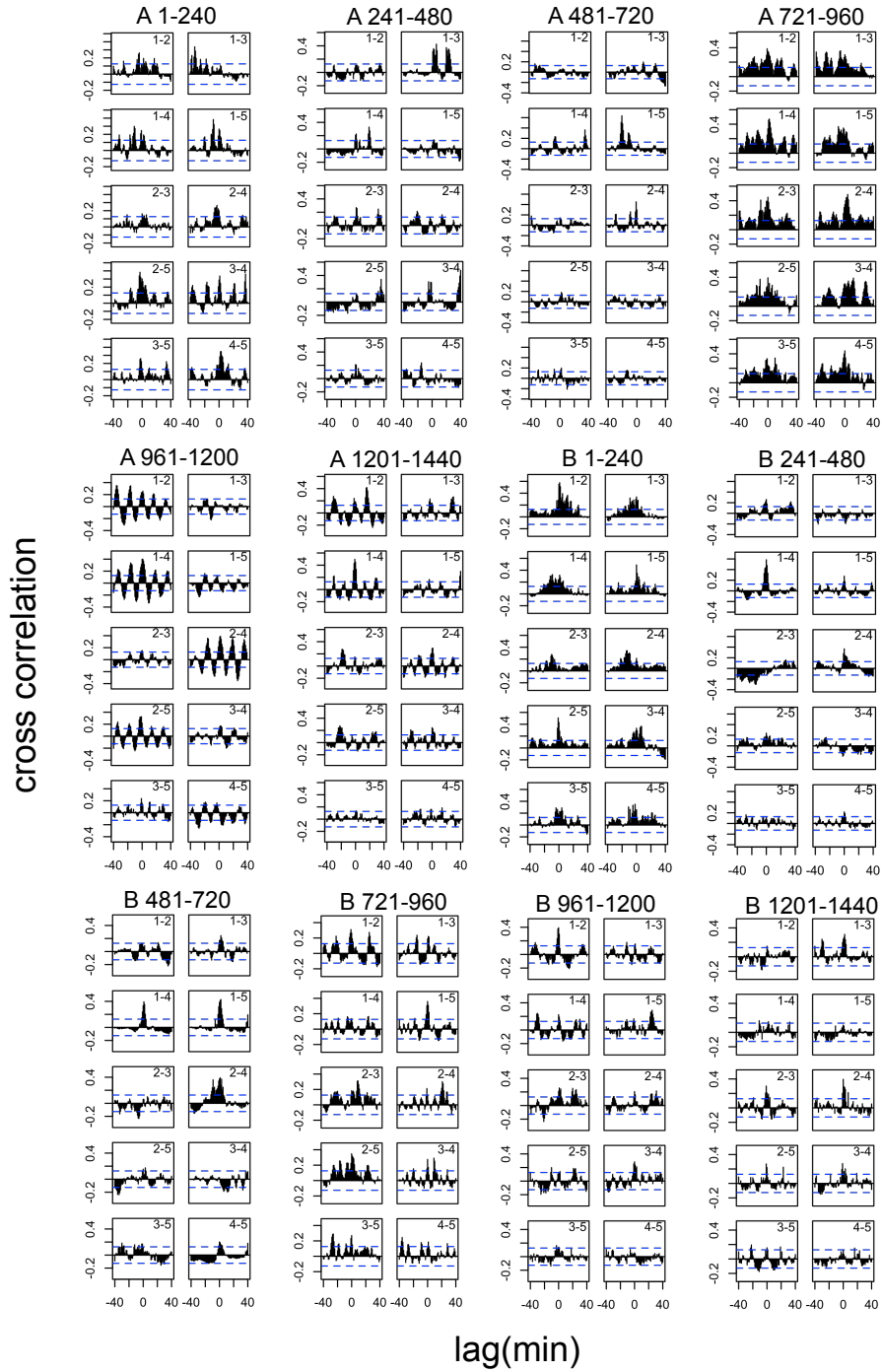




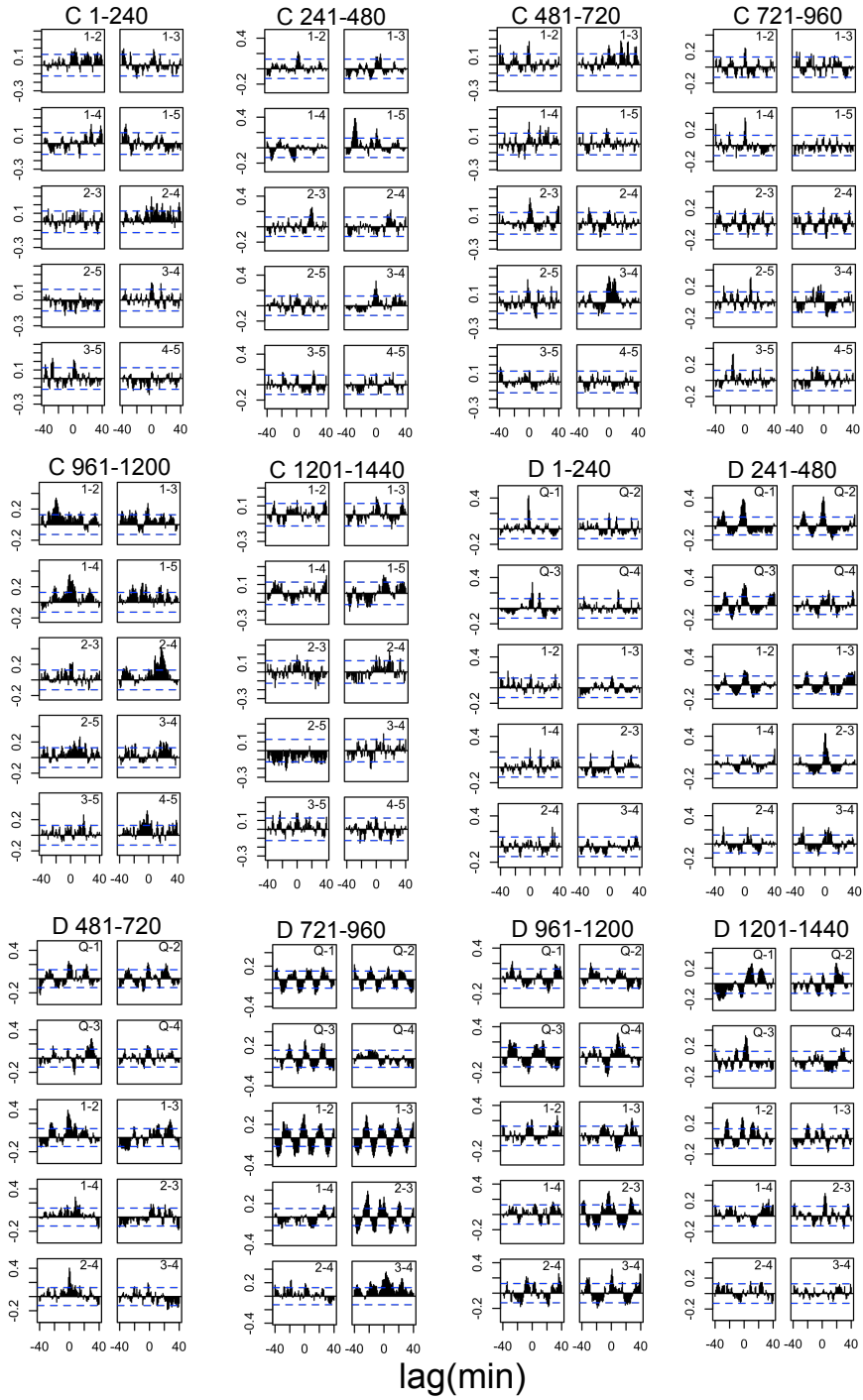
**Figures 4-S3-S4. The autocorrelation of ant's activity.**

The horizontal axis represents the time lag (min) and the vertical axis means autocorrelation. The character and number in each graph means the group name and time used for calculation of autocorrelation. The solid lines indicate the autocorrelation for each ant and the black dashed line represents the autocorrelation of total activity (i.e., sum of activity of five ant individuals). The autocorrelation of most time-series rapidly declines as the time lag increasing.

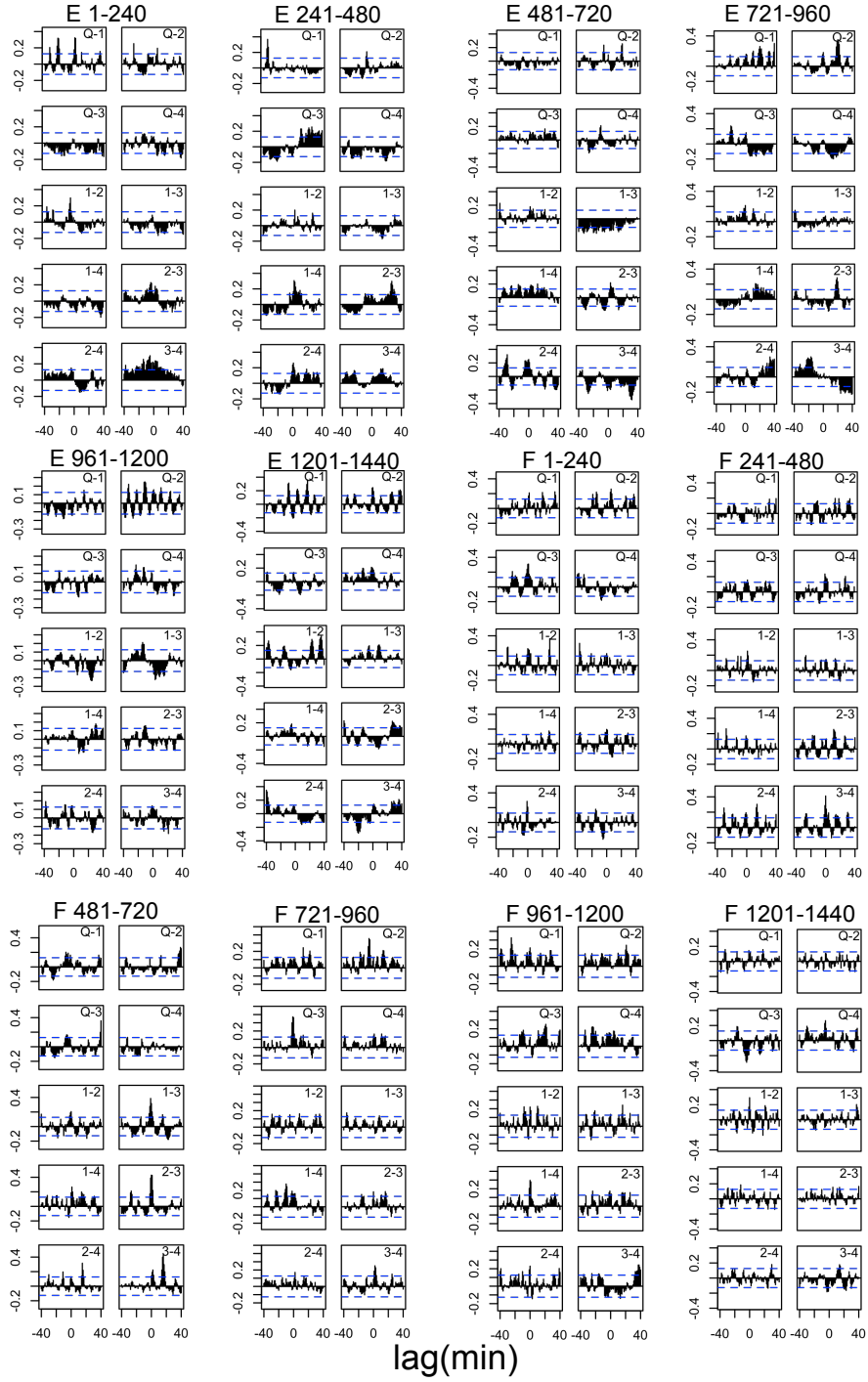




cross correlation



cross correlation

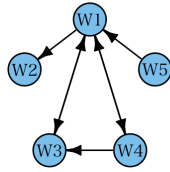


**Figures 4-S5-S7. The crosscorrelation of ant's activities.**

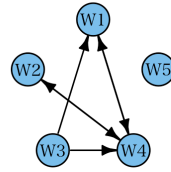
The horizontal axis represents the time lag (min) between a pair of time-series and the vertical axis means cross-correlation. The blue dashed line represents 95% confidence interval. The character and number over graphs means the group name and time used for analysis. The characters in each graph represent the pair of individuals.

Group B

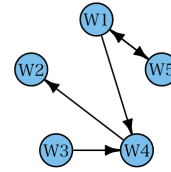
1-240



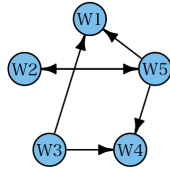
241-480



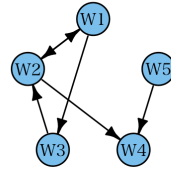
481-720



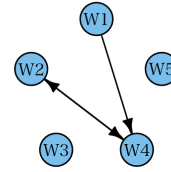
721-960



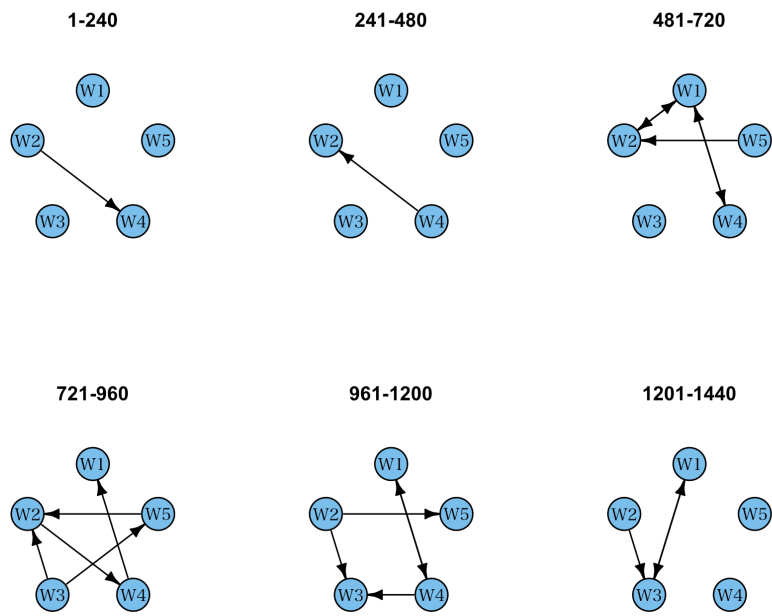
961-1200



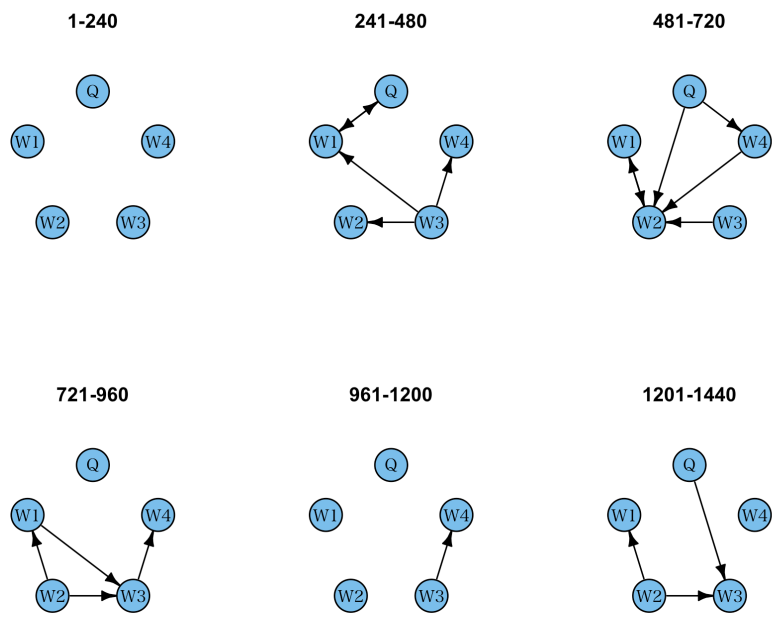
1201-1440



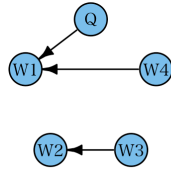
Group C



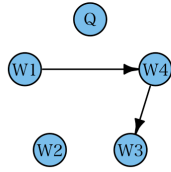
Group D



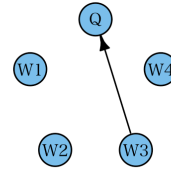
Group E 1-240



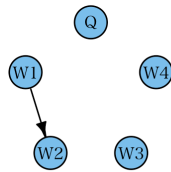
241-480



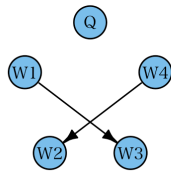
481-720



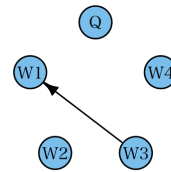
721-960



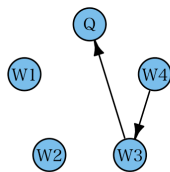
961-1200



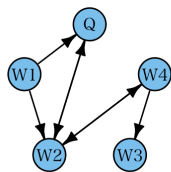
1201-1440



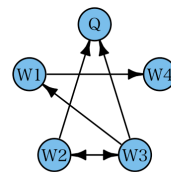
Group F 1-240



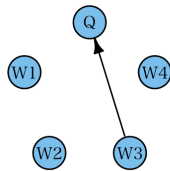
241-480



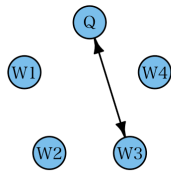
481-720



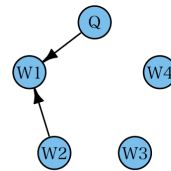
721-960



961-1200



1201-1440



**Figures 4-S8-S12. The time evolution of causality networks.**

The causality networks of group B-F are derived from results of CCM. The number over a network means the time used for CCM. The characters in a node mean the name of an ant individual. For instance, W1 and Q mean worker 1 and queen, respectively.



# **Chapter 5**

## **Network structure of dominance hierarchy of ant workers**

### **Introduction**

Dominance interaction such as aggressive physical interaction and ritualized displays between dominant (i.e., high-ranked in the hierarchy) and subordinate (i.e., low-ranked) individuals is widespread in animals. Dominance hierarchies are a regulatory mechanism of the social system and observed in a wide range of taxa from vertebrates to invertebrates (Wilson, 1975; Drews, 1993; Keller and Reeve, 1999; Earley and Dugatkin, 2010). Dominant individuals would have a high chance to access to resources and can enhance their fitness, whereas subordinates have a small chance of resource acquisition and as a result in some taxa undertake a role of helper that does not reproduce (Queller et al., 2000; Clutton-Brock et al., 2001).

Eusocial insects characterized by reproductive division of labor provide opportunities for studying complex social organisations (Wilson, 1975; Gadau and Fewell, 2009; Bourke, 2011). In many eusocial Hymenoptera (e.g., ants, honey bees, and wasps), workers cannot mate but do produce males through arrhenotokous parthenogenesis. Kin selection theory suggests that colony members are in conflict over male production because a worker gains genetic benefit by rearing her own sons (Hamilton, 1964a; Hamilton, 1964b; Ratnieks, 1988). At the same time, worker reproduction is costly to a colony because reproductive workers allocate their workforces to personal reproduction rather than to household chores for maintaining the colony (Cole, 1986; Tsuji et al. 2012) (see also Bourke, 2011). In fact, most workers facing this conflict remain sterile. Dominance interaction is also found in various species of ants and regulates worker reproduction (Cole, 1986; Bourke and Franks, 1995; Heinze et al., 1997; Monnin and Peeters, 1999; Gobin and Ito, 2003).

A prevalent theoretical approach to dominance hierarchy is to rank individuals in a group on the basis of observed dyadic interactions. By inferring the direction of missing interactions between pairs of individuals if necessary, one can construct a so-called tournament, which is an assignment of directed links to all pairs of individuals (Appleby, 1983; de Vries, 1995). If cyclic dominance relationship (e.g., rock-scissors-paper relationship among three individuals) is absent, the linear ordering uniquely exists such that a dominant individual always has a higher rank than the subordinate individual in any pair (Chase, 1982; Shizuka and McDonald, 2012). The degree of linear hierarchy is related to relative abilities of individuals in controlling resources such as mates and food (Earley and Dugatkin, 2010) and to group stability (Monnin and Ratnieks, 1999; Lindquist and Chase, 2009).

However, linear hierarchy is commonly violated in large groups of animals in various species (Chase, 1980; Chase, 1982; de Vries, 1995; Shizuka and McDonald, 2012; McDonald and Shizuka, 2013). In particular, pair-flips, i.e., bidirectional links (Lindquist and Chase, 2009), and intransitive triads represented by the rock-scissors-paper relationship (Shizuka and McDonald, 2012; Chase, 1980; McDonald and Shizuka, 2013) are basic building blocks that make dominance networks not linear. The loss of linearity is intuitive given that an individual would not be able to recognize all peers and many individuals would have similar strengths in a large group.

In the present study, I observe aggressive behavior among workers of an ant species *Diacamma* sp. on a large scale (i.e., 58–214 workers). I show that the observed dominance networks are directed acyclic graphs (DAGs) or approximately DAGs such that they are consistent with (almost) perfect linear hierarchy, despite the relatively large group sizes. Furthermore, using network analysis tools specialized for directed networks, particularly those recently developed for DAGs, I analyze rank-dependent aggression behavior of individuals and randomness inherent in global structure of the observed networks.

## **Materials and methods**

## Ant species

*Diacamma* sp. is a ponerine species. In Japan, this is the only species of the genus *Diacamma*. Colonies are monogynous containing at most one functional queen in each colony together with 20–300 workers (Kikuchi et al., 2008). Precisely speaking, queens of this species are called gamergates, i.e., mated reproductive workers (Peeters and Crewe, 1984), because unlike many other ants the role differentiation between queens and workers in this species occurs not through the larval development but via the specialized social manipulation after the adult eclosion called the gemmae mutilation (Fukumoto et al., 1989). In the current study, I use the terms queen and worker for simplicity. The queen monopolizes the production of female offspring. Workers, i.e., those whose gemmae are mutilated, cannot mate but retain the ability to produce male-destined haploid eggs. Aggressive behaviors are frequently observed among workers when the queen is absent or the colony is large (Kikuchi et al., 2008; Peeters and Tsuji, 1993). Such behavior is considered to reflect competition over direct male production, because the dominant workers, usually the most dominant one, actually lay eggs even in the presence of the queen especially in large colonies (Kikuchi et al., 2008; Nakata and Tsuji, 1996). The queen never participates in dominance hierarchy.

There is another type of aggressive interaction among nestmate workers in this species, i.e., worker policing (Kawabata and Tsuji, 2005). Worker policing is behaviorally distinct from aggressive behavior underlying dominance hierarchy. In worker policing, multiple individuals simultaneously attack one victim to immobilize it. In contrast, aggression takes the form of one-on-one interaction, i.e., biting and jerking (Peeters and Tsuji, 1993), which has led me to study the dominance hierarchy by network analysis tools; a network is by definition composed of a collection of pairwise interactions.

I collected six colonies of *Diacamma* sp. in peninsula Motobu, northern part of the main island of Okinawa, in March-May 2011 and in August 2012. Each colony contained a queen and 58–214 workers. I individually marked all the adult ants by enamel markers. Then, I housed each colony in “double container” artificial nests (Kikuchi et al., 2008), which comprised a small plastic container (10 cm × 10 cm × 2.5 cm high) serving as

a breeding chamber. The container was located in the centre of a larger container (15 cm × 21 cm × 13.5 cm high). The colonies had been maintained in the laboratory (25 ± 1 °C, 14 L: 10 D cycle) for two to three months before the observation began. The workers were fed ad libitum on honey worms (caterpillars of *Galleria mellonella*) and water placed outside the smaller container. It should be noted that I recorded aggressive behavior among workers in the presence of the queen in each colony.

### **Recording aggressive behavior**

I recorded all aggressive behavior events between all pairs of workers in each colony for 300 min per day for consecutive four days using a digital video camera (HDR-CX700V, Sony, Japan). The aggressive interaction was defined as bite and jerk (Peeters and Tsuji, 1993). I counted the number of aggressive interactions between each pair of workers and constructed a directed social network for each colony. The nodes are workers. A directed link represents a pair of workers that have interacted at least once and emanates from the attacking worker to the attacked worker.

### **Triangle transitivity metric**

Due to high sparseness of the recorded networks (see Results), I should resort to a measurement different from well-known indices such as Landau's  $h$  and Kendall's  $K$  to quantify linearity (i.e., orderliness) of a dominance network. To this end, I calculate the triangle transitivity metric (Shizuka and McDonald, 2012). The triangle transitivity is defined as a normalized value of the number of transitive triads (A attacks B, A attacks C, and B attacks C) divided by the sum of the number of transitive triads and that of cycles (A attacks B, B attacks C, and C attacks A). See Electronic Supplementary Material for the mathematical definition.

### **Generation of thinned linear tournaments**

I generate a thinned linear tournament possessing  $N$  nodes and  $|E|$  expected number of links, which is used as a null model for probing structure of observed networks,

as follows (equivalent to the cascade model used in food web research (Cohen and Newman, 1985)). Consider the linear tournament with  $N$  nodes, in which all pairs of individuals interact (i.e., complete graph) and perfectly ranked in the sense that the higher-ranked individual dominates the lower-ranked individual in any pair (Wilson, 1975; Haray and Moser, 1966). Then, I independently retain each of the  $N(N-1)/2$  directed links with probability  $p$ . Otherwise, I remove the link. I call the generated network a thinned linear tournament. I set

$$p = \frac{2|E|}{N(N-1)} \quad (5.1)$$

such that the expected number of the links in the generated network is equal to  $|E|$ .

## CV

The in-degree of a worker is defined as the number of directed links incoming to the worker, i.e., number of workers that attack the focal worker. The out-degree of a worker is defined as the number of directed links outgoing from the worker, i.e., number of workers that the focal worker attacks. If I convert the bidirectional links to unidirectional links by discarding one of the two directions whose link weight is smaller than the other (Electronic Supplementary Material, section S.4), the out-degree is identical to the *Netto* dominance index (Hemelrijk et al., 2005).

To quantify the heterogeneity in the in- and out-degree, I measure the coefficient of variation (CV), i.e., the ratio of the standard deviation of in- or out-degree to the mean. If all workers have the same degree, CV is equal to zero. The exponential degree distribution yields CV equal to unity. A CV value much larger than unity implies that the distribution is heavily tailed.

## CV for the thinned linear tournament

In the thinned linear tournament, the probability that the worker with rank  $k$  ( $1 \leq k \leq N$ ) has in-degree  $d^{\text{in}}$  ( $0 \leq d^{\text{in}} \leq k-1$ ) is given by

$$P(d^{\text{in}} | k) = \frac{(k-1)!}{d^{\text{in}}!(k-1-d^{\text{in}})!} p^{d^{\text{in}}} (1-p)^{k-1-d^{\text{in}}}. \quad (5.2)$$

Therefore, the in-degree distribution not conditioned by the rank is given by

$$\begin{aligned} P(d^{\text{in}}) &= \frac{1}{N} \sum_{k=d^{\text{in}}+1}^N P(d^{\text{in}} | k) \\ &= \frac{1}{N} \sum_{k=d^{\text{in}}+1}^N \frac{(k-1)!}{d^{\text{in}}!(k-1-d^{\text{in}})!} p^{d^{\text{in}}} (1-p)^{k-1-d^{\text{in}}}. \end{aligned} \quad (5.3)$$

Similarly, the conditional and unconditional distributions of the out-degree

$d^{\text{out}}$  ( $0 \leq d^{\text{out}} \leq N-k$ ) are given by

$$P(d^{\text{out}} | k) = \frac{(N-k)!}{d^{\text{out}}!(N-k-d^{\text{out}})!} p^{d^{\text{out}}} (1-p)^{N-k-d^{\text{out}}} \quad (5.4)$$

and

$$\begin{aligned} P(d^{\text{out}}) &= \frac{1}{N} \sum_{k=1}^{N-d^{\text{out}}} P(d^{\text{out}} | k) \\ &= \frac{1}{N} \sum_{k=1}^{N-d^{\text{out}}} \frac{(N-k)!}{d^{\text{out}}!(N-k-d^{\text{out}})!} p^{d^{\text{out}}} (1-p)^{N-k-d^{\text{out}}} \\ &= \frac{1}{N} \sum_{k'=d^{\text{out}}+1}^N \frac{(k'-1)!}{d^{\text{out}}!(k'-1-d^{\text{out}})!} p^{d^{\text{out}}} (1-p)^{k'-1-d^{\text{out}}}, \end{aligned} \quad (5.5)$$

respectively. Because the unconditional in- and out-degree distributions are the same, the expected in-degree and out-degree are given by

$$E(d^{\text{in}}) = E(d^{\text{out}}) = \sum_{d=0}^{N-1} dP(d) = \frac{(N-1)p}{2}. \quad (5.6)$$

The variance of the in- and out-degree is given by

$$V(d^{\text{in}}) = V(d^{\text{out}}) = \sum_{d=0}^{N-1} P(d) \left[ d - \frac{(N-1)p}{2} \right]^2 = \frac{(N-1)p[(N-5)p+6]}{12}. \quad (5.7)$$

By combining equations (1), (6), and (7), I obtain the CV for the thinned linear tournament as follows:

$$CV = \frac{\sqrt{V(d^{\text{in}})}}{E(d^{\text{in}})} = \frac{\sqrt{V(d^{\text{out}})}}{E(d^{\text{out}})} = \sqrt{\frac{|E|(N-5) + 3N(N-1)}{3|E|(N-1)}}. \quad (5.8)$$

### Bottom-up leaf-removal algorithm and ranking of workers

I determine the ranks of nodes (i.e., workers) in a DAG using the so-called bottom-up leaf-removal algorithm (Eades et al., 1993; Ma et al., 2004) as follows (see Figure 5-S1 for a schematic). First, I remove the nodes without outgoing links. The set of the removed nodes is denoted by  $W_1$ . I also remove the incoming links incident to the removed nodes. Second, I remove the nodes without outgoing links in the remaining network and the incoming links incident to these nodes. The set of the nodes removed in the second round is denoted by  $W_2$ . I repeat the same procedure until all the nodes are removed. The set of the nodes removed in the  $i$ -th round is denoted by  $W_i$ . Now, a given DAG is assigned with a layer structure  $\{W_1, W_2, \dots, W_L\}$ , where  $L$  is the number of layers.

The rank of a node belonging to layer  $W_i$  is given by  $L-i+1$ . The most and least dominant nodes possess ranks 1 and  $L$ , respectively. By construction, any directed link emanates from a worker with the higher rank to a worker with the lower rank. Multiple nodes may possess the same rank value. There is no link between nodes with the same rank (equivalently, nodes in the same layer).

### Generation of random DAGs

I generate random DAGs that possess the same in-degree and out-degree of each node and the same distribution of the connected component size as those of the observed networks. The random DAGs are also used as null models for probing structure of observed networks. To generate networks, I use a previously proposed rewiring method (method c in Goñi et al. (2010)).

The rewiring process begins by applying the bottom-up leaf-removal algorithm to an observed network. Then, I randomly order the  $N$  nodes in the network under the

condition that a node with a higher rank (i.e., smaller rank value) appears earlier. This is tantamount to randomly ordering the nodes within each layer and align them from the last (i.e.,  $L$ -th) to the first layer. Then, I select a directed link  $k \rightarrow j$  (i.e., directed link from the  $k$ -th node to the  $j$ -th node) with the equal probability and then randomly select two nodes  $i$  and  $\ell$  such that (i) links  $i \rightarrow k$  and  $\ell \rightarrow j$  exist or (ii) links  $k \rightarrow i$  and  $j \rightarrow \ell$  exist. If condition (i) holds true,  $\ell \rightarrow k$  does not exist,  $i \rightarrow j$  does not exist,  $\ell < k$  and  $i < j$ , then I replace  $i \rightarrow k$  and  $\ell \rightarrow j$  by  $\ell \rightarrow k$  and  $i \rightarrow j$ , respectively. If condition (ii) holds true,  $k \rightarrow \ell$  does not exist,  $j \rightarrow i$  does not exist,  $k < \ell$  and  $j < i$ , I replace  $k \rightarrow i$  and  $j \rightarrow \ell$  by  $k \rightarrow \ell$  and  $j \rightarrow i$ , respectively. If any of these conditions is not satisfied, I repeat the same procedure with a different directed link  $k \rightarrow j$  until a successful rewiring event occurs. Once I have rewired two links, I carry out the entire procedure starting from the leave-removal algorithm and iterate it until a desired number of links is rewired.

I verified that the generated DAG was random enough by measuring the so-called dissimilarity (Goñi et al., 2010) (Supplementary Material).

## Out-strength

The out-strength of a worker is defined as the sum of the weights of the links outgoing from the worker. It corresponds to the number of aggression behavior that the worker has exerted on other workers and is identical to the *AttFr* dominance index (Hemelrijk et al., 2005).

## Reversibility

The reversibility from non-maximal nodes (i.e., workers) to maximal nodes, denoted by  $H$ , quantifies the variety of paths in the DAG (Corominas-Murtra et al., 2010). In a DAG, the maximal node is defined as the most dominant node, i.e., a node without incoming link. The  $H$  value is the average amount of information necessary for reversely traveling from non-maximal to maximal nodes (see Supplementary Material for definition). If  $H$  is equal to zero, the network is a (heterogeneous) directed tree, including the case of the directed chain, such that any subordinate worker is attacked by just one worker. A large



$H$  value indicates that subordinate workers would often receive multiple incoming links and there tend to be various reversed pathways to reach one of the most dominant workers from a subordinate worker. The reversibility is a quantity exclusively defined for DAGs.

## Hierarchy index

The hierarchy index denoted by  $\nu$  ranges between  $-1$  and  $1$  and quantifies the extent to which the network has pyramidal structure and reversibility of paths (Corominas-Murtra et al., 2011) (see Supplementary Material for definition). A network with  $\nu = 1$  is perfect (possibly heterogeneous) tree such that all nodes except a single root node have in-degree unity and all nodes except leaves, which possess out-degree zero, have out-degree at least two. In addition, the distance from the unique root node to any leaf node is the same. The network with  $\nu = -1$  is an inverted (possibly heterogeneous) tree such that all nodes except a single leaf has out-degree unity and all nodes except roots, which possess in-degree zero, have in-degree at least two. In addition, the distance from any root to the unique leaf is the same. Networks having  $\nu$  values close to zero are considered to lack hierarchical structure in both downward and upward directions. The hierarchical index is also a quantity exclusively defined for DAGs.

## Global reaching centrality

The global reaching centrality  $GRC$  is defined as follows (Mones et al., 2012). The local reaching centrality of node  $i$ , denoted by  $C_R(i)$ , is defined as the proportion of the other nodes reachable from node  $i$  by following outgoing links. On the basis of  $C_R(i)$ , I define

$$GRC = \frac{\sum_{i=1}^N [C_R^{\max} - C_R(i)]}{N - 1}, \quad (5.9)$$

where  $C_R^{\max}$  is the maximum of  $C_R(i)$  ( $1 \leq i \leq N$ ).  $GRC$  ranges between 0 and 1. It is an indicator similar to the CV in the meaning that it quantifies the heterogeneity of the out-degree. However,  $GRC$  also quantifies the level of hierarchy in a network. A large  $GRC$

value indicates that directed paths starting from a small fraction of nodes reach a majority of nodes such that the network has strong hierarchical structure. In particular, if the *GRC* value is equal to unity, the network is the directed outward star, in which a single hub sends a directed link to every other node. The *GRC* is a quantity defined for general directed networks including DAGs.

## **Network motif**

Network motifs are overrepresented small subgraphs in a given network (Milo et al., 2002). Out of the 13 possible directed and weakly connected three-node patterns, only four patterns (motifs 1, 2, 4, and 5 as defined in Milo et al. (2002)) are possible in a DAG. It should be noted that here I am not concerned with the frequency of intransitive triads such as bidirectional links (Lindquist and Chase, 2009) and cycles (Shizuka and McDonald, 2012; Chase, 1980; McDonald and Shizuka, 2013) because my observed networks are (approximately) DAGs (see Results), which are devoid of intransitive triads. I calculate the number of each of the four three-node patterns in the observed networks, thinned linear tournaments, and randomized DAGs. I perform the motif analysis using the *igraph* package implemented in R.

## **Z score**

To assess the significance of the quantities measured for the observed networks, such as *GRC*, I compare them with those calculated for null model networks, which are either thinned linear tournaments or random DAGs. To this end, I calculate the *Z* score, i.e., the distance between, for example, the *GRC* value for the observed network and the mean of *GRC* for the null model divided by the standard deviation of *GRC* for the null model. The mean and standard deviation for the null model are calculated on the basis of  $10^3$  realisations of the null model. A large absolute value of the *Z* score implies that the observed network deviates from the null model in terms of the examined variable, e.g., *GRC*. The *Z* score is conventionally used in the motif analysis (Milo et al., 2002).

## Results

### Observed dominance networks are perfect or approximate DAGs

I observed dominance networks from six colonies. A directed link was assumed between two ants if aggressive behavior between them was observed at least once during the recording period. I also counted the number of aggression in each interacting pair. In the following, I focus on the largest weakly connected component (i.e., connected component when the direction of the links is ignored) of each colony, which I refer to as the dominance network. In fact, the second largest weakly connected component in each colony contained at most two workers, such that it was negligible. The statistics of the six dominance networks is summarized in Table 5-1. Further statistics of the networks (modified Landau's  $h$  index (de Vries, 1995), triangle transitivity metric (Shizuka and McDonald, 2012), and total number of observed interactions) is shown in Table 5-S1. The dominance network contained 24–38% of workers in each colony. The full information about the structure of the six networks and network-related properties of workers used in the following analysis are available as Electronic Supplementary Material.

I mainly analyzed the unweighted directed network (where the number of attacks on each link was reduced to unity). All observed dominance networks apparently had hierarchical structure as shown in Fig. 5-1. They were sparse networks, i.e., only approximately 10% of pairs of workers among the possible pairs interacted, yielding large sparseness values (Table 5-1; the definition of sparseness is given in the table's caption). The triangle transitivity, a measurement of linearity suitable for sparse networks, was equal to unity for five of the six observed networks; they have perfect transitivity. It was equal to 0.96 for the other network (i.e., colony C5).

In fact, the five dominance networks were DAGs. Colony C5 was almost a DAG in the sense that it was a DAG if I removed two bidirectional links (Table 5-1; red thick lines in Figure 5-1(e)). Even this colony did not have any directed cycle of length larger than two, which contrasted to the results of previous studies showing the presence of some cycles in various dominance networks (Shizuka and McDonald, 2012; Chase, 1980;

McDonald and Shizuka, 2013).

### **Purely random sampling of links from a linear tournament does not explain observed dominance networks**

The complementary cumulative distribution of the in-degree (number of other workers that attack a given worker) and that of the out-degree (number of other workers that a worker attacks) are shown in Figure 5-2 (non-cumulative distributions are shown in Figure 5-S3). For all colonies, both in-degree and out-degree were inhomogeneous among workers.

To quantify the heterogeneity in the degree, I measured its CV. I found that the CV values for the in-degree distribution for the observed dominance networks were much smaller than unity (Table 5-1); the in-degree was rather homogeneously distributed. In fact, most workers were attacked by just one or two other workers. In contrast, the CV for the out-degree distribution was much larger than unity in all colonies (Table 5-1). This result implies that some workers have dominated many others, and many workers have dominated few others. The results did not noticeably change upon the removal of the bidirectional links from C5 to make it a DAG (CV = 0.60 and 2.31 for the in- and out-degree, respectively).

Every DAG is consistent with the linear tournament, in which all pairs of individuals interact and are perfectly ranked such that the higher-ranked individual dominates the lower-ranked individual in any pair (Haray and Moser, 1966; Wilson, 1975). However, the observed networks were sparse (i.e., small average degree and large sparseness; see Table 5-1). Therefore, I compared each observed networks with thinned linear tournaments having the same number of nodes and the same expected number of directed links as the observed network.

The CV value for both in-degree and out-degree predicted from the thinned linear tournament (Eq. (5.8)) was equal to 0.98 for C1, 0.93 for C2, 0.81 for C3, 0.87 for C4, 0.85 for C5, and 0.88 for C6. In short, the thinned linear tournament yielded CV values slightly smaller than unity. These CV values were consistently larger than those for the

in-degree and much smaller than those for the out-degree for the observed networks. Therefore, the thinned linear tournament does not explain the observed dominance networks in terms of the CV.

### **Origin of the heterogeneity in the frequency of aggression behavior**

To further understand the origin of the heterogeneity of the out-degree, I classified the workers according to their ranks (determined by the bottom-up leaf-removal algorithm) in the hierarchy and calculated the mean out-degree of the workers having the same rank. In general, multiple workers may possess the same rank. Because this algorithm as well as the reversibility and hierarchy index analyzed in the next section is exclusively applicable to DAGs, I preprocessed colony C5 by removing the two bidirectional links to make it a DAG for the present and following analysis.

The out-degree averaged over the workers with the same rank is plotted against the rank by the squares in Figure 5-3. A small rank value indicates a high rank in the hierarchy. The corresponding results for the thinned linear tournament are shown by the circles in Figure 5-3. The relationship between the out-degree and the rank was dissimilar between the observed networks (squares) and the thinned linear tournament (circles) even if I normalized the rank by the depth of the hierarchy, i.e., the total number of ranks. This result lends another support to my claim that the thinned linear tournament fails to explain the observed data. Figure 5-3 also indicates that the workers with disproportionately large out-degree values have a high but not the highest rank in all colonies.

The out-strength (i.e., the total number of aggression behavior that the worker has exerted on other workers) averaged over the workers with the same rank is plotted against the rank in Figure 5-4. The figure indicates that workers near the top of the hierarchy have disproportionately large out-strength values. In some colonies, the averaged out-strength is the largest at the highest rank. In other colonies, the largest out-strength is realized by a high but not the highest rank, as is the case for the out-degree. To summarize the results shown in Figures 5-3 and 5-4, I conclude that workers near the top of the hierarchy have paid a disproportionately large amount of cost in attacking subordinates.

## **Observed networks resemble randomized DAGs given the in-degree and out-degree of each worker**

In this section, I focus on unweighted dominance networks and examine the proximity of the observed networks, which are (approximate) DAGs, to thinned linear tournaments and randomized DAGs, using the following four types of analysis.

**Reversibility:** First, I measured the reversibility,  $H$ , to evaluate the variety of paths in the DAG. In all observed networks, the  $H$  values were positive (Table 5-2). Then, I calculated the  $Z$  score, i.e., distance between the  $H$  value for the observed network and the mean of  $H$  for the null model (either the thinned linear tournament or randomized DAG) divided by the standard deviation of  $H$  for the null model. For three out of the six colonies, the  $Z$  score was significantly positive when the null model was the thinned linear tournament. However, when the null model was the randomized DAG, the  $Z$  score in four of the five colonies was close to zero such that the observed networks were not significantly different from the randomized DAGs (Table 5-2). It should be noted that, for colony C1, the  $H$  value for any randomized DAG coincided with that for the observed network, making it impossible to calculate the  $Z$  score.

I assumed that directed links emanated from attacking workers to attacked workers. If I adopt the opposite definition for the direction of links (i.e., from attacked to attacking), the  $H$  value is generally altered. Therefore, I carried out the same statistical test for networks in which all links were reversed. The results were qualitatively the same as those for the original networks. In other words, the  $Z$  score was significantly positive and insignificant when the null model was the thinned linear tournament and randomized DAG, respectively (Table 5-S2).

**Hierarchy index:** Second, I measured the hierarchical index,  $\nu$ , to find that  $\nu$  averaged over the six colonies was somewhat positive (mean  $\pm$  SE:  $0.30 \pm 0.07$ ). Therefore, the dominance networks had some hierarchical structure. For four colonies,  $\nu$  was significantly larger for the observed networks than the thinned linear tournaments. However,

for all colonies,  $\nu$  was not significantly different from the value for the randomized DAG (Table 5-2).

Reversing the direction of all links in a given network only flips the sign of  $\nu$ . In addition, the link reversal of a thinned linear tournament is a thinned linear tournament. Therefore, the absolute values of the  $Z$  score calculated for the link-reversed dominance networks were the same as those for the original dominance networks, up to statistical fluctuations (Table 5-S2). In contrast, the randomized DAG is affected by the link reversal because a node generally has different in-degree and out-degree values. I confirmed that the results for the link-reversed networks with the randomized DAG as the null model were qualitatively the same as those for the original networks (Table 5-S2). I conclude that, for a majority of observed networks, the hierarchical structure of the empirical networks is as expected from randomized DAGs.

**Global reaching centrality:** Third, I measured the global reaching centrality,  $GRC$ , to find that the  $GRC$  value was large for all colonies (Mean  $\pm$  SE;  $0.86 \pm 0.04$ ), suggesting hierarchical structure. For all colonies, the  $GRC$  value was significantly larger for the observed network than the thinned linear tournament. However, for all but one colony, the  $GRC$  value was statistically indifferent from that for the randomized DAG (Table 5-2). The results were almost the same when I retained the bidirectional links in C5 ( $GRC = 0.83$ ). The results were also qualitatively the same when the same statistical test was applied to the dominance networks in which the direction of all links was reversed (Table 5-S2).

**Network motif:** Fourth, I carried out motif analysis. The  $Z$  scores for the four three-node patterns are shown in Fig. 5-5. The  $Z$  score was significant for most three-node patterns when the null model was the thinned linear tournament. In contrast, the  $Z$  score was insignificant in most cases when the null model was the randomized DAG.

Reversal of all links in a given network simply swaps motifs 1 and 4, and conserves motifs 2 and 5. Therefore, the link reversal conserved the  $Z$  score when the null model was the thinned linear tournament except for statistical fluctuations and the swapping of the results for motif 1 and those for motif 4 (Figure 5-S4). As shown in the

same figure, the results for the link-reversed networks with the randomized DAG as the null model were qualitatively the same as those for the original networks.

To summarize the analysis of the four quantities in this section, I conclude that the randomized DAG, but not the thinned linear tournament, roughly approximates the observed dominance networks.

## Discussion

I examined dominance networks formed by worker ants. By analysing the dominance networks as directed networks, I reached four main conclusions. First, the observed dominance networks are DAGs or approximately DAGs, which are consistent with perfect linear hierarchy despite their large sizes (Figure 5-1). Second, the out-degree obeys a much more heterogeneous distribution than the in-degree does (Figure 5-2 and Table 5-1). Third, the workers with high ranks showed a larger amount of aggressive behavior than those with low ranks (Figures 5-3 and 5-4). Fourth, the dominance networks are indistinguishable from random DAGs under the condition that the in-degrees and out-degrees of all nodes are given (Figures 5-5 and 5-S4, and Tables 5-2 and 5-S2).

Empirical studies for various species often failed to detect perfect linear hierarchy in particular when networks were large (de Vries, 1995; Chase, 1980; Chase, 1982; Shizuka and McDonald, 2012; McDonald and Shizuka, 2013). In large groups, it would be impossible for individuals to recognize and interact with all other peers (Appleby, 1983; de Vries, 1995; Galimberti et al., 2003; Shizuka and McDonald, 2012). The cost of exerting aggressive behavior (Clutton-Brock et al., 2010; Bell et al., 2012; Nelson-Flower et al., 2013) may also contribute to the sparseness (i.e., low density of links) because the number of potential links per individual linearly increases with group size. For sparse networks, inference of the direction of missing links by previously established methods (Appleby, 1983; de Vries, 1995) may be unreliable (Galimberti et al., 2003; Izar et al., 2006; Klass and Cords, 2011; Shizuka and McDonald, 2012). To overcome this sparseness problem, the frequency of transitive triads (i.e., A dominates B, B dominates C, and A dominates C) has been used as an indicator of linear hierarchy (Chase, 1980; Shizuka and



McDonald, 2012; Dey et al., 2012; McDonald and Shizuka, 2013; Pinter-Wollman et al., 2014). In contrast, I analyzed the dominance networks as DAGs. The triad census and my analysis methods are common in that they are suitable to large and sparse dominance networks. However, the triad census neglects emergent structure derived from a collection of more than three nodes. In contrast, I analyzed global structure of networks to reveal that the observed networks were (approximate) DAGs. More importantly, my approach revealed the depth of hierarchy, hierarchical ranks of individual workers, and workers' behavior depending on the rank. These parameters may be also informative in various biological and nonbiological contexts. In addition, the DAG analysis may be useful when dominance networks are very sparse and the triad census fails to detect significant orderliness of the network due to the paucity of triads. In fact, the  $P$  value for the triangle transitivity metric (Shizuka and McDonald, 2012) was not small enough for C1, C2, C5, and C6 (Table 5-S1). This issue deserves further investigations.

The hierarchical ranking through the leaf-removal algorithm, redundancy, and hierarchy index are exclusively defined for DAGs. Therefore, I cannot immediately apply these methods to other dominance network data that I cannot transform to DAGs by removing just a few links, as I did for C5. Adapting the present methods to such data warrants future work.

It should be noted that the bottom-up leaf-removal algorithm for DAGs used in the present study produced multiple equal ranks, in particular for workers low in the hierarchy. In contrast, other established ranking methods produce a higher uniqueness of ranks, i.e., more different rank values for a given network (Gammell et al., 2003; Hemelrijk et al., 2005). The former may be adequate when pairwise interaction occurs sparsely as in the present study such that the relative strength of many pairs of workers is unclear.

It has been discussed that linearity disappears in large dominance networks for the following proximate reason. In small groups, individuals can easily recognize each other and form a perfectly linear tournament even with a limited cognitive ability (Chase, 1982; Shizuka and McDonald, 2012). In contrast, in large groups, as described above, it would not be possible for individuals to recognize and interact with all other peers

(Appleby, 1983; de Vries, 1995; Galimberti et al., 2003; Shizuka and McDonald, 2012). My colonies contained up to 214 workers. However, the fraction of workers in the colony belonging to the dominance network, including purely subordinate workers, was not large, i.e., 24–38% (Table 5-1). In addition, the number of workers entering the hierarchy (i.e., showing aggressive behavior) was small (5, 10, 11, 8, 18, and 16 workers in colonies C1, C2, C3, C4, C5, and C6, respectively) relative to the colony size. This number would even decrease if I only regard the workers showing frequent aggressive behavior as entering the hierarchy (Monnin et al., 2003). The fact that only a small number of workers entered hierarchy and possibly had to recognize many others might contribute to the resultant nearly perfect linear hierarchy.

The present result that only a small fraction of workers has entered the hierarchy supports the prediction of inclusive fitness models (Monnin and Ratnieks, 1999; Molet et al., 2005) in which workers are assumed to obtain direct fitness benefit by entering the hierarchy while suffer from indirect fitness costs. The prediction that a small fraction of workers enters the hierarchy is also consistent with empirical evidence for other ant species (Cole, 1981; Bourke, 1988; Monnin and Peeters, 1999; Monnin et al., 2003) although the prediction quantitatively differs depending on intracolony relatedness and the offspring sex that workers directly produce (Monnin and Ratnieks, 1999; Molet et al., 2005). Furthermore, the same model (Monnin and Ratnieks, 1999; Molet et al., 2005) predicts that the hierarchy is long for a large colony. This is intuitive because a worker in a large colony represents a small fraction of work force such that a worker joining the hierarchy without working does not much harm the colony. In the present study, the length of the hierarchy was operationally defined as the number of workers showing aggressive behavior or the number of distinct ranks determined by the bottom-up leaf-removal algorithm. The latter quantity was equal to 4, 7, 8, 7, 11, and 8 for C1, C2, C3, C4, C5, and C6, respectively (squares in Figure 5-3). According to either definition of the hierarchy length, the present results are roughly consistent with the theoretical prediction. It should be noted that the observed networks possessed redundancy in terms of the density of links. The minimum number of directed links necessary to maintain a connected DAG is equal to  $N-1$ . In fact,

each observed network had more than twice this number of directed links. Therefore, the observed short length of the hierarchy is not simply due to infrequent interactions.

I found new patterns in dominance networks of *Diacamma* sp. that were not anticipated. In particular, the out-degree was more heterogeneous than the in-degree. This result implies that a relatively few workers near the top of the hierarchy have attacked many workers, whereas many workers has not attacked any others, rendering themselves the most subordinate. The extent of heterogeneity was beyond that expected by the thinned linear tournament. High rankers may accept the cost of attacking because they have high chances to reproduce in this species (Nakata et al., 1996; Kikuchi et al., 2008). However, the high ranked, but not the highest ranked, workers had the largest out-degree on average (Figure 5-3). In three of the six colonies, this property held true even when I counted the total frequency of aggression per worker of a given rank (Figure 5-4). The most dominant workers tended to attack a relatively small number of workers, and the frequency of attacks on each of such subordinate workers was large. In contrast, the high-ranked but not the highest-ranked workers attacked many workers, and the number of attacks on each attacked worker was relatively small. The reason for this difference is unclear. Mathematical models may help explain the rationale behind this observation.

The observed dominance networks did not statistically differ from random DAGs given the in-degree and out-degree of each individual. In this sense, the observed networks may not be so complex as they apparently look. This result coincides with that for acyclic networks investigated in other domains such as citation networks (Karrer and Newman, 2009). The relative simplicity revealed in the present study paves the way to, above all, construction of new generative models for dominance networks and development of statistical procedures to interrogate structure of observed and artificial dominance networks. These tasks as well as clarifying the extent to which my results generalize to other species warrant future work.

The most important limitation of the present study is that I have constructed the dominance networks on the basis of the observation for four days. In fact, dominance networks may be dynamic, as has been reported for interaction networks of ants (Blonder

and Dornhaus, 2011). At the same time, the observed networks seem to grow in terms of the density of links as the observation time increases at least up to four days. Therefore, I should not overemphasize the sparseness of the observed networks. Clarification of this issue requires analysis methods for time-dependent networks (Holme and Saramäki, 2012) in addition to longer longitudinal data.

## Supplementary information

### Randomness of rewired DAGs

The randomness of a DAG generated by the randomisation algorithm (article main text, section 2.6) depends on the number of successful rewiring events. To guarantee that I rewired the links sufficiently many times such that the generated DAG was random enough, I measured the dissimilarity (Goñi et al., 2010) defined as

$$D = \frac{1}{2|E|} \sum_{i,j} [1 - \delta(A_{ij}, A'_{ij})], \quad (5.S1)$$

where  $A = (A_{ij})$  and  $A' = (A'_{ij})$  were the adjacency matrices of the empirical network and the randomized network, respectively, and  $\delta$  is the Kronecker delta. To obtain one random DAG from the degree sequence of an empirical network, I iterated the rewiring process until I successfully rewired the links 5000 times. The mean time courses of  $D$  during the rewiring process are shown in Fig. 5-S2. The figure shows that  $D$  saturates sufficiently fast.

### Definition of reversibility

The reversibility  $H$  is defined as follows (Corominas-Murtra et al., 2010). In a DAG, the maximal node is defined as a node without incoming link, corresponding to the most dominant worker in the colony. There may be multiple maximal nodes in a DAG. I denote the set of all paths (consistent with the direction of links) from any maximal node to node  $i$  by  $\phi(i)$ . Let  $v(\pi_k)$  be the set of nodes participating in path  $\pi_k \in \phi(i)$  except the maximal node.

$P(\pi_k | i)$  represents the probability of the reversed path of path  $\pi_k$  starting from node  $i$  under the unbiased random walk, i.e.,

$$P(\pi_k | i) = \prod_{j \in v(\pi_k)} \frac{1}{d_j^{\text{in}}}, \quad (5.S2)$$

where  $d_j^{\text{in}}$  is the in-degree of node  $j$ . The uncertainty associated with the reversed paths

starting from node  $i$  is defined by

$$H(i) = - \sum_{\pi_k \in \phi(i)} P(\pi_k | i) \log P(\pi_k | i). \quad (5.S3)$$

The average of  $H(i)$  over all non-maximal starting nodes defines the reversibility as follows:

$$H = - \sum_{i \in V \setminus M} \frac{1}{N - |M|} \sum_{\pi_k \in \phi(i)} P(\pi_k | i) \log P(\pi_k | i). \quad (5.S4)$$

Here,  $V = \{1, 2, \dots, N\}$  is the set of nodes,  $M$  is the set of the maximal nodes, and  $|\cdot|$  denotes the number of nodes in the set. In practice, I can efficiently calculate  $H$  from the adjacency matrix (Corominas-Murtra et al., 2010).

### Definition of hierarchy

To define the hierarchy index  $\nu$  (Corominas-Murtra et al., 2011), I first define the minimal node as a node without any outgoing link, corresponding to the most subordinate workers in the colony. The set of the minimal nodes is denoted by  $\mu$ . Similar to equation (S4), the uncertainty value averaged over the minimal nodes, which are used as the starting nodes of paths, is equal to

$$H(\mu) = - \sum_{i \in \mu} \frac{1}{|\mu|} \sum_{\pi_k \in \phi(i)} P(\pi_k | i) \log P(\pi_k | i). \quad (5.S5)$$

The degree of pyramidal structure is defined by

$$H^{\text{fwd}}(M) = - \sum_{i \in M} \frac{1}{|M|} \sum_{\pi_k \in \phi^{\text{fwd}}(i)} P^{\text{fwd}}(\pi_k | i) \log P^{\text{fwd}}(\pi_k | i) \quad (5.S6)$$

and

$$P^{\text{fwd}}(\pi_k | i) = \prod_{j \in \nu^{\text{fwd}}(\pi_k)} \frac{1}{d_j^{\text{out}}}, \quad (5.S7)$$

where  $\phi^{\text{fwd}}(i)$  is the set of all forward paths from  $i$  to a minimal node,  $\nu^{\text{fwd}}(\pi_k)$  is defined as the set of the nodes participating in path  $\pi_k \in \phi^{\text{fwd}}(i)$  except the minimal node, and  $d_j^{\text{out}}$  is the out-degree of node  $j$ . I define the balance between  $H(\mu)$  and  $H^{\text{fwd}}(M)$  as

$$f(G) = \frac{H^{\text{fwd}}(M) - H(\mu)}{\max\{H^{\text{fwd}}(M), H(\mu)\}}. \quad (5.S8)$$

For a later use, I explicitly indicated that  $f$  is a function of a given network  $G$  in equation (S8). The denominator is the normalisation factor to ensure  $-1 \leq f(G) \leq 1$ .

The hierarchical index  $\nu$  is defined as the  $f$  value averaged over the networks obtained in the course of two leaf-removal algorithms. It is given by

$$\nu = \frac{1}{2L-3} \left\{ f(G) + \sum_{i < L-1} [f(G_i) + f(\tilde{G}_i)] \right\}, \quad (5.S9)$$

where  $G_i$  and  $\tilde{G}_i$  are the networks obtained after the application of the first  $i$  rounds of the bottom-up leaf-removal algorithm and the top-down leaf-removal algorithm (i.e., successively removing the nodes without incoming links) to the original network  $G$ , respectively. It should be noted that the number of layers,  $L$ , is the same for the bottom-up and top-down leaf-removal algorithms. The hierarchy index  $\nu$  ranges from  $-1$  to  $1$ . When  $\nu$  is close to  $1$ , the network has pyramidal structure and needs little information for walking backward from the minimal nodes to maximal nodes. In other words, most nodes of the network have one incoming link and multiple outgoing links. Conversely, when  $\nu$  is close to  $-1$ , most nodes have multiple incoming links and one outgoing link.

### **Modified Landau's $h$ index and triangle transitivity metric**

To calculate two orderliness measures for dominance networks, I treat the observed networks as unweighted networks in this section. I regard the two bidirectional links in C5 as unidirectional links by discarding one of the two directions whose link weight is smaller than the other (Appleby, 1983; Shizuka and McDonald, 2012).

The modified Landau's  $h$  index, denoted by  $h'$ , is calculated as follows (de Vries, 1995; Shizuka and McDonald, 2012). First, I fill all the missing dyads randomly. In other words, I assume a unidirectional link in either direction with probability  $1/2$  for all node pairs between which a link is originally absent. The obtained network, which I call the

imputed network according to (Shizuka and McDonald, 2012), is a directed complete graph (also called tournament). Second, I calculate

$$h \equiv \frac{12}{N^3 - N} \sum_{i=1}^N \left( d_i^{\text{out}} - \frac{N-1}{2} \right)^2, \quad (5.S10)$$

where  $d_i^{\text{out}}$  is the out-degree of node  $i$  in the imputed network.  $h$  ranges from 0 to 1, and the perfectly linear tournament yields  $h = 1$ . Finally,  $h'$  is the average of  $h$  over  $10^4$  independent imputed networks. To calculate the  $P$  value for  $h'$  as defined in (de Vries, 1995; Shizuka and McDonald, 2012), I compare each of the  $10^4$  values of  $h$  used for calculating  $h'$  and the  $h$  value calculated for a randomized imputed network. I generate a randomized imputed network by independently reassigning one of the two directions with probability 1/2 to each link in the imputed network, which is the complete graph. To make the comparison  $10^4$  times, I generate  $10^4$  independent randomized imputed networks. Then, I count the fraction of times out of the  $10^4$  times in which  $h$  for the randomized network is larger than or equal to that obtained from the original imputed network. This fraction defines the one-tailed  $P$  value for  $h'$ .

The triangle transitivity metric  $t_{\text{tri}}$  is defined by

$$t_{\text{tri}} = 4 \left( \frac{N_{\text{transitive}}}{N_{\text{transitive}} + N_{\text{cycle}}} - 0.75 \right), \quad (5.S11)$$

where  $N_{\text{transitive}}$  and  $N_{\text{cycle}}$  are the frequencies of transitive triads (i.e., A dominates B, A dominates C, and B dominates C) and cyclic triads (i.e., A dominates B, B dominates C, and C dominates A) in the given dominance network, respectively (Shizuka and McDonald, 2012). A network in which all triangles are transitive yields  $t_{\text{tri}} = 1$ . A random network yields  $t_{\text{tri}} \approx 0$ . To calculate the one-tailed  $P$  value for  $t_{\text{tri}}$ , I generate  $10^3$  random directed networks possessing the same numbers of nodes and links as those of the observed network, calculate  $t_{\text{tri}}$  for each random network, count the number of the random networks yielding  $t_{\text{tri}}$  values larger than or equal to that obtained from the observed network, and divide the count by  $10^3$ .

The values of  $h'$ ,  $t_{\text{tri}}$ , and their  $P$  values for the six colonies are shown in Table 5-S1. It should be noted that these quantities are measured for the largest weakly connected



component of each colony, whose size is shown in Table 5-1. The total number of observed interactions, including those observed in the small components, is also shown in the table. Table 5-S1 indicates that the  $P$  values for  $h'$  and  $t_{tri}$  are larger than or equal to 0.05 (i.e., no significant linearity) except for colonies C3 and C4 (and C5 in case of  $t_{tri}$ ). It should be noted that the  $P$  value for  $t_{tri}$  is large although  $t_{tri}$  for the observed network takes the maximum possible value (i.e., =1) in C1, C2, and C6. This is because randomized networks often yield  $t_{tri} = 1$  owing to the sparseness of the network.

Figure 1

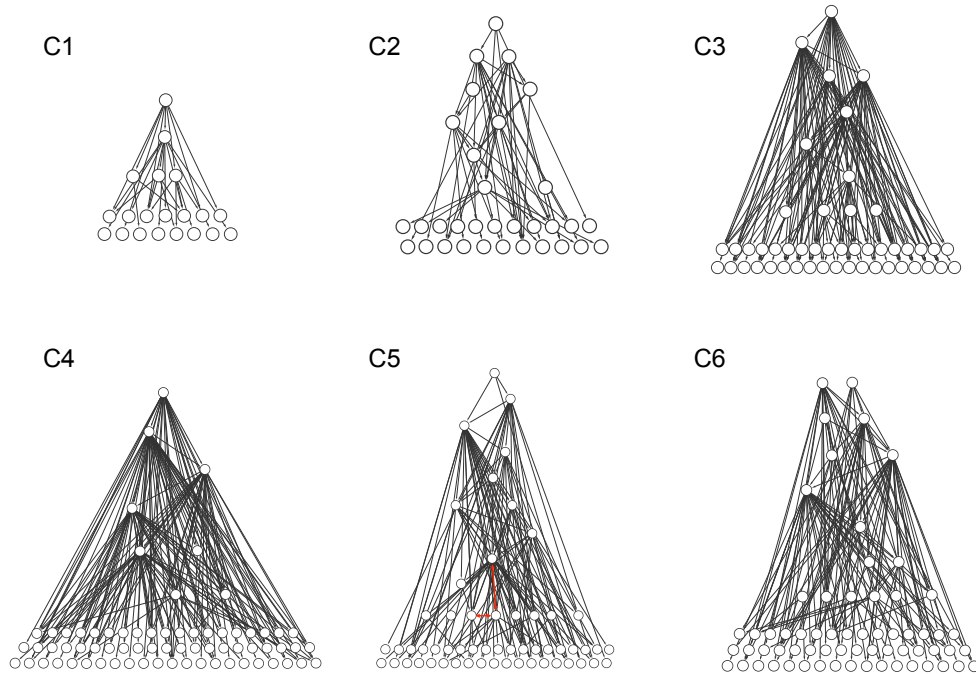


**Figure 5-1. Observed dominance networks.**

Each panel corresponds to a colony. The largest connected component is drawn for each colony. A circle represents a worker. The workers are aligned according to their hierarchical ranks as determined by the bottom-up leaf-removal algorithm. An arrow represents aggressive behavior exerted by an attacking worker toward an attacked worker. The two bidirectional links in C5 are shown by the red thick bidirectional arrows.

Figure 2

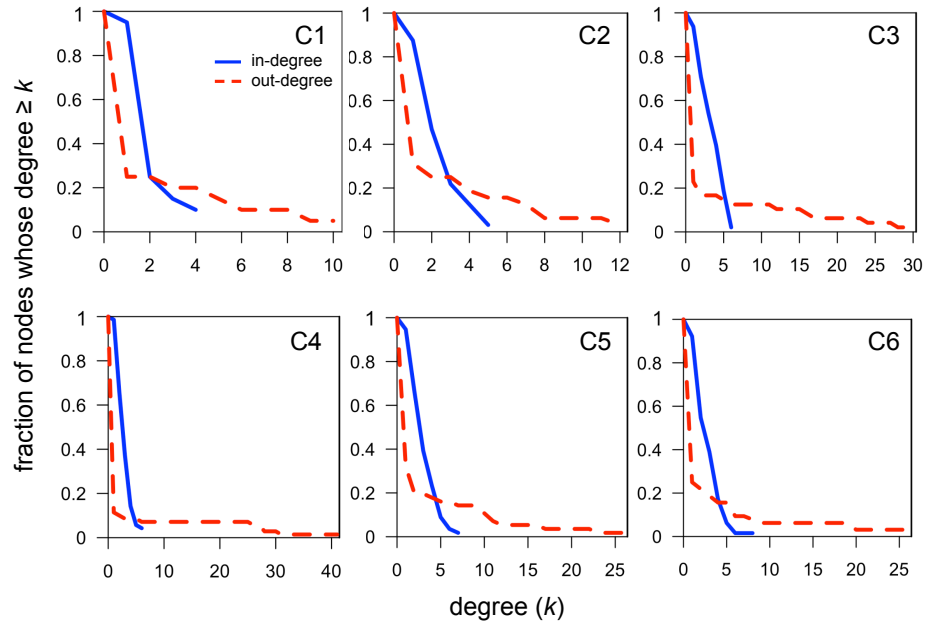


**Figure 5-2. Complementary cumulative distributions of the in-degree and out-degree in dominance networks.**

The fraction of nodes with the in-degree and out-degree larger than or equal to the value shown on the horizontal axis is plotted for the six dominance networks. The solid and dashed lines correspond to the in-degree and out-degree, respectively.

Figure 3

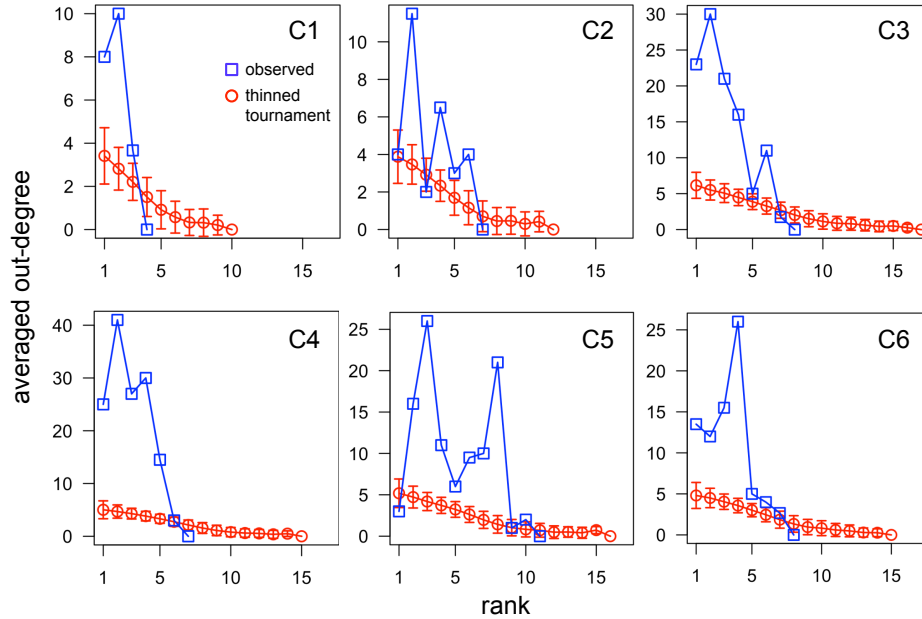


**Figure 5-3. Dependence of the average out-degree on the worker's rank.**

The out-degree averaged over the workers possessing the same rank is plotted against the rank for each colony. The squares and circles represent the results for the observed dominance networks and the corresponding thinned linear tournament averaged over  $10^3$  realisations, respectively. The error bars accompanying the circles represent the standard deviation.

Figure 4

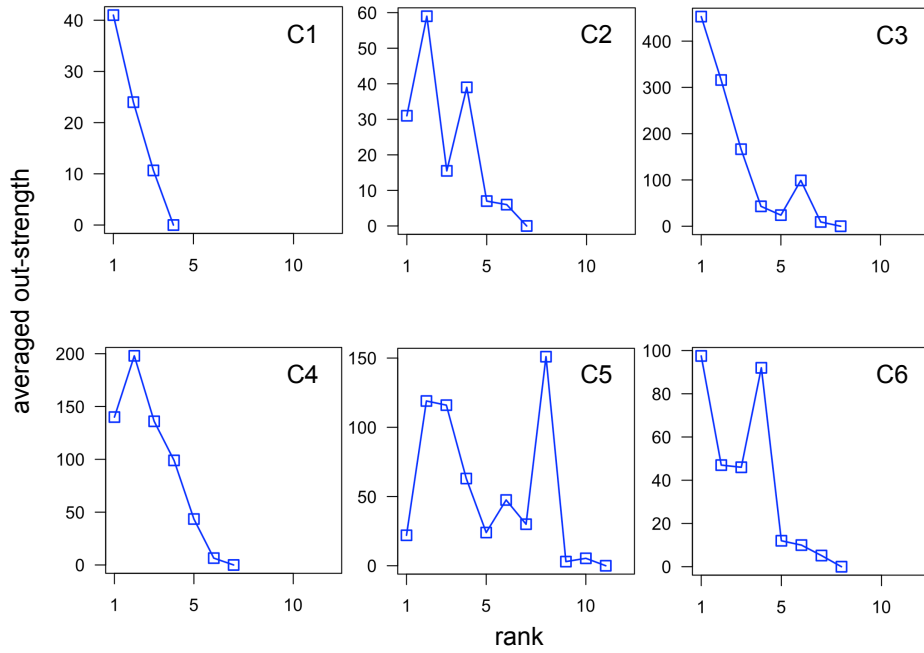


**Figure 5-4. Dependence of the average out-strength on the worker's rank.**

The out-strength, i.e., the sum of the link weights over the outgoing links of a worker, averaged over the workers possessing the same rank is plotted against the rank for each colony.

Figure 5

Colony	Motif 1		Motif 2		Motif 4		Motif 5	
	Thinned tournament	Randomised DAG	Thinned tournament	Randomised DAG	Thinned tournament	Randomised DAG	Thinned tournament	Randomised DAG
C1	6.64**	0.08	-0.99	0.08	-1.46	0.08	0.99	-0.08
C2	7.42**	0.93	1.23	0.93	-2.20*	0.93	4.85**	-0.93
C3	25.91**	-2.14*	-3.31**	-2.14*	-4.81**	-2.14*	13.65**	2.14*
C4	49.23**	-0.45	-1.77	-0.45	-5.25**	-0.45	22.80**	0.45
C5	18.73**	0.99	2.95**	0.99	-4.00**	0.99	13.93**	-0.99
C6	24.67**	1.82	1.91	1.82	-3.32**	1.82	14.22**	-1.82

**Figure 5-5. Results of the motif analysis.**

I calculated the  $Z$  score for the frequency of each three-node network against each null model (i.e., thinned linear tournament or randomized DAG). Asterisks indicate significance levels (\*:  $p < 0.05$ , i.e.,  $|Z| > 1.96$ ; \*\*:  $p < 0.01$ , i.e.,  $|Z| > 2.58$ ).

**Table 5-1. Statistics of observed dominance networks.**

The size represents the number of workers in the colony. The number of nodes represents the number of workers contained in the largest weakly connected component. The other quantities shown in the table are calculated for the largest component. Apart from the largest component, there is a weakly connected component composed of two workers and a directed link between them in C1, C2, C3, and C6. Colonies C4 and C5 contain a unique weakly connected component. The sparseness is defined as the number of noninteracting pairs of workers divided by all possible pairs, i.e.,  $N(N-1)/2$  (Shizuka and McDonald, 2012). The sparseness ranges from 0 to 1, with 0 corresponding to the all-to-all network and 1 to the null network.

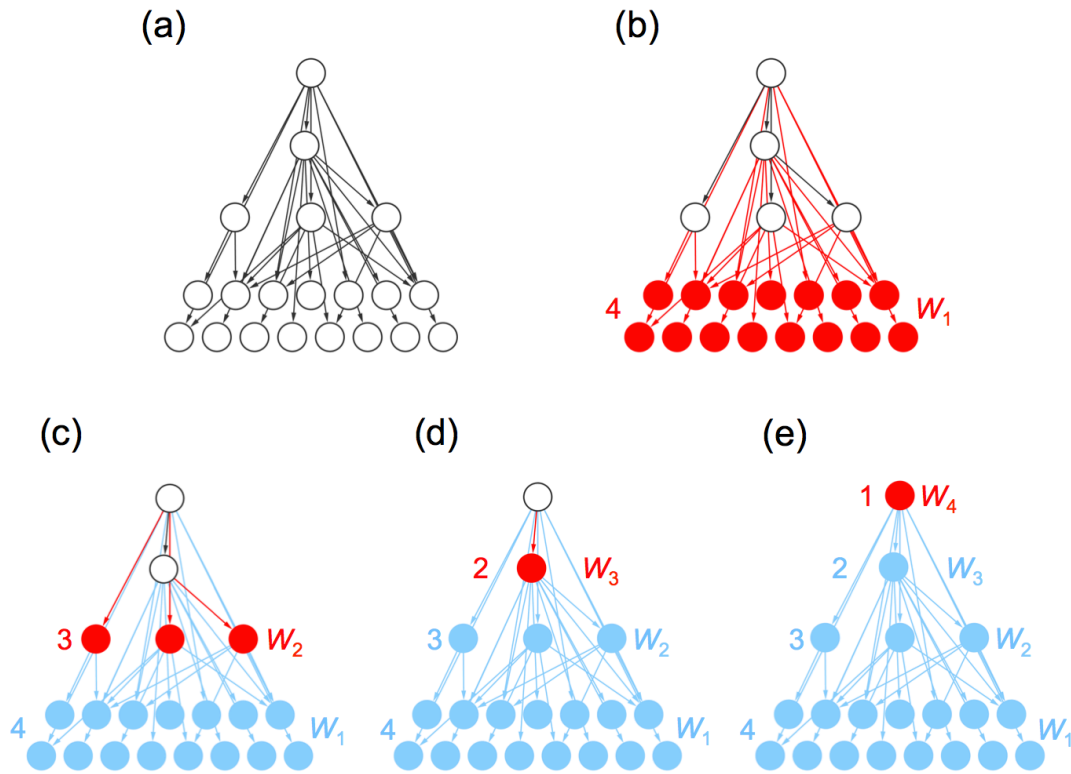
Colony	Size	Number of nodes ( $N$ )	Number of links ( $ E $ )	Average degree	CV of in-degree	CV of out-degree	Bidir. links	Sparseness
C1	58	20	29	2.90	0.71	1.99	0	0.85
C2	132	32	55	3.44	0.73	1.90	0	0.89
C3	149	48	134	5.58	0.58	2.55	0	0.88
C4	183	70	158	4.51	0.58	3.49	0	0.93
C5	200	56	133	4.75	0.64	2.29	2	0.91
C6	214	64	137	4.28	0.71	2.63	0	0.93

**Table 5-2. Statistical results for the reversibility, hierarchy, and global reaching centrality.**

For each index, I calculated the  $Z$  score against each null model (i.e., thinned linear tournament or randomized DAG). The thinned linear tournament and randomized DAG are abbreviated as tournament and DAG in the table. Asterisks indicate significance levels (\*:  $p < 0.05$ , i.e.,  $|Z| > 1.96$ ; \*\*:  $p < 0.01$ , i.e.,  $|Z| > 2.58$ ).

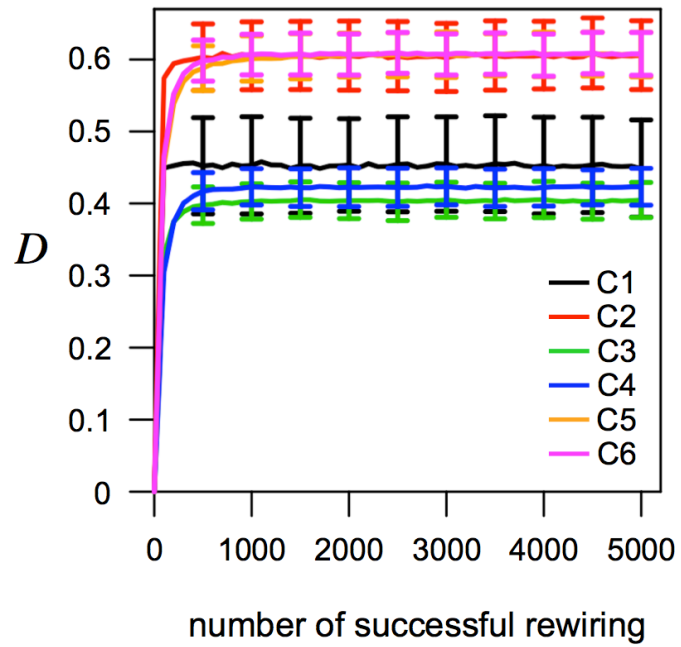
Colony	Reversibility ( $H$ )			Hierarchy ( $v$ )			GRC		
	value	Z score (tournament)	Z score (DAG)	value	Z score (tournament)	Z score (DAG)	value	Z score (tournament)	Z score (DAG)
C1	0.28	-2.36*	-	0.59	3.68**	-0.33	0.94	4.45**	1.01
C2	1.41	1.86	1.76	0.14	1.05	-1.70	0.71	2.72**	-2.11*
C3	1.73	0.24	2.33*	0.31	3.32**	0.05	0.88	4.93**	-1.40
C4	1.33	-0.36	-1.33	0.32	3.90**	-1.08	0.96	6.60**	1.66
C5	2.37	4.98**	0.20	0.28	3.15**	0.74	0.86	4.82**	-0.89
C6	2.02	4.09**	1.69	0.14	1.72	0.66	0.82	4.54**	-0.64





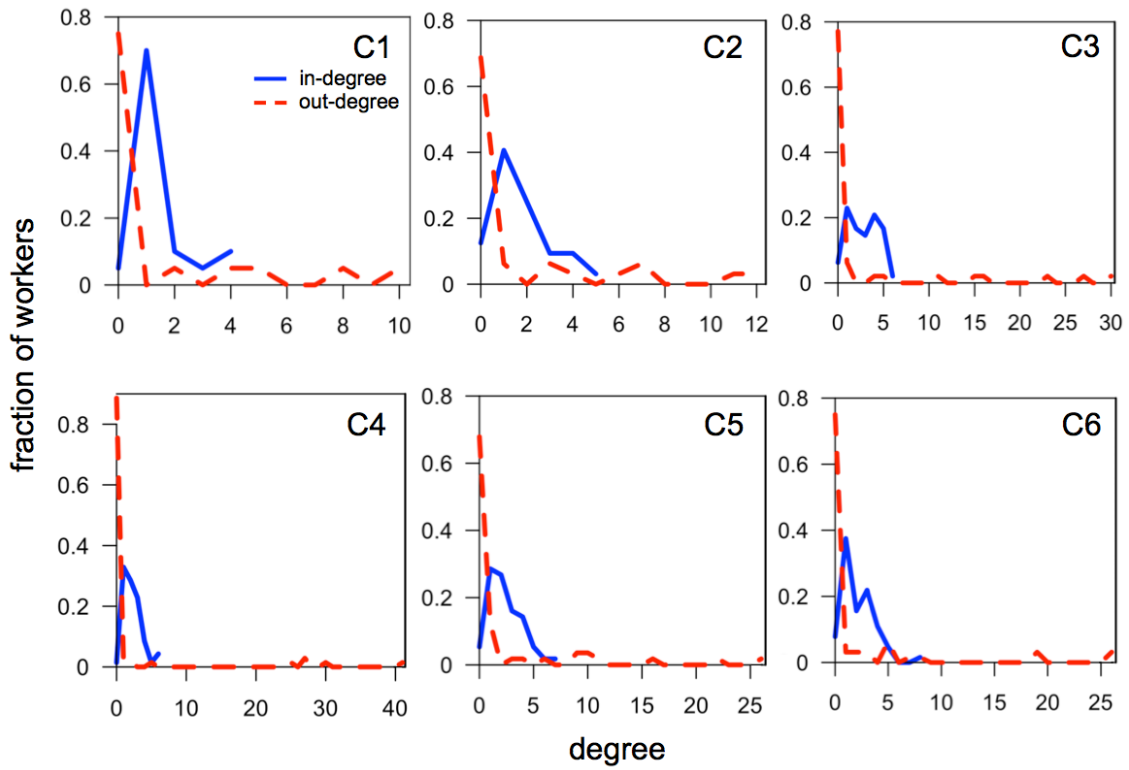
**Figure 5-S1. Bottom-up leaf-removal algorithm.**

(a) Colony C1, replicating the left-top panel in Figure 5-1. In the first step of the algorithm, the nodes shown in red in (b) are removed because their out-degree is equal to zero. These nodes form layer  $W_1$  and in fact receive rank value 4 because it turns out at the end of the algorithm that there are four layers. I also remove the links incident to the removed nodes. Second, the three nodes shown in red in (c) are removed because their out-degree is zero in the reduced network. These nodes form layer  $W_2$  and receive rank value 3. Third, the node shown in red in (d), which constitutes layer  $W_3$  and receives rank value 2, is removed. Finally, the node shown in red in (e), which constitutes layer  $W_4$  and receives rank value 1, is removed.

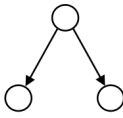
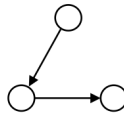
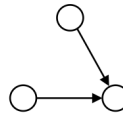
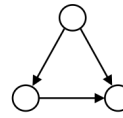


**Figure 5-S2. Time courses of dissimilarity during the rewiring process.**

Each curve represents the time course of the dissimilarity (i.e.,  $D$ ) for one colony averaged over  $10^3$  realisations of the randomisation runs, each starting from the observed network. The error bars represent standard deviations.



**Figure 5-S3. Distributions of the in-degree and out-degree in dominance networks of colonies C1 to C6.**

	Motif 1		Motif 2		Motif 4		Motif 5	
								
Colony	Thinned tournament	Randomised DAG	Thinned tournament	Randomised DAG	Thinned tournament	Randomised DAG	Thinned tournament	Randomised DAG
C1	-1.40	-0.21	-0.96	-0.21	6.84**	-0.21	1.02	0.21
C2	-2.11*	0.67	1.12	0.67	7.17**	0.67	4.73**	-0.67
C3	-4.96**	-2.35*	-3.23**	-2.35*	25.77**	-2.35*	13.79**	2.35*
C4	-5.39**	-0.51	-1.78	-0.51	51.36**	-0.51	22.90**	0.51
C5	-4.04**	0.51	3.05**	0.51	18.59**	0.51	13.41**	-0.51
C6	-3.29**	0.59	1.90	0.59	24.35**	0.59	14.37**	-0.59

**Figure 5-S4. Results of the motif analysis for the link-reversed networks.**

For the networks generated by reversing all links in the observed dominance networks, I calculated the  $Z$  score for the frequency of each motif against each null model (i.e., thinned linear tournament or randomized DAG). Asterisks indicate significance levels (\*:  $p < 0.05$ , i.e.,  $|Z| > 1.96$ ; \*\*:  $p < 0.01$ , i.e.,  $|Z| > 2.58$ ).

**Table 5-S1. Other statistics of observed dominance networks.**

The modified Landau's  $h'$  index,  $h'$ , triangle transitivity metric  $t_{\text{tri}}$ , their  $P$  values, and the total number of observed interactions for each colony are shown. I calculated the number of interactions for the entire colony and the other quantities for the largest weakly connected component of the colony.

<b>Colony</b>	<b><math>h'</math></b>	<b><math>P</math> value for <math>h'</math></b>	<b><math>t_{\text{tri}}</math></b>	<b><math>P</math> value for <math>t_{\text{tri}}</math></b>	<b>Number of interactions</b>
C1	0.21	0.18	1.00	0.39	98
C2	0.12	0.23	1.00	0.23	278
C3	0.13	0.0003	1.00	0.001	1306
C4	0.08	0.0005	1.00	0.029	673
C5	0.07	0.09	0.96	0.024	680
C6	0.07	0.05	1.00	0.053	537

**Table 5-S2. Statistical results for the reversibility, hierarchy, and global reaching centrality for the dominance networks with reversed links.**

See the caption of Table 5-2 for the legends.

Colony	Reversibility ( <i>H</i> )			Hierarchy ( <i>v</i> )			<i>GRC</i>		
	value	Z score (tournament)	Z score (DAG)	value	Z score (tournament)	Z score (DAG)	value	Z score (tournament)	Z score (DAG)
C1	1.76	3.84**	-0.78	-0.59	-3.41**	0.19	0.16	-2.23*	1.10
C2	2.21	5.12**	-0.05	-0.14	-1.04	-0.36	0.14	-2.88**	-2.43*
C3	2.13	2.09*	-0.66	-0.31	-3.32**	-0.98	0.08	-5.83**	-1.29
C4	2.57	6.87**	-0.40	-0.32	-3.91**	-0.41	0.05	-5.09**	-1.10
C5	1.92	2.75**	-2.42*	-0.28	-3.17**	-3.13**	0.12	-4.04**	-1.39
C6	2.06	4.21**	-1.26	-0.14	-1.59	-2.23*	0.11	-4.08**	-1.28

# Chapter 6

## General discussion

The central questions in behavioral science are how and why animals move in nature (Nussbaum, 1978; Nathan et al., 2008). Currently, several fields, including behavioral ecology, neuroscience, and psychology, are trying to address these questions (Krebs and Davies, 1978; Zupanc, 2010). Movement ecology is a novel research area that aims to quantify and analyze movements over a large scale and comprehensively examine the internal and external factors that affect the observed movement patterns (Nathan et al., 2008). Although the effects of individual interactions are crucial to animals, as described in Chapter 1, their relationships are poorly understood. In this thesis, I focused on the movements and individual interactions of animals and investigated the relationships between them.

All animals need to move to search for food, prey, and mates. For two decades, it has been reported that, when animals are searching for something, their movements can be random patterns, such as the movement pattern called the Lévy walk (Viswanathan et al., 1996; Viswanathan et al., 1999; Bartumeus et al., 2003; Sims et al., 2008; Humphries et al., 2010; Raichlen et al., 2014), which was discovered by quantifying the movements of animals in nature. However, this claim has been sometimes questioned (Edwards et al., 2007; Benhamou, 2007; Petrovskii et al., 2011). Previous theoretical studies have reported that Lévy walks have higher encounter rates of targets compared with Brownian walks (Viswanathan et al., 2011). In Chapter 2, I theoretically examined the precise conditions in which the Lévy walk search strategy was superior to the Brownian walk in terms of maximizing fitness. These findings indicated that the parameter range of the Lévy walk was smaller than previously thought, as discussed in Chapter 2. In Chapter 3, I theoretically and empirically analyzed the Lévy walk in terms of an avoidance strategy. This is the first study to analyze the Lévy walk as an avoidance strategy. Thus, I found an evolutionary reason why animals exhibit the Lévy walk. My results in Chapter 2 and 3 addressed the question

of why animals sometimes exhibit the Lévy walk in nature and not in other cases, which suggested the high impact of interactions with predators on optimizing the movements.

In Chapter 2 and 3, I analyzed the spontaneous patterns of an individual movement, and revealed the importance of such patterns in an evolutionary and ecological context. On the one hand, animals in most situations can respond to external stimuli, form memories and change the behavior by the operation of nervous systems and brains (Zupanc, 2010). A number of behavioral scientists have tried to uncover the mechanisms of such an input/output (i.e., stimulus and response) system. The functions of input/output systems are undoubtedly important for animal's survival in the complex and fluctuating environment. Here, the questions arise: how the movement patterns vary by stimuli and how the spontaneous activity interacts with the dynamics of sensory-motor coupling. The studies on movement patterns included the experiment and field study so far. The former limits the scale of experiments. For example, the extremely long straight movements cannot be observed due to the limitation of the experiment apparatus. Moreover, the experiments would include the unnatural conditions. On the other hand, although the latter can reveal the large-scale pattern under natural conditions, the cause of the observed movement patterns includes the several factors. Therefore, to distinguish them, the controlled experiments are needed. Recently, the sophisticated experimental apparatus to solve this problem has developed. For instance, they can propose the virtual reality to the small animals such as insects while the animals can walk on the sphere (Stowers et al., 2014). Consequently, the movement can be tracked at large scale under a controlled condition, so that we can analyze the role and mechanisms of the input/out system and address the above questions. Thus, we could integrate the ultimate and proximate factors.

Animals are likely to have diverse movement patterns depending on the interactions with other individuals or other ecological factors. Therefore, a future research for investigating this involves empirical tests on the effects of the interactions. For example, an interstrain comparison between species living in environments with low- and high-predation pressures might uncover the effects of predators on movement patterns and the evolutionary origin of spontaneous activity. Furthermore, it is worth noting that



spontaneous activity patterns could influence population dynamics, food web stability, and spatial patterns (Nathan et al., 2008). A highly efficient search might lead to instability because very strong interactions between species have been shown to most likely destabilize the equilibrium in the Lotka-Volterra model (May, 1973). Future research topics include theoretically analyzing the effects of movement patterns on such dynamic phenomena. It is expected that this knowledge will enable us to predict and estimate, for example, the density of other species and the food web structure from the movement data of animals. Another role of spontaneous activity to consider is the ability to detect novel resources with learning (i.e., operant conditioning) (Brembs, 2011). Therefore, the phenomena ranging from individual to ecological and evolutionary time scales are critically and inseparably connected through movements and interactions.

Animals often form groups because they can benefit from collective behavior. The sophisticated collective motions of strongly coupled groups, such as schools of fish or flocks of birds, have been analyzed theoretically and empirically (Camazine et al., 2003; Sumpter, 2010; Vicsek and Zafeiris, 2012). In Chapter 4, I investigated weakly coupled groups in terms of dynamics, especially social insects, and proposed a framework for analyzing interactions from the movement data by using Convergent Cross Mapping. This is based on dynamical systems (Sugihara et al., 2012), and it can reveal interaction patterns that cannot be detected from a distance between individuals. The methods can be applied to other animals, and they might detect novel interaction patterns. Previous studies examined the various dynamics, the stable state, the stable limit cycle and chaotic dynamics of social insects at a collective level (Cole, 1991a, b; Boi et al., 1999; Beekman et al., 2001; Nicolis et al., 2013). I observed the periodic and (chaotic) non-periodic dynamics of ant activities from individual movements. Such dynamics might be widespread in animal society. Although periodicity is considered to work as mutual exclusion that can spread cares to more broods (Hatcher et al., 1992), the role of non-periodic dynamics is poorly understood. In that case, the complex dynamics may not be inevitable noise but adaptation to the environment, which raises the open question of how such instability promotes efficient information transfer or division of labor.

In Chapter 5, I observed interactions that were definitely identified as aggressive behavior in ant groups and analyzed them as directed networks. The results showed novel-type networks with clearly hierarchical structures. When studying dominance interactions, most analyses to date have only examined linearity (de Vries, 1995; Shizuka and McDonald, 2012). I developed the new perspective of global network structures, which can characterize the dominance hierarchies of several taxa. In *Diacamma*.sp, workers have reproductive potential, but the dominance hierarchy is considered to serve to prevent workers from reproducing males. The individual at the highest rank can reproduce the male (i.e., direct fitness) before colony fission. If the top individual dies, then the second or third rank individual could become the top individual. A lot of lower rank individuals cannot reproduce males, but receives indirect fitness by working for the colony. Then, how does the hierarchical structure increase the fitness and stabilize the society? The conventional method, calculating linearity of dominance relationship, cannot address this question. Future studies will include the construction of an individual-based model in order to analyze the evolutionary consequences. By evolving the interaction rules of individuals, we will reveal how the network structures emerge from the interactions and how the network structures increase the fitness at group level and stabilize the society. In addition, the meta-analysis allows us for comparison of many types of dominance hierarchy in various species. Shizuka and McDonald (2012) re-analyzed 107 dominance hierarchies obtained from previous papers. Thus, we will discuss the evolutionary implications by comparing network structures (Pasquaretta et al., 2014).

The interaction patterns can be described as networks in a conventional way. The networks observed in Chapter 4 differed from the network that was derived from dominance behavior in Chapter 5 and that had hierarchical structure, which indicated that there may be several relationships on different time scales. This finding corresponds with the idea that networks on multiple scales interact with each other (Flack, 2012), but the interactions between these networks were not clearly detected in my study. Moreover, future topics will include an analysis of how the interaction patterns influence movements

and spatial patterns and should lead to a better understanding of why the interaction patterns emerge from an evolutionary perspective.

Moreover, the robustness of the collective properties such as networks and dynamics is less understood in my study. The perturbation to individuals or knockout of an individual may alter these patterns (Flack et al., 2006). If the patterns are robust to the perturbation, it is considered to be essentially important for the group. We must find the relationship between collective properties and environmental variables.

Collective behavior is considered to have the advantage such as efficient foraging or predator avoiding in a group level. However, there are few direct evidences of relationship between collective behavior and fitness. For ant colonies, we need to analyze the colony size and reproduction rate as fitness to claim the importance of interaction patterns observed in my study. One possible method may be the long-term observation by a novel method discussed below.

The automatic quantification of the movements and interactions of individuals at the individual level and at the collective level is a challenging task (Dell et al., 2014). The performance of machine learning that can detect specific patterns in a movie and method to analyze the movement data have recently improved (Takahashi et al., 2008; Horibe, 2011; Viswanathan et al., 2011; Sugihara et al., 2012; Kabra et al., 2013; Dell et al., 2014). Future studies focusing on the detection of movements and interactions in heterogeneous environments and differentiation of the various kinds of interactions based on long-term observation data will lead to a better understanding of how and why animals move.

# Acknowledgement

I would like to show my sincerest appreciation to Prof. Masakazu Shimada for all kinds of helps and advices throughout this study.

I wish to thank Prof. Takehito Yoshida and Prof. Takashi Ikegami for valuable discussions. Since my research life started, they have continued to encourage me.

I am grateful to all other members of the jury for their evaluation of this thesis and their valuable opinion. They are Prof. Akira Sasaki and Prof. Michio Kondoh.

I wish to express my gratitude to Minoru Kasada, Prof. Naoki Masuda, Dr. Hiroyuki Shimoji, Prof. Kazuki Tsuji, Dr. Shin-ichiro Nakayama, Haruna Fujioka and Prof. Yasukazu Okada for their collaboration. In particular, the discussions with Minoru Kasada led me to an exciting scientific world.

I wish to thank Prof. Shigeto Dobata, Dr. Naoto Horibe and Prof. Yoshito Hirata for fruitful advices and discussions. I also thank Hisashi Murakami, Dr. Yuta Nishiyama, Kotaro Kagawa, Yutaka Osada and Kazeto Shimonishi for interesting discussions and study sessions.

I wish to thank all members of Shimada laboratory and Yoshida laboratory for helpful discussion and encouragement.

I would like to show my appreciation to SYMAP (Satoshi Kobayashi, Yuji Yamauchi, Minoru Kasada, Koji Pedio Nishimura). I have developed through friendly competition with them.

Finally, I would like to express my heartfelt gratitude to my family.

January, 2015

Masato Abe

## References

- Appleby MC (1983) The probability of linearity in hierarchies. *Anim. Behav.* 31: 600–608.
- Barabási AL (2005) The origin of bursts and heavy tails in human dynamics. *Nature* 435: 207–211.
- Bartumeus F, Catalan J, Fulco UL, Lyra ML, Viswanathan GM (2002) Optimizing the encounter rate in biological interactions: Lévy versus Brownian strategies. *Phys. Rev. Lett.* 88: 097901.
- Bartumeus F, Peters F, Pueyo S, Marrasé C, Catalan J (2003) Helical Lévy walks: Adjusting searching statistics to resource availability in microzooplankton. *Proc. Natl. Acad. Sci. USA* 100: 12771–12775.
- Bartumeus F, da Luz MGE, Viswanathan GM, Catalan J (2005) Animal search strategies: A quantitative random-walk analysis. *Ecology* 86: 3078–3087.
- Bartumeus F, Levin SA (2008) Fractal reorientation clocks: Linking animal behavior to statistical patterns of search. *Proc. Natl. Acad. Sci. USA* 105: 19072–19077.
- Beekman M, Sumpter DJT, Ratnieks LW (2001) Phase transition between disordered and ordered foraging in Pharaoh's ants. *Proc. Natl. Acad. Sci. USA* 98: 17.
- Bell MBV, Nichols HJ, Gilchrist JS, Cant MA, Hodge SJ (2012) The cost of dominance: suppressing subordinate reproduction affects the reproductive success of dominant female banded mongooses. *Proc. R. Soc. B* 279: 619–624.
- Benhamou S (2007) How many animals really do the Lévy walk? *Ecology* 88: 1962–1969.
- Bénichou O, Loverdo C, Moreau M, Voituriez R (2011) Intermittent search strategies. *Rev. Mod. Phys.* 83: 81–129.
- Blonder B, Dornhaus A (2011) Time-ordered networks reveal limitations to information flow in ant colonies. *PLoS ONE* 6: e20298.
- Boi S, Couzin ID, Buono ND, Franks NR, Britton NF (1999) Coupled oscillators and activity waves in ant colonies. *Proc. R. Soc. B* 266: 371–378.
- Bonabeau E, Dorigo M, Theraulaz G (2000) Inspiration for optimization from social insect

- behaviour. *Nature* 406: 39–42.
- Bourke AFG (1988) Dominance orders, worker reproduction, and queen-worker conflict in the slave-making ant *Harpagoxenus sublaevis*. *Behav. Ecol. Sociobiol.* 23: 323–333.
- Bourke AFG, Franks NR (1995) *Social Evolution in Ants*. Princeton, NJ: Princeton University Press.
- Bourke AFG (2011) *Principles of Social Evolution*. Oxford: Oxford University Press.
- Brembs B (2011) Towards a scientific concept of free will as a biological trait: spontaneous actions and decision-making in invertebrates. *Proc. R. Soc. B* 278: 930–939.
- van den Broek B, Lomholt MA, Kalisch S-MJ, Metzler R, Wuite GJL (2008) How DNA coiling enhances target localization by proteins. *Proc. Natl. Acad. Sci. USA* 105: 15738–15742.
- Butail S, Ladu F, Spinello D, Porfiri (2014) Information flow in animal-robot interactions. *Entropy* 16: 1315–1330.
- Camazine S, Deneubourg JL, Franks NR, Sneyd J, Theraulaz G et al. (2003) *Self-organization in biological systems*. New Jersey: Princeton University Press.
- Castellano C, Fortunato S, Loreto V (2009) Statistical physics of social dynamics. *Rev. Mod. Phys.* 81: 591–646.
- Cavagna A, Cimarelli A, Giardina I, Parisi G, Santagati R et al. (2010) Scale-free correlations in starling flocks. *Proc. Natl. Acad. Sci. USA* 107: 11865–11870.
- Charnov EL (1976) Optimal foraging, the marginal value theorem. *Theor. Popul. Biol.* 9: 129–136.
- Chase ID (1980) Social process and hierarchy formation in small groups: a comparative perspective. *Am. Sociol. Rev.* 45: 905–924.
- Chase ID (1982) Dynamics of hierarchy formation: the sequential development of dominance relationships. *Behaviour* 80: 218–240.
- Chen X, Dong X, Be'er A, Swinney HL, Zhang HP (2012) Scale-invariant correlations in dynamic bacterial clusters. *Phys. Rev. Lett.* 108: 148101.
- Clutton-Brock TH, Brotherton PNM, Russell AF, O'Riain MJ, Gaynor D, et al. (2001)

- Cooperation, control, and concession in meerkat groups. *Science* 291: 478–481.
- Clutton-Brock TH, Hodge SJ, Flower TP, Spong GF, Young AJ (2010) Adaptive suppression of subordinate reproduction in cooperative mammals. *Am. Nat.* 176: 664–673.
- Cohen JE, Newman CM (1985) A stochastic theory of community food webs: I. Models and aggregated data. *Proc. R. Soc. B* 224: 421–448.
- Cole BJ (1981) Dominance hierarchies in *Leptothorax* ants. *Science* 212: 83–84.
- Cole BJ (1986) The social behavior of *Leptothorax allardycei* (Hymenoptera, Formicidae): time budgets and the evolution of worker reproduction. *Behav. Ecol. Sociobiol.* 18: 165–173.
- Cole BJ (1991a) Short-term activity cycles in ants: Generation of periodicity by worker interaction. *Am. Nat.* 137: 244–259.
- Cole BJ (1991b) Is animal behaviour chaotic? Evidence from the activity of ants. *Proc. R. Soc. B* 244: 253–259.
- Cole BJ (1995) Fractal time in animal behaviour: The movement activity of *Drosophila*. *Anim. Behav.* 50: 1317–1324.
- Corominas-Murtra B, Rodríguez-Caso C, Goñi J, Solé R (2010) Topological reversibility and causality in feed-forward networks. *New J. Phys.* 12: 113051.
- Corominas-Murtra B, Rodríguez-Caso C, Goñi J, Solé R (2011) Measuring the hierarchy of feedforward networks. *Chaos* 21: 016108.
- Couzin ID, Krause J (2003) Self-organization and collective behavior in vertebrates. *Advances in the study of behavior* 32: 1–75.
- Couzin ID, Franks NR (2003) Self-organized lane formation and optimized traffic flow in army ants. *Proc. R. Soc. B* 270: 139–146.
- Couzin ID, Krause J, Franks NR, Levin SA (2006) Effective leadership and decision-making in animal groups on the move. *Nature* 433: 513–516.
- van Dartel M, Postma E, van den Herik J, de Croon G (2004) Macroscopic analysis of robot foraging behaviour. *Connect. Sci.* 16: 169–181.
- Delgado J and Solé RV (2000) Self-synchronization and task fulfillment in ant colonies. *J.*

- Theor. Biol. 205: 433–441.
- Dell AI, Bender JA, Branson K, Couzin ID, de Polavieja GG, et al. (2014) Automated image-based tracking and its application in ecology. *Trends. Ecol. Evol.* 29: 417–428.
- Dey CJ, Reddon AR, O'Connor CM, Balshine S (2012) Network structure is related to social conflict in a cooperatively breeding fish. *Anim. Behav.* 85: 395–402.
- Domenici P, Booth D, Blagburn JM, Bacon JP (2008) Cockroaches keep predators guessing by using preferred escape trajectories. *Curr. Biol.* 18: 1792–1796.
- Domenici P, Blagburn JM, Bacon JP (2011a) Animal escapology I: theoretical issues and emerging trends in escape trajectories. *J. Exp. Biol.* 214: 2463–2473.
- Domenici P, Blagburn JM, Bacon JP (2011b) Animal escapology II: escape trajectory case studies. *J. Exp. Biol.* 214: 2474–2494.
- Drews C (1993) The concept and definition of dominance in animal behaviour. *Behaviour* 125: 283–313.
- Eades P, Lin X, Smyth WF (1993) A fast and effective heuristic for the feedback arc set problem. *Info. Process. Lett.* 47: 319–323.
- Earley RL, Dugatkin LA (2010) Behavior in Group. In *Evolutionary Behavioral Ecology* (ed. D. F. Westneat & C. W. Fox), pp. 285–307. Oxford: Oxford University Press.
- Edwards AM, Phillips RA, Watkins NW, Freeman MP, Murphy EJ, et al. (2007) Revisiting Lévy flight search patterns of wandering albatrosses, bumblebees and deer. *Nature* 449: 1044–1048.
- Einstein A (1905) On the movement of small particles suspended in stationary liquids required by the molecular-kinetic theory of heat. *Ann. Phys.* 17: 549–560.
- Faustino CL, da Silva LR, da Luz MGE, Raposo EP, Viswanathan GM (2007) Search dynamics at the edge of extinction: Anomalous diffusion as a critical survival state. *Europhys. Lett.* 77: 30002.
- Flack JC, Girvan M, de Waal FBM, Krakauer DC (2006) Policing stabilizes construction of social niches in primates. *Nature* 439: 426–429.
- Flack JC (2012) Multiple time-scales and the developmental dynamics of social systems. *Phil. Trans. R. Soc. B* 367: 1802–1810.



- Fukumoto Y, Abe T, Taki A (1989) A novel form of colony organization in the “queenless” ant *Diacamma rugosum*. *Physiol. Ecol. Japan* 26: 55–61.
- Gadau J, Fewell J (2009) Organization of insect societies: From genome to sociocomplexity. Cambridge, MA: Harvard University Press.
- Galimberti F, Fabiani A, Boitani L (2003) Socio-spatial levels in linearity analysis of dominance hierarchies: a case study on elephant seals. *J. Ethol.* 21: 131–136.
- Gammell MP, de Vries H, Jennings DJ, Carlin CM, Hayden TJ (2003) David’s score: a more appropriate dominance ranking method than Clutton-Vrock et al.’s index. *Anim. Behav.* 66: 601–605.
- Getz WM, Saltz D (2008) Movement ecology special feature: A framework for generating and analyzing movement paths on ecological landscapes. *Proc. Natl. Acad. Sci. USA* 105: 19066–19071.
- Gobin B, Ito F (2003) Sumo wrestling in ants: major workers fight over male production in *Acanthomyrmex ferox*. *Naturwissenschaften* 90: 318–321.
- Goñi J, Corominas-Murtra B, Solé RV, Rodríguez-Caso C (2010) Exploring the randomness of directed acyclic networks. *Phys. Rev. E* 82: 066115.
- Goss S, Aron S, Deneubourg JL, Pasteels JM (1989) Self-organized shortcuts in the Argentine ant. *Naturwissenschaften* 76: 579–581.
- Granger CWJ (1969) Investigating causal relations by econometric models and cross-spectral methods. *Econometrica* 37: 424–438
- Haefner JW, Crist TO (1994) Spatial model of movement and foraging in harvester ants (*Pogonomyrmex*) (I): The roles of memory and communication. *J. Theor. Biol.* 166: 299–313.
- Hamilton WD (1964a) The genetical evolution of social behaviour. I. *J. Theor. Biol.* 7: 1–16.
- Hamilton WD (1964b) The genetical evolution of social behaviour. II. *J. Theor. Biol.* 7: 17–52.
- Harary F, Moser L (1966) The theory of round robin tournaments. *Am. Math. Month.* 73: 231–246.

- Harris TH, Banigan EJ, Christian DA, Konradt C, Wojno EDT, et al. (2012) Generalized Lévy walks and the role of chemokines in migration of effector CD8<sup>+</sup> T cells. *Nature* 486: 545–548.
- Hatcher MJ, Tofts C, Franks NR (1992) Mutual exclusion as a mechanism for information exchange within ant nests. *Naturwissenschaften* 79: 32–34.
- Hays GC, Bastian T, Doyle TK, Fossette S, Gleiss AC, et al. (2012) High activity and Lévy searches: Jellyfish can search the water column like fish. *Proc. R. Soc. B* 279: 465–473.
- Heinze J, Puchinger W, Hölldobler B (1997) Worker reproduction and social hierarchies in *Leptothorax* ants. *Anim. Behav.* 54: 849–864.
- Hemelrijk CK, Wantia J, Gygax L (2005) The construction of dominance order: comparing performance of five methods using an individual-based model. *Behaviour* 142: 1037–1058.
- Hidalgo J, Grilli J, Suweis S, Muñoz MA, Banavar JR et al. (2014) Information-based fitness and the emergence of criticality in living systems. *Proc. Natl. Acad. Sci. USA* 111: 10095–10100.
- Holme P, Saramäki J (2012) Temporal networks. *Phys. Rep.* 519: 97–125.
- Horibe N (2011) Theoretical analysis of living and non-living systems with memory structure. PhD thesis. The University of Tokyo.
- Humphries DA, Driver PM (1970) Protean defence by prey animals. *Oecologia* 5: 285–302.
- Humphries NE, Queiroz N, Dyer JRM, Pade NG, Musyl MK, et al. (2010) Environmental context explains Lévy and Brownian movement patterns of marine predators. *Nature* 465: 1066–1069.
- Humphries NE, Weimerskirch H, Queiroz N, Southall EJ, Sims DW (2012) Foraging success of biological Lévy flights recorded in situ. *Proc. Natl. Acad. Sci. USA* 109: 7169–7174.
- Ishii Y, Shimada M (2012) Learning predator promotes coexistence of prey species in host-parasitoid systems. *Proc. Natl. Acad. Sci.* 109: 5116–5120.
- Izar P, Ferreira RG, Sato T (2006) Describing the organization of dominance relationships

- by dominance-directed tree method. *Am. J. Primatol.* 68: 189–207.
- de Jager M, Weissing FJ, Herman PMJ, Nolet BA, van de Koppel J (2011) Lévy walks evolve through interaction between movement and environmental complexity. *Science* 332: 1551–1553.
- de Jager M, Bartumeus F, Kölzsch A, Weissing FJ, Hengeveld GM, et al. (2014) How superdiffusion gets arrested: ecological encounters explain shift from Lévy to Brownian movement. *Proc. R. Soc. B* 281: 20132605.
- Proekt A, Banavar JR, Maritan A, Pfaff DW (2012) Scale invariance in the dynamics of spontaneous behavior. *Proc Natl Acad Sci USA* 109: 10564–10569.
- Kabra M, Robie AA, Rivera-Alba M, Branson S, Branson K (2013) JAABA: interactive machine learning for automatic annotation of animal behavior. *Nature Methods* 10: 66–70.
- Kaneko K (1990) Clustering, coding, switching, hierarchical ordering, and control in a network of chaotic elements. *Physica D* 41: 137–172.
- Karrer B, Newman MEJ (2009) Random graph models for directed acyclic networks. *Phys. Rev. E* 80: 046110.
- Katz Y, Tunsrøm K, Ioannou CC, Huepe C, Couzin ID (2011) Inferring the structure and dynamics of interactions in schooling fish. *Proc. Natl. Acad. Sci. USA* 108: 18720–18725.
- Kawabata S, Tsuji K (2005) The policing behavior “immobilization” towards ovary-developed workers in the ant, *Diacamma* sp. from Japan. *Ins. Soc.* 52: 89–95.
- Keller L, Reeve HK (1999) Dynamics of Conflicts within insect societies. In *Levels of Selection in Evolution* (ed. L. Keller), pp. 153–175. Princeton, NJ: Princeton University Press.
- Kikuchi T, Nakagawa T, Tsuji K (2008) Changes in relative importance of multiple social regulatory forces with colony size in the ant *Diacamma* sp. from Japan. *Anim. Behav.* 76: 2069–2077.
- Klass K, Cords M (2011) Effect of unknown relationships on linearity, steepness and rank ordering of dominance hierarchies: Simulation studies based on data from wild

- monkeys. *Behav. Proc.* 88: 168–176.
- Kondoh M (2003) Foraging adaptation and the relationship between food-web complexity and stability. *Science* 299: 1388–1391.
- Krebs JR, Davies NB (1978) *Behavioural ecology: An evolutionary approach*. New Jersey: Wiley-Blackwell.
- Lenz F, Ings T, Chittka L, Chechkin A, Klages R (2012) Spatiotemporal dynamics of bumblebees foraging under predation risk. *Phys. Rev. Lett.* 108: 098103.
- Li L, Peng H, Kurths J, Yang Y, Schellnhuber HJ (2014) Chaos-order transition in foraging behavior of ants. *Proc. Natl. Acad. Sci. USA* 111: 23.
- Lima SL, Valone TJ, Caraco T (1985) Foraging-efficiency-predation-risk trade-off in the grey squirrel. *Anim. Behav.* 33: 155–165.
- Lindquist WB, Chase ID (2009) Data-based analysis of winner-loser models of hierarchy formation in animals. *Bull. Math. Biol.* 71: 556–584.
- Ma HW, Buer J, Zeng AP (2004) Hierarchical structure and modules in the *Escherichia coli* transcriptional regulatory network revealed by a new top-down approach. *BMC Bioinformatics* 5: 199.
- MacArthur RH, Pianka ER (1966) On optimal use of a patchy environment. *Am. Nat.* 100: 603–609.
- Martin JR, Faure P, Ernst R (2001) The power law distribution for walking-time intervals correlates with the ellipsoid-body in *Drosophila*. *J. Neurogenet.* 15: 205–219.
- May RM (1973) *Stability and complexity in model ecosystem*. New Jersey: Princeton University Press.
- May RM (2006) Network structure and the biology of populations. *Trends. Ecol. Evol.* 21: 394–399.
- Maye A, Hsieh CH, Sugihara G, Brembs B (2007) Order in spontaneous behavior. *PLoS ONE* 2: e443.
- Mischiati M, Lin HT, Herold P, Imler E, Olberg R, et al. (2015) Internal models direct dragonfly interception steering. *Nature* 517: 333–338.
- McDonald DB, Shizuka D (2013) Comparative transitive and temporal orderliness in

- dominance networks. *Behav. Ecol.* 24: 511–520.
- Mersch DP, Crespi A, Keller L (2013) Tracking individuals shows spatial fidelity is a key regulator of ant social organization. *Science* 340: 1090–1093.
- Milo R, Shen-Orr S, Itzkovitz S, Kashtan N, Chklovskii D, et al. (2002) Network motifs: simple building blocks of complex networks. *Science* 298: 824–827.
- Miramontes O, Solé RV, Goodwin BC (1993) Collective behaviour of random-activated mobile cellular automata. *Physica D* 63:145–160.
- Molet M, Van Baalen M, Monnin T (2005) Dominance hierarchies reduce the number of hopeful reproductives in polygynous queenless ants. *Ins. Soc.* 52: 247–256.
- Mones E, Vicsek L, Vicsek T (2012) Hierarchy measure for complex networks. *PLOS ONE* 7: e33799.
- Monnin T, Peeters C (1999) Dominance hierarchy and reproductive conflicts among subordinates in a monogynous queenless ant. *Behav. Ecol.* 10: 323932.
- Monnin T, Ratnieks FLW (1999) Reproduction versus work in queenless ants: when to join a hierarchy of hopeful reproductives? *Behav. Ecol. Sociobiol.* 46: 413–422.
- Monnin T, Ratnieks FLW, Brandão CRF (2003) Reproductive conflict in animal societies: hierarchy length increases with colony size in queenless ponerine ants. *Behav. Ecol. Sociobiol.* 54: 71–79.
- Nagy M, Ákos Z, Biro D, Vicsek T (2010) Hierarchical group dynamics in pigeon flocks. *Nature* 464: 890–893.
- Nahin PJ (2007) *Chases and escapes: The mathematics of pursuit and evasion*. New Jersey: Princeton University Press.
- Nakata K, Tsuji K (1996) The effect of colony size on conflict over male-production between gamergate and dominant workers in the ponerine ant *Diacamma* sp. *Ethol. Ecol. Evol.* 8: 147–156.
- Nathan R, Getz WM, Revilla E, Holyoak M, Kadmon R, et al. (2008) A movement ecology paradigm for unifying organismal movement research. *Proc. Natl. Acad. Sci. USA* 105: 19052–19059.
- Nelson-Flower MJ, Hockey PAR, O'Ryan C, English S, Thompson AM, et al. (2013)

- Costly reproductive competition between females in a monogamous cooperatively breeding bird. *Proc. R. Soc. B* 280: 20130728.
- Nicolis SC, Fernández J, Pérez-Penichet C, Noda C, Tejera F, et al. (2013) Foraging at the edge of chaos: Internal clock versus external forcing. *Phys. Rev. Lett.* 110: 268104.
- Nowak MA (2006) Five rules for the evolution of cooperation. *Nature* 314: 1560–1563.
- Nussbaum MC (1978) *Aristotle's De Motu Animalium*. Princeton, NJ: Princeton University Press.
- Pasquaretta C, Levé M, Claidière N, van de Waal, Whiten A et al. (2014) Social networks in primates: smart and tolerant species have more efficient networks. *Sci. Rep.* 4: 7600.
- Peeters C, Crewe R (1984) Insemination controls the reproductive division of labour in a ponerine ant. *Naturwissenschaften* 71: 50–51.
- Peeters C, Tsuji K (1993) Reproductive conflict among ant workers in *Diacamma* sp. from Japan: dominance and oviposition in the absence of the gamergate. *Ins. Soc.* 40: 119–136.
- Petrovskii S, Mashanova A, Jansen VAA (2011) Variation in individual walking behavior creates the impression of a Lévy flight. *Proc. Natl. Acad. Sci. USA* 108: 8704–8707.
- Pinter-Wollman N, Wollman R, Guetz A, Holmes S, Gordon DM (2011) The effect of individual variation on the structure and function of interaction networks in harvester ants. *J. R. Soc. Interface* 8: 1562–1573.
- Pinter-Wollman N, Hobson EA, Smith JE, Edelman AJ, Shizuka D, et al. (2014) The dynamics of animal social networks: analytical, conceptual, and theoretical advances. *Behav. Ecol.* 25: 242–255.
- Proekt A, Banavar JR, Maritan A, Pfaff DW (2012) Scale invariance in the dynamics of spontaneous behavior. *Proc. Natl. Acad. Sci. USA* 109: 10564–10569.
- Queller DC, Zacchi F, Cervo R, Turillazzi S, Henshaw MT, et al. (2000) Unrelated helpers in a social insect. *Nature* 405: 784–787.
- Raichlen DA, Wood BM, Gordon AD, Mabulla AZP, Marlowe FW, et al. (2014) Evidence of Lévy walk foraging patterns in human hunter-gatherers. *Proc. Natl. Acad. Sci. USA*

111: 728–733.

- Raposo EP, Buldyrev SV, da Luz MGE, Santos MC, Stanley HE, et al. (2003) Dynamical robustness of Lévy search strategies. *Phys. Rev. Lett.* 91: 240601.
- Raposo EP, Bartumeus F, da Luz MGE, Ribeiro-Neto PJ, Souza TA, et al. (2011) How landscape heterogeneity frames optimal diffusivity in searching processes. *PLoS Comput. Biol.* 7: e1002233.
- Ratnieks FLW (1988) Reproductive harmony via mutual policing by workers in eusocial Hymenoptera. *Am. Nat.* 132: 217–236.
- Reynolds AM, Frye MA (2007) Free-flight odor tracking in *Drosophila* is consistent with an optimal intermittent scale-free search. *PLoS ONE* 2: e354.
- Reynolds AM, Smith AD, Reynolds DR, Carreck NL, Osborne JL (2007) Honeybees perform optimal scale-free searching flights when attempting to locate a food source. *J. Exp. Biol.* 210: 3763–3770.
- Reynolds AM (2008) Optimal random Lévy-loop searching: New insights into the searching behaviours of central-place foragers. *Europhys. Lett.* 82: 20001.
- Reynolds AM, Bartumeus F (2009) Optimising the success of random destructive searches: Lévy walks can outperform ballistic motions. *J. Theor. Biol.* 260: 98–103.
- Reynolds AM, Rhodes CJ (2009) The Lévy flight paradigm: random search patterns and mechanisms. *Ecology* 90: 877–887.
- Reynolds AM (2010) Balancing the competing demands of harvesting and safety from predation: Lévy walk searches outperform composite Brownian walk searches but only when foraging under the risk of predation. *Physica A* 389: 4740–4746.
- Reynolds A (2013) Beyond optimal searching: Recent developments in the modeling of animal movement patterns as Lévy walks. In: Lewis MA, Maini P, Petrovskii S. *Dispersal, individual movement and spatial ecology*. Berlin: Springer Verlag. pp. 53–76.
- Rutz C, Hays GC (2009) New frontiers in biologging science. *Biol. Lett.* 5: 289–292.
- Santos MC, Raposo EP, Viswanathan GM, da Luz MGE (2004) Optimal random searches of revisitable targets: Crossover from superdiffusive to ballistic random walks.

- Europhys. Lett. 67: 734–740.
- Schneider J, Dickinson MH, Levine JD (2012) Social structures depend on innate determinants and chemosensory processing in *Drosophila*. Proc. Natl. Acad. Sci. USA 109: 17174–17179.
- Shimoji H, Abe MS, Tsuji K, Masuda N (2014) Global network structure of dominance hierarchy of ant workers. J. R. Soc. Interface 11: 20140599.
- Shizuka D, McDonald DB (2012) A social network perspective on measurements of dominance hierarchies. Anim. Behav. 83: 925–934.
- Sims DW, Southall EJ, Humphries NE, Hays GC, Bradshaw CJA, et al. (2008) Scaling laws of marine predator search behaviour. Nature 451: 1098–1102.
- Sims DW, Humphries NE, Bradford RW, Bruce BD (2012) Lévy flight and Brownian search patterns of a free-ranging predator reflect different prey field characteristics. J. Anim. Ecol. 81: 432–442.
- Solé RV, Bascompte J (2006) Self-organization in complex ecosystems. Princeton, NJ: Princeton University Press.
- Sorribes A, Armendariz BG, Lopez-Pigozzi D, Murga C, de Polavieja GG (2011) The origin of behavioral bursts in decision-making circuitry. PLoS Comput. Biol. 7: e1002075.
- Stowers JR, Fuhrmann A, Hofbauer M, Streinzer M, Dickinson MH, Straw AD (2014) Reverse engineering animal vision with virtual reality and genetics. Computer 14: 38–45.
- Strogatz SH, Stewart I (1993) Coupled oscillators and biological synchronization. Scientific American 269: 102–109.
- Sugihara G, May R, Ye H, Hsieh C, Deyle E, Forgarty M, et al. (2012) Detecting causality in complex ecosystems. Science 338: 496–500.
- Sumpter DJT (2010) Collective animal behavior. New Jersey: Princeton University Press.
- Takahashi DY, Narayanan DZ, Ghazanfar AA (2013) Coupled oscillator dynamics of vocal turn-taking in monkeys. Curr. Biol. 23: 2162–2168.
- Takahashi H, Horibe N, Shimada M, Ikegami T (2008) Analyzing house fly's exploration



- behavior with AR methods. *J. Phys. Soc. Jap.* 77: 084802-1-6.
- Takens F (1981) Detecting strange attractors in turbulence. In: Rand D A and Young L S, *Lecture Notes in Mathematics* 898, 366–381. Berlin Heidelberg: Springer-Verlag.
- Thiel M, Romano MC, Kurths J (2004) How much information is contained in a recurrence plot? *Physcis Letters A* 330: 343-349.
- Thiel M, Romano MC, Kurths J, Rolfs M, Kliegl R (2006) Twin surrogates to test for complex synchronization. *Europhysics Ltters* 75: 535-541.
- Tsuji K, Kikuta N, Kikuchi T (2012) Determination of the cost of worker reproduction via diminished life span in the ant *Diacamma* sp. *Evolution* 66: 1322–1391.
- Tunrsøm K, Katz Y, Ioannou CC, Huepe C, Lutz MJ, Couzin ID (2013) Collective states, multistability and transitional behavior in schooling fish. *PLoS Comput. Biol.* 9: e1002915.
- Vicsek T, Zafeiris A (2012) Collective motion. *Phys. Rep.* 517: 71–140.
- Visser AW (2007) Motility of zooplankton: fitness, foraging and predation. *J. Plankton Res.* 29: 447–461.
- Viswanathan GM, Afanasyev V, Buldyrev SV, Murphy EJ, Prince PA, et al. (1996) Lévy flight search patterns of wandering albatrosses. *Nature* 381: 413–415.
- Viswanathan GM, Buldyrev SV, Havlin S, da Luz MGE, Raposo EP, et al. (1999) Optimizing the success of random searches. *Nature* 401: 911–914.
- Viswanathan GM, da Luz MGE, Raposo EP, Stanley HE (2011) *The physics of foraging: An introduction to random searches and biological encounters.* New York: Cambridge University Press.
- de Vries H (1995) An improved test of linearity in dominance hierarchies containing unknown or tied relationships. *Anim. Behav.* 50: 1375–1389.
- Ward AJW, Herbert-Read JE, Sumpter DJT, Krause J (2011) Fast and accurate decisions through collective vigilance in fish shoals. *Proc. Natl. Acad. Sci. USA* 108: 2312–2315.
- Waters JS, Fewell JH (2012) Information processing in social insect networks. *PLoS ONE* 7: e40337.

- Wearmouth VJ, McHugh MJ, Humphries NE, Naegelen A, Ahmed MZ, et al. (2014) Scaling laws of ambush predator ‘waiting’ behaviour are tuned to a common ecology. *Proc. R. Soc. B* 281: 20132997.
- Wey T, Blumstein DT, Shen W, Jordán F (2008) Social network analysis of animal behaviour: a promising tool for the study of sociality. *Anim. Behav.* 75: 333–344.
- Wilson EO (1975) *Sociobiology*. Cambridge, MA: Harvard University Press.
- Wittemyer G, Polansky L, Douglas-Hamilton I, Getz WM (2008) Disentangling the effects of forage, social rank, and risk on movement autocorrelation of elephants using Fourier and wavelet analyses. *Proc. Natl. Acad. Sci. USA* 105: 19108–19113.
- Zollner PA, Lima SL (1999) Search strategies for landscape-level interpatch movements. *Ecology* 80: 1019–1030.
- Zupanc GKH (2010) *Behavioral neurobiology: an integrative approach*. Oxford: Oxford University Press.